Fundamental issues, mechanisms and models of flow boiling heat transfer in microscale channels

CHENG, Lixin and XIA, Guodong

Published version

CHENG, Lixin and XIA, Guodong (2017). Fundamental issues, mechanisms and models of flow boiling heat transfer in microscale channels. International Journal of Heat and Mass Transfer, 108 (Part A), 97-127.

Fundamental issues, mechanisms and models of flow boiling heat transfer in microscale channels

Lixin Cheng[1,2*] and Guodong Xia[1*]

[1]College of Environmental and Energy Engineering, Beijing University of Technology, Beijing, China,

[2]Department of Engineering and Mathematics, Sheffield Hallam University, City Campus, Howard Street, Sheffield, S1 1WB, UK

Abstract

This paper presents state-of-the-art review on the fundamental and frontier research of flow boiling heat transfer, mechanisms and prediction methods including models and correlations for heat transfer in microscale channels. First, fundamental issues of current research on flow boiling in microscale channels are addressed. These mainly include the criteria for macroscale and microscale channels. Then, studies on flow boiling heat transfer behaviours and mechanisms in microscale channels are presented. Next, the available correlations and models of flow boiling heat transfer in microscale channels are reviewed and analysed. Comparisons of 12 correlations with a database covering a wide range of test parameters and 8 fluids are presented. It shows that

* Corresponding author, e-mail address: lixincheng@hotmail.com; xgd@bjut.edu.cn.

all correlations poorly agree to the database. No generalized model or correlation is able to predict all flow boiling heat transfer data. Furthermore, comparisons of the mechanistic flow boiling heat transfer models based on flow patterns including the Thome at al. three-zone heat transfer model for evaporation in microchannel and the flow pattern based model combining the Thome et al. three zone heat transfer models with the Cioncolini-Thome annular flow model for both macro- and microchannel to the database are presented. It shows that the flow pattern based model combining the three zone model with the annular flow model gives better prediction than the three zone heat transfer model alone. The flow pattern based heat transfer model favourably agrees with the experimental database collected from the literature. According to the comparison and analysis, suggestions have been given for improving the prediction methods in the future. Next, flow patterned based phenomenological models and their applications to microscale channels are presented. Finally, as an important topic, unstable and transient flow boiling phenomena in microscale channels are briefed and recommendations for future research are given. According to this comprehensive review and analysis of the current research on the fundamental issues of flow boiling, mechanisms and prediction methods in microscale channels, the future research needs have been identified and recommended. In general, systematic and accurate experimental data of flow boiling heat transfer in microscale channels are still needed although a large amount of work has been done over the past decades. The channel size effect on the flow boiling behaviours should be systematically investigated. Heat transfer mechanisms in microscale channels should be further understood and related to the corresponding flow patterns. Furthermore, effort should be made to develop and improve generalised mechanistic prediction methods and theoretical models for flow boiling heat transfer in microscale channels according to the physical phenomena/mechanisms and the corresponding flow structures. The effects of the

channel size and a wide range of test conditions and fluid types should be considered in develop new methods. Furthermore, systematic experimental, analytical and modelling studies on unstable and transient flow boiling heat transfer in microscale channels should be conducted to understand the physical mechanisms and theoretical models.

Keywords: Flow boiling, heat transfer, microscale channel, fundamental, model, mechanistic method, correlation, transient, unstable, instability, mechanism and theory

Table of Contents

1. Introduction

Flow boiling phenomena in microscale channels are essential processes involved in a wide range of industrial applications such as micro-heat exchangers, micro reactors, microfluidic device, high heat fluxes cooling and the like in mechanical, chemical, aerospace, automotive, energy and renewable energy, electronic and microelectronic, biological and medical engineering etc.[1-6]. It is nowadays one of the most important research subjects in the field of heat transfer with various industrial and practical applications for the past decades [7-11]. For instance, as a highly efficient cooling technology, it has a lot of advantages of high heat transfer performance, chip temperature uniformity, hot spots cooling capability for cooling electronic chips and elements [4, 12-16]. The micro-electronics technology continues to develop very fast with very high heat flux to be dissipated up to 300 W/cm^2 or even more for cooling the electronic devices [2-5, 13-16]. One possible solution is to use flow boiling heat transfer in microscale channels such as multi-microscale channels made in silicon or copper cooling elements attached to CPUs or the electric elements, or directly in the silicon chip itself by utilizing the latent heat of flow boiling in a microscale channel evaporator for high heat flux cooling as shown in Fig. 1. Figure 1(a) shows a cross-section of a board of chips (about 30 chips per board) with the microchannel evaporator. Schmidt and Notohardjono [15] have demonstrated the successful use of a refrigeration unit with a microscale channel evaporator to cool IBM S/390 G4 server as shown in Fig. 2. Flow boiling in multi-channel evaporators is one of the most promising heat transfer mechanisms for electronics cooling by utilizing the latent heat of evaporation of a fluid to extract the heat in an energy efficient manner. As a result of the enhanced thermal performance compared to other processes, better axial temperature uniformity, reduced coolant flow rates, and

thus smaller pumping powers are obtained in flow boiling and two phase flow cooling technology. Cheng and Thome [16] have presented simulation results of flow boiling and two phase frictional pressure drop of CO_2 evaporating in a multi-microchannel evaporator shown in Fig. 1 (b) for chips cooling with the CO_2 flow boiling and two phase flow phenomenological models of Cheng et al based on flow patterns [25, 26]. They have found that superior heat transfer performance may be achieved with flow boiling in microscale channels. Figure 3 shows the comparison of the simulated based temperatures in the multi-microchannel using CO_2 and R236fa flow boiling in the microchannel in Fig. 1(b). In general, flow boiling heat transfer characteristics and mechanisms in microscale channels are quite different from those in conventional channels [3-8]. The channel size and confinement have a significant on the flow boiling characteristics, the corresponding heat transfer mechanisms and the models for predicting heat transfer coefficients. Compared to those in macroscale channels, flow boiling phenomena in microscale channels have not yet been well understood although a number of experiments have been conducted so far. The available studies of flow boiling heat transfer phenomena in microscale channels have exhibited contradictory results although a large amount of experimental work, theory and prediction methods for flow boiling in microscale channels have extensively been conducted over the past decades. Due to the large discrepancies between experiment results from different researchers, systematic knowledge of understanding the fundamentals of flow boiling including characterization, mechanisms and model development in microscale channels is urgently needed to be achieved. Furthermore, a number of heat transfer prediction methods such as correlations and models have been proposed for flow boiling heat transfer in microscale channels. However, nearly all these methods were based on limited test fluids, channel shapes and diameters under limited parametric conditions such as limited range of

saturation temperatures, mass fluxes, heat fluxes and working fluids etc. Therefore, the extrapolation of the available prediction methods to other fluids and channels do not work properly. It must be stressed here that big discrepancies among the experimental data from different independent laboratories may be caused due to different surface roughness of the test channels, channel dimension uncertainties, improper data reduction methods, flow boiling instabilities, improper designed test facility, test sections and experimental procedures. In some cases, the published results are unreasonable such as too big or too small heat transfer coefficients, some or complete wrong heat transfer behaviours and trends and correlations of various parameters and physical properties even if they have been published in journals. For instance, quite anomaly heat transfer trends are presented but they cannot be explained according to the corresponding flow boiling mechanisms in some papers although it is said that such mechanisms account for the heat transfer behaviours as detailed in a recent analysis in a comprehensive review by Ribatski et al. [7]. Furthermore, some flow boiling heat transfer correlations and models were proposed by simply regressing limited experimental data at limited test parameter ranges without considering the heat transfer mechanisms. Therefore, it is necessary to evaluate these correlations to validate their applicability before using these correlations. In fact, in most cases, such correlations do not work properly for other fluids and conditions. Therefore, it is essential to analyse and evaluate these correlations to identify further research needs in this important field.

The objectives of this paper are to discuss the fundamental issues by analysing the available experimental data of flow boiling heat transfer in the literature, the flow boiling heat transfer mechanisms accounting for the effects of channels size, bubble dynamics and flow regimes, the correlations and models for predicting flow boiling heat transfer coefficients in

microscale channels and some ideas for developing new mechanistic and phenomenological methods through relating the heat transfer behaviours to the bubble behaviours and flow regimes. In particular, a number of selected correlations and two mechanistic heat transfer models based on flow patterns for flow boiling in microchannel were evaluated with a database consisting of a wide range of test conditions. Furthermore, as an important topic, research of unstable and transient flow boiling heat transfer in microscale channel is addressed and future research needs have been pointed out. Through the analysis of the prediction results and heat transfer mechanisms in this comprehensive review, further research needs in the aspects of fundamental issues, mechanisms and model development of flow boiling in micoscale channels have been identified and recommended.

2. Fundamental issues on flow boiling heat transfer in microscale channels

2.1. Criteria for distinction of macroscale and microscale channels

Due to the quite different flow boiling phenomena in microscale channels as compared to conventional size channels or macroscale channels, the first and most important issue should be clarified about the distinction between micro-scale channels and macro-scale channels. However, a universal agreement is not yet established so far. Instead, there are various definitions on this issue, which are based on the engineering applications, bubble confinements or others.

Shah [17] defined a compact heat exchanger as an exchanger with a surface area density ratio > 700 m^2/m^3. This limit translates into a hydraulic diameter of < 6 mm. According to this definition, the distinction between macro- and micro-scale channels is 6 mm.

Mehendale et al. [18] defined various small and mini heat exchangers in terms of hydraulic diameter D_h, as:

- Micro heat exchanger: $D_h = 1 – 100$ μm.
- Meso heat exchanger: $D_h = 100$ μm – 1 mm.
- Compact heat exchanger: $D_h = 1 – 6$ mm.
- Conventional heat exchanger: $D_h > 6$ mm.

According to this definition, the distinction between macro- and micro-scale channels is somewhere between 1 to 6 mm.

Based on engineering practice and application areas such as refrigeration industry in the small tonnage units, compact evaporators employed in automotive, aerospace, air separation and cryogenic industries, cooling elements in the field of microelectronics and micro-electro-mechanical-systems (MEMS), Kandlikar [3] defined the following ranges of hydraulic diameters D_h which are attributed to different channels:

- Conventional channels: $D_h > 3$ mm.
- Minichannels: $D_h = 200$ μm – 3 mm.
- Microchannels: $D_h = 10$ μm – 200 μm.

According to this definition, the distinction between small and conventional size channels is 3 mm.

Several important dimensionless numbers are used to represent the feature of flow boiling and two phase flow in micro-scale channels by various researchers. According to these dimensionless numbers, the distinction between macro- and micro-scale channels may be classified. Triplett et al. [19] defined flow channels with hydraulic diameters D_h of the order, or smaller than, the Laplace constant L:

$$L = \frac{\sigma}{g(\rho_l - \rho_g)} \tag{1}$$

as micro-scale channels, where σ is surface tension, g is gravitational acceleration, and ρ_l and ρ_g are respectively liquid and gas/vapor densities.

Kew and Cornwell [20] proposed the Confinement number Co for the distinction of macro- and micro-scale channels, which is actually based on the Laplace number Eq. (1) as

$$Co = \frac{1}{D_h}\sqrt{\frac{\sigma}{g(\rho_l - \rho_g)}} \tag{2}$$

When the confinement number Co is less than 0.5, the channel is considered as microscale channel.

Based on a linear stability analysis of stratified flow and the argument that neutral stability should consider a disturbance wavelength of the order of channel diameter, Brauner and Moalem-Maron [21] derived the Eotvös number Eö criterion for the dominance of surface tension for micro-scale channels:

$$Eö = \frac{(2\pi)^2 \sigma}{(\rho_l - \rho_g) D_h^{\,2} g} > 1 \tag{3}$$

It is obvious that the definition of a micro-scale channel is quite confusing because there are different criteria available as described above. Cheng and Mewes [12] made a comparison of these different criteria for micro-scale channels. Figure 4 shows their comparable results for

water and CO_2, which shows the big difference among these criteria. It is obvious that no general definition of micro-scale channels has been agreed so far.

More recently, Harirchian and Garimella [22] has proposed a microscale to macroscale criterion as follows:

$$\mathrm{Bd}^{0.5} \times \mathrm{Re} = \frac{1}{\mu_l}\left(\frac{\mathrm{g}(\rho_l - \rho_g)}{\sigma}\right)^{0.5} \mathrm{GD}^2 = 160 \tag{4}$$

$$\mathrm{Bd} = \left(\frac{\mathrm{g}(\rho_l - \rho_g)}{\sigma}\right)^{0.5} \tag{4a}$$

$$\mathrm{D} = \sqrt{\mathrm{A}_{cs}} \tag{4b}$$

where Bd is the Bond number, Re is the Reynolds number, G is mass velocity and D is length scale, A_{cs} is cross-sectional area of microscale channels. Figure 5 shows their macrocale to microscale channel transition from confined flow to unconfined flow according to their experimental data. This distinction criterion is based on the flow characteristics, which is different from the afore-mentioned criteria. It is based on the convective confinement number which is the product of the Bond number and the Reynolds number with the assumption that the total gas liquid two-phase mixture flows as liquid. Compared to the criteria simply using a threshold diameter, the criterion of Harirchian and Garimella needs to be further validated with extensive experimental data because it is only based on their own experimental data which is very limited in test conditions, channel size and shape. The proposed criterion may have limitation when applied to other cases. In particular, it should be realised that their experiments

were conducted in microscale channels. As such, all flows are actually confined in the microchannels. Therefore, it is better to clarify what unconfined flow means in this case.

Ong and Thome [23] have proposed a new macro-to-micro channel criterion using the confinement number Co defined by Eq. (2) according to their experimental data and observed liquid films for different flow regimes. In annular flows, for the confinement numbers greater than 1, they observed symmetric liquid film distribution along the channel wall and micro-scale flow boiling behavior. For the confinement numbers lower than about 0.3, they observed non-symmetric liquid film distribution along the channel wall. They observed isolated bubbles and bubbles coalescence and the flow boiling is microscale behavior for the confinement number greater than 1. For the confinement number is less than 0.3, they observed the plug-slug flow pattern and flow boiling exhibits macroscale channel behaviors. For confinement numbers between 1.0 and values within the range of 0.3 to 0.4, they observed the mesoscale channel behaviour according to their test conditions and test channels. However, it should be realized that the transition from macroscale-to-micoscale is a continuous and progress process which corresponds to the flow regime, heat transfer behaviors and mechanisms. Therefore, the most important point is to relate flow regimes to flow boiling heat transfer behaviours such as heat transfer, CHF and fluid behaviour such as pressure drops as pointed out by Cheng et al. [11]. Relating flow regime behaviors to the corresponding flow boiling heat transfer and gas liquid two phase flow behaviors is a practical and effective method to develop mechanistic or phenomenal predictions for both macroscale and microscale channels due to the continuously progressive change from macroscale channels to microcale channels. This has been validated by the flow pattern based CO_2 flow boiling model of Cheng et al. [24-26], which covers both macroscale and microscale channels for CO_2 flow boiling heat transfer and two phase flow.

Their generalized flow pattern based CO_2 flow boiling heat transfer model predicts both macroscale and microscale channel flow patterns and heat transfer reasonably well. Especially, their CO_2 flow pattern map captured well the independent flow pattern observations in microscale channels by Gasche [27]. It gives a hint that the macroscale and microscale channels may be determined according to the flow boiling heat transfer behaviour due to the intrinsic links between the heat transfer mechanisms and the flow structures in both macroscale and microscale channels. A mechanistic distinction criterion may be more of practice and effectiveness in developing new flow boiling heat transfer prediction models. However, such criteria need to be further developed in future. In this sense, using Kandlikar's criterion of 3 mm to distinct the macroscale and microscale channels is quite reasonable when developing mechanistic models because it covers the transitional region from macroscale to microcale flow boiling. It should be realised here that the transition between microscale and macroscale channels has neither been well defined nor seriously experimentally investigated as evidenced according the afore-going analysis and discussion. However, one may distinguish between flow boiling behaviours such as heat transfer, fluid flow and flow patterns behaviours in macroscale and microscale channels [11, 28-30, 33, 34, 37, 38]. It is definitely effective from a practical application viewpoint if the flow patterns can be incorporated into flow boiling heat transfer and two phase frictional pressure drop prediction methods simultaneously with the corresponding heat transfer mechanisms such as those by Katten et al. [46], Wojtan et al. [31, 32], Cheng et al. [24-26] and Moreno Quibén [35, 36]. Such a prediction method actually works reasonably well if related flow regimes and bubble dynamics to the corresponding heat transfer behaviours.

It should be stressed here that in most cases the dimensionless number such as the confinement number has been given different values according to individual observations and

experimental data with limited test fluids, test channels and test conditions. Although a number of such criteria have been proposed by various researchers so far, it is obvious that no universal agreement has been reached according to the dimension less numbers. The main reason is due to the limited experimental parameter ranges and test channel sizes and shapes.

In the present paper, the distinction between macro- and micro-channels by the threshold diameter of 3 mm is adopted due to the lack of a well-established theory, but is in line with that recommended by Kandlikar [3] as mentioned in the fore-going. Using this threshold diameter enables more relevant studies to be included and thus the different flow boiling heat transfer characteristics, mechanisms and models in various channels with different sizes can be compared and analysed.

2.2. Fundamental issues of flow boiling heat transfer in microscale channels

Flow boiling heat transfer in conventional channels is governed by two basic mechanisms of nucleate boiling dominant mechanism (relating to the formation of vapour bubbles at the tube wall surface and bubble dynamics) and convection dominant mechanism (relating to conduction and convection through a thin liquid film with evaporation on the channel wall and at the liquid–vapour interface). It should stressed here that the flow boiling heat transfer mechanisms are intrinsically related to the bubble dynamics and flow pattern behaviors [5, 24-25, 31, 33, 35-38]. The gravity becomes important for flow boiling in horizontal conventional channels and affects the flow patterns and heat transfer behaviour. The flow boiling heat transfer is strongly dependent on the heat flux in nucleation dominant boiling while the heat transfer is less dependent on the heat flux and strongly dependent on the mass flux and vapour quality in convection dominant boiling. It should be pointed out that one may assume that these boiling

mechanisms function independently of one another for simplicity. However, the two main flow boiling mechanisms may actually coexist at high vapor qualities, where the convective boiling gradually suppresses the nucleate boiling [5]. Therefore, the nucleate and convective boiling contributions to the heat transfer process can be superimposed by very complex mechanisms which are not yet fully understood so far. In general, the flow boiling heat transfer mechanisms in macroscale channels have laid a good foundation to investigating the flow boiling heat transfer mechanisms in microscale channels which needs to be systematically explored through considering more affecting factors such as bubble confinement, channel size and shape effects, surface roughness, accurate liquid film and heat transfer measurement and corresponding flow regime observation with state-of-the-art experimental technique and proper data analysis methods.

Despite numerous investigations in the field of microchannel flow boiling for many years, the characteristics of flow boiling still need to be better clarified. Quite different parametric trends of heat transfer coefficient versus quality, mass velocity, and heat flux have been reported in the literature. Figure 6 shows the various variations of heat transfer coefficient with vapor quality in the literature as illustrated by Ribatski et al. [7] in their review. In most case, the heat transfer coefficient decreases with increasing the vapor quality and the hydraulic diameter, and the heat transfer coefficient increases with increasing mass velocity at a given vapor quality. However, other variations are also observed as illustrated in Fig. 6. Just to show two comparisons of the experimental data obtained at similar test conditions by different researchers here as shown in Figs. 7(a) and (b) [7]. Figure 7(a) shows the comparison for R22 flow boiling heat transfer coefficients at similar test conditions in two micrcoscale channels whose diameter difference is very little. The flow boiling heat transfer coefficient increases from 3 to 8 kW/m^2K

for increasing vapor qualities from 0.2 to 0.8 according to the experimental data of Kim et al. [67] while the flow boiling heat transfer coefficient keeps at nearly a constant value of 2 kW/m^2K for the experimental data of Bang and Choo [66]. It can be seen that there are big difference of the experimental results for two similar test conditions in the microscale channel. Figure 7(b) shows the comparison of the experimental flow boiling heat transfer coefficients of R410A by Yun et al. [68] and Pamitran and Choi [54] in two microscale channels whose diameter difference is very little. Again, remarkable discrepancies between the heat transfer coefficients are observed. According to the experimental results of Yun et al. [68], the flow boiling heat transfer coefficient increases with increasing the vapor quality up to 0.8 while for the experimental results of Pamitran and Choi [54] the flow boiling heat transfer coefficient is almost constant until increasing the vapor quality up to 0.4 and it then decreases monotonically with further increasing the vapor quality. Furthermore, at the test conditions: vapor quality of 0.4, saturation temperature of 10 ^oC and heat flux of 15 kW/m^2, the flow boiling heat transfer coefficients of Yun et al. [68] are almost 3 fold those of Pamitran and Choi [54] at lower vapor qualities and up to 10 fold at higher vapor qualities. It is very difficult to explain the observations from the flow boiling heat transfer mechanisms. It seems that the high mass fluxes are not related to such differences for the heat transfer coefficients of Pamitran and Choi as it is obvious that the effects of the mass flux on the heat transfer coefficient are almost negligible as indicated in Fig. 7(b). It also seems impossible that the difference is caused due to the transition from macroscale- to microscale channel behaviors because both experiments were performed in microscale channels with similar tube diameters using the same working fluid and at similar test conditions. Both Kim et al. and Yun et al. conducted experiments of flow boiling in rectangular multi-channels and obtained similar parametric trends which are the heat transfer coefficient increases

with increasing the vapor quality. However, Bang and Choo and Pamitran and Choi conducted experiments of flow boiling heat transfer in single circular channels. The variations of the heat transfer coefficients versus vapor qualities are almost flat at lower vapor qualities and then decrease at higher vapor qualities for both studies. In a rectangular channel, the surface tension effects on the liquid flow play a key role in the corners of the channel and result in a thinner film on the channel wall than in the corners, which may result in higher evaporation heat transfer coefficients. However, it is unable to explain the huge differences of the flow boiling heat transfer coefficients in these examples according to the flow boiling heat transfer mechanisms.. Something might go wrong in the experiments and results. Obviously, when performing experiments of flow boiling in microscale channels, well designed test facility, accurate calibration and measurement systems, validation of the systems careful planned test procedure and data analysis methods should be used. It is also important to do energy balance using single phase heat transfer before the flow boiling experiments.

Furthermore, it should be pointed out here that the flow regimes should be related to flow boiling heat transfer behaviours to indicate the corresponding heat transfer mechanisms [11, 37, 38]. Understanding the bubble dynamics and flow regimes in microscale channels is extremely important when investigating the corresponding flow boiling characteristics. The effects of multiple channels, single channels and channel shapes should be considered as well. Generally, flow regimes in multi-microscale channels are similar to those in single microscale channels. However, flow instability becomes important in microscale channels due to the confinement effect of bubble dynamics. As such, reversible flow occurs as observed by Qu and Mudawar show in Fig. 8. The complex flow instability issue is beyond the scope of this paper. Simply considering the flow pattern in such flow boiling in microscale channels, there are several studies

relevant to flow patterns in multi-microscale channels [37]. Here just to illustrate one example, Wang et al. [48] conducted flow visualization and measurement study on the effects of inlet/outlet configurations on flow boiling instabilities in eight parallel microscale channels, having a length of 30 mm and a hydraulic diameter of 186 μm. The arrangement of their test multi-channels are shown in Fig. 9. Figure 10 shows their observed flow patterns in the parallel channels at steady flow condition. Elongated bubbles were observed due to the confinement of the microscale channels. Other flow patterns include isolated bubble flow, coalescence bubble flow and annular flow. Furthermore, Understanding bubble dynamics is essential to investigate the heat transfer mechanisms [37]. Wang et al. [48] also observed high-speed images of bubble nucleation process were obtained for different mass velocities, tube diameter and fluid. Figure 11(a) shows that flow boiling exhibited nucleate boiling characteristics with small isolated bubbles at a negative local vapor quality (x_e = -0.034). Figure 11(b) shows that when the local vapor quality was nearly equal to zero (x_e = 0.005), the bubbles filled the entire cross-section and then were flushed out of the channels. This resulted in the maximum value of heat transfer coefficient, as discussed below. Figure 11(c) shows that at an exit vapor quality of x_e = 0.26, local dryout was observed instantaneously from t = 24.6–65.9 ms, and the lifetime of the dryout increased with the increasing vapor quality. It can be speculated that the liquid film in the Taylor bubbles ruptures easily, causing dryout in microchannels.

For flow boiling in microscale channels, both mass flux and heat flux can affect the boiling process significantly, depending on the channel sizes and shapes, fluid type and operation conditions. The inlet subcooling may also play a role in the microchannel flow boiling heat transfer mechanisms but less investigation in this aspect is available in the literature. Although a large number of studies suggest the two flow boiling heat transfer mechanisms in microscale

channels, which are actually similar to those in macroscale channels, quite different microchannel flow boiling heat transfer trends have been observed for similar test channels and experimental conditions by different researchers, which sometimes cannot be explained by a single mechanism. Therefore, the dominant heat transfer mechanisms still need to be well clarified and they should be related to the relevant bubble and flow regime behaviours in microscale channels. Figure 12 show schematically the two dominant flow boiling heat transfer mechanisms in microscaole channels: nucleate boiling dominant heat transfer and convective boiling dominant heat transfer [33]. However, the actual heat transfer mechanisms in microscale channels are much more complex than the two mechanisms. The channel size and shape effects on flow boiling heat transfer and the mechanisms become more important as they have a significant effect on the corresponding bubble evolution flow patterns [37-39]. For instance, the bubbly and the elongated slug regimes are said to exhibit the characteristics of the nucleate boiling while the annular regime exhibits the convective boiling trend. This is quite similar to what is observed in conventional sized (macro) channels. In conventional channel flow boiling, different heat transfer mechanisms are dominant according to the vapour quality range, heat flux and mass flux levels. At low vapour qualities, nucleate boiling effects prevail while at high vapour qualities and prior to the liquid dryout, the heat transfer coefficient is mainly controlled by convective effects. These heat transfer mechanisms are commonly considered when developing flow boiling heat transfer correlations in conventional channels such as the Chen correlation [40] and others [41-46]. However, nearly all conventional flow boiling heat transfer correlations have been found to be inadequate to predict the flow boiling heat transfer data in the microscale channels [38]. On a general basis, although by chance they sometimes work for a particular data set, the failure of these methods to accurately predict the heat transfer coefficient

in microscale channels means that more complex flow boiling heat transfer mechanisms dominate the flow boiling processes in microscale channels. This is due to significant differences in the phase change phenomena in the transition region between macro- and micro-channels and also in the bubble growth and flow pattern evolution affected by the microscale channels. Many extrapolations of macroscale channel prediction methods to microscale channel flow boiling conditions were performed without a sound physical basis and clearly understanding of the fundamental issues such as bubble dynamics and flow patterns representing the corresponding flow boiling heat transfer mechanisms in microscale channels. Apparently these fundamental issues have not been well solved although experimental data are continuously published. Careful research work, deep analysis of the experimental data and development of reasonable mechanisms governing the microscale channel flow boiling phenomena are urgently needed.

3. State-of-the-art review on studies on flow boiling heat transfer and mechanisms in microscale channels

Experiments of flow boiling in microscale channels have been extensively conducted by researchers over the past years. Both single- and multi-microscale channels with various shapes such as rectangular, trapezoidal, circular and triangular etc. were used in the tests. Various fluids such as water, Nitrogen, CO_2, refrigerants, dielectric fluids and others have been employed as the working fluid in the experiments under different test conditions. Table 1 summarizes the selected experimental studies on flow boiling heat transfer in microscale channels and the corresponding heat transfer mechanisms in the literature.

As one of the pioneer studies, Lazarek and Black [49] conducted experimental studies of flow boiling in small diameter tube. They measured the local heat transfer coefficients for saturated flow boiling of R-113 in a vertical circular tube with an internal diameter of 3.1 mm, a heated length of 12.6 cm over the static pressure range of 1.3 to 4.1 bar and mass flux from 140 to 740 kg/m^{2}s. They have found that the flow boiling heat transfer mechanisms is controlled by nucleate boiling dominant due to the independence of the heat transfer coefficient with the local vapour quality. They proposed a correlation for the local flow boiling heat transfer coefficients using the Nusselt number as a function of the liquid Reynolds number and the boiling number based on their experimental data. However, it should be mentioned that such a correlation may be difficult to be extended to other conditions due to the limited working fluids, test conditions and channel sizes and shapes. It should also be mentioned here that other heat transfer mechanisms may occur in different cases.

Bao et al. [50] conducted experiments of flow boiling heat transfer with R-11 and HCFC123 in a horizontal circular tube with an inner diameter of 1.95 mm. Their test parameter ranges are: mass fluxes from 50 to 1800 kg/m^{2}s, heat fluxes from 5 to 200 kW/m^2 and saturation pressures from 200 to500 kPa. According to their study, flow boiling heat transfer coefficients are independent of mass flux and vapour quality but are strongly affected by the heat flux and saturation pressure. It means that the main heat transfer mechanisms are nucleate boiling dominant. In their experimental observation, the flow boiling heat transfer behaves as the nucleate boiling dominant mechanisms up to vapour quality of 70%. Their results shows trends and mechanisms similar to those found by Lazarek and Black [49] using R-113 in a 3.1 mm diameter tube, by Tran et al [70] using R-12 in a 2.46 mm diameter horizontal tube, and by Owhaib et al. [71] using R-134a in vertical tubes with inner diameters of 0.826, 1.224, and 1.7

mm. It should be realised that their results were based on only one tube diameter and two test fluids as different heat transfer mechanisms may occur for other cases.

Huo et al. [72] conducted experiments of flow boiling of R134a in vertical tubes with two diameters of 2.01 and 4.26 mm. They have found a more complex behaviour especially for vapor quality larger than 20%, as shown in Fig. 13, where the flow boiling heat transfer coefficient is plotted versus the vapor quality for different heat fluxes. Similar results have been found by Yan and Lin [73] using R-134a in a 2.0 mm 28 parallel tubes channel, and by Lin et al. [75] using R-141b in a 1.1 mm circular tube. Huh and Kim [74] have argued that major flow pattern is similar with annular flow in their study, which would not support the nucleate boiling dominant mechanism associated with an independency of heat transfer coefficient on mass flux or vapour quality in their experimental data. It has to mention here that a 4.26 mm inner diameter tube falls into the macroscale channel range but their heat transfer data cannot be explained by the well documented flow boiling mechanisms.

Warrier et al. [51] took FC-84 as test fluid flowing through 5 parallel channels with each channel having the following dimensions: hydraulic diameter of 0.75mm and length to diameter ratio of 409.8. Their test parameter ranges are mass fluxes from 557 to1600 kg/m^{2}s, heat fluxes from 0 to 59.9 kW/m^2 and the inlet liquid temperatures of 26, 40 and 60^{o}C. Based on their flow boiling heat transfer data, they proposed a correlation for saturated flow boiling heat transfer only using the Boiling number. Their saturated flow boiling correlation is valid in their test ranges: $0.00027 \leq$ Bo ≤ 0.00089 and $0.03 \leq x \leq 0.55$. It should be pointed out that only using one dimensionless number to develop a flow boiling heat transfer correlation does not really capture the governing heat transfer mechanisms. Also such a correlation is difficult to be extended to other fluids and conditions due to the limited data used.

Zhang et al. [52] conducted extensive comparisons of the existing correlations for flow boiling heat transfer in mini-channels. They have found that the available flow boiling heat transfer correlations do not work for microscale channels. They have found that a common feature of flow boiling heat transfer in many mini-channels is liquid-laminar and gas-turbulent flow, and thus it may not be applicable in principle to predict the flow boiling heat transfer coefficients by using the general existing correlations developed for liquid-turbulent and gas-turbulent flow conditions, such as the Chen [40] flow boiling correlation. They proposed a new correlation for microscale channel flow boiling based on various existing experimental data in the literature. It should be pointed out that such a correlation is actually the Chen type correlation with proposed new nucleate enhancement factor and suppression factor. As already mentioned, from the mechanistic aspects, no flow regime information is considered in their methods. It is important to correlate the flow regimes to the heat transfer mechanisms and the heat transfer prediction methods although the correlation of Zhang et al. works well for global data in some cases but it does not capture the heat transfer trends, like the Chen correlation does.

Lee and Mudawar [53] conducted experiments on flow boiling heat transfer of R134a in horizontal rectangular parallel microscale channels with 231 μm wide and 713 μm deep groves in a copper block. They have found that flow boiling heat transfer is associated with different mechanisms for low, medium and high vapor qualities. Bubbly flow and nucleate boiling occur only at low qualities less than 0.05 and low heat fluxes, which suggests the heat transfer mechanism is nucleate boiling dominant. At medium qualities from 0.05 to 0.55 or high qualities larger than 0.55 and high heat fluxes, the flow boiling heat transfer is dominated by annular film evaporation. They proposed a new flow boiling heat transfer correlation for these three ranges of vapour qualities, which is recommended for both R134a and water flow boiling in microscale

channels. Due to the limited working fluids, test conditions and channel sizes and shapes, the proposed correlation needs to be verified before applied to other cases.

Pamitran et al. [54] investigated the convective boiling heat transfer of binary mixture refrigerant R410A in horizontal circular tubes with inner diameters of 1.5 and 3.0 mm lengths of 1500 and 3000 mm, respectively. Local heat transfer coefficients were obtained for heat fluxes from10 to 30 kW/m^2, mass fluxes from 300 to 600 kg/m^2s, a saturation temperature of 10^{o}C and vapour quality up to 1.0. They proposed a new flow boiling heat transfer correlation based on the superposition principle of nucleate boiling dominant and convective dominant mechanisms. However, as already mentioned in the afore-going, their heat transfer are quite different from others at similar test conditions and test channel size. It is difficult to explain the heat transfer mechanisms according to their data. Furthermore, it should be mentioned here that their test mass flux range is rather narrow and their correlation is only based on one fluid. Thus, it is necessary to valid their correlation with independent data due to the limited working fluids, test conditions, channel sizes and shapes.

Bertsch et al. [55] proposed a new heat transfer correlation for flow boiling in microscale channels using a database of 3899 experimental heat transfer data points collected from 14 studies in the literature. Their database covers 12 different wetting and non-wetting fluids flow boiling in channels with the hydraulic diameters from 0.16 to 2.92 mm. The test conditions of the database cover the mass fluxes from 20 to 3000 kg/m^2s, the heat fluxes from 4 to1150 kW/m^2, the saturation temperatures from 94 to 97^{o}C and the vapor qualities from 0 to 1. Their flow boiling heat transfer correlation predicts the flow boiling heat transfer database reasonably. Although some of the data sets show opposing trends with respect to some parameters, the mean absolute error is still acceptable for the new flow boiling heat transfer correlation. However, as

already mentioned in afore-going, a reasonable heat transfer prediction method should not only be able to capture the heat transfer trends but also be able to explain the physical phenomena and the corresponding heat transfer mechanisms. In this aspect, relating flow patterns to the heat transfer behaviors and mechanisms are essential. Therefore, effort should be made to develop mechanistic or phenomenological prediction methods which should be based on the well understanding the flow boiling heat transfer mechanisms and the corresponding flow regime behaviours.

Ong and Thome [56] conducted experiments of flow boiling heat transfer with three working fluids R134a, R236a and R245fa in a 1.03 mm horizontal circular channel. Their test parameter ranges cover a wide range of mass fluxes from 200 to 1600 kg/m^{2}s and heat fluxes from 2.3 to 250 kW/m^2. However, only one saturation temperature of 31^{o}C was tested in their investigation. According to their experimental results, the local saturated flow boiling heat transfer coefficients depend on the heat flux and the mass flux. The variation of flow boiling heat transfer coefficients trends correspond well with flow regime transitions of a flow map for microchannel developed by Thome's group. However, it should be mentioned here that the physical properties of a fluid are related to saturation temperature or pressure. In their study, based only on one test saturation temperature of 31^{o}C, it is difficult to identify how the physical properties would affect the flow boiling heat transfer behavior and mechanisms. Therefore, it is essential to reasonably define a range of saturation temperatures and other test parameters when designing test runs in an experiment campaign. This is the basis to understand how the heat transfer mechanisms would change with the physical properties and test parameters.

Sun and Mishima [57] evaluated thirteen prediction methods for flow boiling heat transfer in microscale channels against a database including 2505 experimental heat transfer data for 11

working fluids and tubes with tube diameters from 0.27 to 6.05 mm covering both macroscale and microscale channels. They have found that the Chen correlation [40] and those methods developed based on the Chen correlations are not suitable for flow boiling heat transfer inmicroscale channels, which actually means that the heat transfer mechanisms in macroscale channel cannot explain the flow boiling heat transfer behaviors in microscale channels properly. Furthermore, they have found that the Lazarek and Black [49] flow boiling heat transfer correlation and the Kew and Cornwell [20] flow boiling heat transfer correlation worked better for their database than other prediction methods used in their study. Therefore, their results support the nucleate dominant boiling mechanisms in microscale channel flow boiling. They proposed a new modified flow boiling heat transfer correlation on the basis of the correlations of the Lazareck and Black and the Kew and Cornwell. As already described in the foregoing, various heat transfer mechanisms occur for different studies. Furthermore, a flow boiling heat transfer prediction method based on limited dimensionless numbers may not be sufficient to represent the intrinsic heat transfer mechanisms involved in microscale channel flow boiling. It might predict the experimental data globally but it does not mean that such a method is able to capture the heat transfer variation trends.

Li and Wu [58] evaluated the existing flow boiling heat transfer correlations for flow boiling in microscale channels with more than 3700 experimental data points collected from the literature. Their database covers a wide range of working fluids, operational conditions and different microscale channel dimensions and shapes. They have found that none of the existing flow boiling heat transfer correlations could predict their database properly. Therefore, they proposed a new flow boiling heat transfer correlation based on their database. The boiling number, the Bond number and the Reynolds number are adopted in developing the new

correlation. Their flow boiling heat transfer correlation predicted their database reasonably well. However, it needs to be verified by a wide range of independent experimental data. As already mentioned, the correlation might predict the database globally but it does not mean that such a method is able to capture the heat transfer variation trends. Furthermore, when develop a new prediction method, it is important to incorporate the heat transfer mechanisms into the methods.

Tibirica and Ribatski [59] conducted experiments of flow boiling with R134a and R245fa in a horizontal 2.3 mm inner diameter stainless steel tube with a heating length of 464 mm. Their experimental flow boiling heat transfer results were obtained at the conditions: the mass fluxes from 50 to 700 kg/m^{2}s, the heat fluxes from 5 to 55 kW/m^2, the saturation temperatures of 22, 31 and 41^{o}C, and the vapor qualities from 0.05 to 0.99. According to their test results, the flow boiling heat transfer coefficients are strongly affected by the heat flux, the mass flux and the vapor quality. The heat transfer coefficient increases with increasing the heat flux, the mass flux and the saturation temperature, which can be reasonably explained by the macroscale channel flow boiling nucleate dominant and convective dominant heat transfer mechanisms. However, their results are quite different from those by Huo et al. [72] showing decreasing trends of the heat transfer coefficient with increasing vapour quality at similar test conditions and with the same fluid R134a although the orientations of the test channels are different, which generally does not make massive difference, especially in the respective of heat transfer mechanisms. It should noticed that a 2 mm inner diameter tube may still fall into the macroscale channel range and the heat transfer behaviors should be similar to those in macroscale channels. In this case, their experimental results are quite reasonable.

Lin et al. [75] conducted an experimental investigation of flow boiling with R141b in circular tubes with 3 tube diameters of 1.8, 2.8, 3.6 mm and one square channel of 2 ×2 mm^2.

The mass fluxes range from 50 to 3500 kg/m^{2}s. They have found that both the nucleate boiling dominant and convective dominant heat transfer mechanisms. The local heat transfer coefficient was found to be a weak function of mass flux while the mean heat transfer coefficient was independent of mass flux. They have showed that the transition from nucleate boiling to convective boiling at high heat fluxes occurred at higher qualities. In the absence of dryout in the saturation boiling region, they have found that the mean heat transfer coefficient varied only slightly with the tube diameter and was mainly a function of the heat flux.

Chen and Garimella [77] conducted experiments of flow boiling with a dielectric fluid in a silicon chip-integrated multiple microscale channel heat sink consisting of 24 microscale square channels with 389 μm × 389 μm in cross-section each. The multiple microscale channels were fabricated into a square silicon substrate with 12.7 mm × 12.7 mm. The flow regimes of the corresponding heat transfer behaviors were observed in their tests. They have found that at lower heat fluxes, the main flow regime is the bubbly flow. With increasing the heat flux, the bubbles coalesced and vapor slug flow regimes were formed. With further increasing the heat flux to higher values, the main flow regimes in the downstream portion of the microscale channels are characteristic of alternating wispy-annular flow and churn flow. In the meantime, the reversed flow phenomena were observed in the upstream region near the inlet of the microscale channels. The local heat transfer behaviors are quite different for three flow rates. At lower heat fluxes, the heat transfer coefficient increases with increasing the heat flux. At medium heat fluxes, the heat transfer coefficient is independent of flow rate. At higher heat fluxes, the heat transfer coefficient decreases with further increasing heat flux. This is mainly due to partial dryout ocuring in some of the microscale channels which actually deteriorate the heat transfer.

Liu and Garimella [78] conducted experiments of flow boiling heat transfer with D.I. water in two rectangular microscale channels cut into a copper block. The microscale channels with 275 μm × 636 μm and 406 μm × 1063 μm were used in their tests. The mass fluxes were from 221 to 1283 kg/m^{2}s. Chen and Garimella [79] conducted experiments of flow boiling heat transfer with FC-77 in a copper microchannel heat sink with 10 rectangular channels, each with 504 μm × 2.5 mm. The mass fluxes are from 80 to 133 kg/m^{2}s. Both experimental results are similar to those by Chen and Garimella [77]. All these studies have showed that beyond the onset of nucleate boiling heat transfer, the boiling curves collapsed on a single curve for all mass flow rates. With further increasing the heat flux, the boiling curves diverged and became dependent on the mass flux. It means that the two flow boiling heat transfer mechanisms exist in their study. Apparently, their results are quite different from those of Lazarek and Black [49], Bao et al. [50], Tran et al [70] and Owhaib et al. [71]. As already mentioned, it is very important to understand the heat transfer trends and mechanisms by observing the flow phenomena and flow regimes [76]. These studies have provided good examples but systematic studies in this aspect are needed to better understand the heat transfer mechanisms.

The channel size has a significant effect on the two phase flow and heat transfer behaviors in microchannel. So far, few have systematically investigated the effect of microscale channel dimensions on the flow boiling heat transfer behaviors. A few studies have considered the effect of microscale channel size on flow boiling patterns and the transition between different flow patterns [37] while the effect of microchannel size on heat transfer coefficient has been largely unexplored.

Saitoh et al. [61] conducted flow boiling heat transfer experiments for R134a in single horizontal channels with inner diameters of 0.51, 1.12 and 3.10 mm. Figure 14a–c show the

effect of heat flux q and mass flux G on the flow boiling heat transfer coefficients for the three different diameter tubes. For the 3.1-mm-ID tube results as shown in Fig. 14a, in the low vapor quality less than 0.6, when the mass flux is fixed at 300 kg/m^{2}s, the heat transfer coefficient for the heat flux of 24 kW/m^2 is higher than that for the heat flux of 12 kW/m^2, whereas when the heat flux is fixed at 12 kW/m^2, the heat transfer coefficient for the mass flux of 150 kg/m^{2}s is similar to that for the mass flux of 300 kg/m^{2}s. However the heat transfer coefficients at vapor quality large than 0.6 and at a fixed heat flux of 12 kW/m^2, the heat transfer coefficient at the mass flux of 300 kg/m^{2}s is higher than that at the mass flux of 150 kg/m^{2}s, whereas at a fixed mass flux of 300 kg/m^{2}s, the heat transfer coefficient at the heat flux of 12 kW/m^2 is similar to that at the heat flux of 24 kW/m^2. According to their experimental results, in the low vapour quality region, nucleate boiling is the dominant heat transfer mechanisms and in the high vapour quality region, forced convective evaporation is the dominant heat transfer mechanisms. According to the 1.12-mm-ID tube test results shown in Fig. 14b, the heat transfer coefficients are slightly higher than those for the 3.1- mm-ID tube shown Fig. 14a, and the effects of heat flux and mass on the heat transfer coefficients are similar for both test tubes and thus the heat transfer mechanisms are the same for these two tubes. Their flow boiling heat transfer results are in consistent with those by Tibirica and Ribatski [57] but again contradictory to those by Huo et al. [70]. For the 0.51-mm-ID tube results shown in Fig. 14c, the flow boiling heat transfer coefficient increases with increasing the heat flux but is not significantly affected by the mass flux, which indicate that nucleate boiling is the dominant heat transfer mechanisms. Of the three tubes, the flow boiling heat transfer coefficients for the 0.51-mm-ID test tube are the highest at the vapor quality less than 0.5. With decreasing the tube diameter, the heat transfer coefficient decreases at lower vapor quality. The vapor quality at which the heat transfer coefficient starts to

decrease is 0.9 for the 3.1-mm-ID test tube, between 0.8 and 0.9 for the 1.12-mm-ID test tube and between 0.5 and 0.6 for the 0.51-mm-ID test tube. According to their experimental results, for the three tubes, the effects of heat flux are strong and nucleate boiling mechanism is the dominant. However, according to their results, the 3.10 mm diameter channel exhibited the strongest effect of mass flux on the heat transfer coefficient as compared with the 1.10 mm test tube while the least effect on mass flux was observed for the 0.51 mm diameter test tube. The onset of dryout was observed to occur earlier in the lower vapor quality region with decreasing channel diameter. According to their study, the convective boiling dominance significantly decreases with decreasing the tube diameter. It is very interesting to see the different heat transfer behaviors and mechanisms affected by the tube diameters. For both 3.1 mm and 1.12 mm diameter tubes, the heat transfer behaviors exhibits the heat transfer behaviors and mechanisms in macroscale channels. However, for the 0.51 mm diameter test tube, the flow boiling heat transfer behaviors and mechanisms have changed signifcantly. As mentioned in fore-going, the distinction between macroscale and microscale channels may be classified according to the flow boiling heat transfer behaviours or mechanisms rather than fixed diameters. This study is a good example to distinct the macrosclae and microscale channels according to the heat transfer mechanisms but further systematic studies are needed to well document the criteria for such a distinction.

It should be mentioned that the experimental data from the different independent studies show somewhat different heat transfer trends at similar test conditions. This may be caused by the channel size, working fluids, heat methods or measurement accuracy etc. Just to show two examples here, Figure 15 shows comparison of the experimental data of flow boiling heat transfer coefficient with CO_2 by Yun et al. [100] for two diameters of 1.53 and 1.54 at the same

test conditions. According to their results, heat transfer coefficients can be higher up to 80% with a very little change of hydraulic diameter from 1.53 mm to 1.54 mm at the same test conditions. No explanation why there is such a big difference even was offered in their paper. Figure 16 shows the comparison of the CO_2 flow boiling heat transfer coefficients of Pettersen [101] with those of Koyama et al. [102] in microscale channels. The biggest difference between them is that in Koyama et al. the heat flux is 32.06 kW/m^2 while in Pettersen it is 10 kW/m^2. The heat transfer coefficients fall off at a vapour quality of about 0.7 in the study of Pettersen while the heat transfer coefficients increase even at qualities larger than 0.7 in the study of Koyama et al. It is difficult to explain why the heat transfer coefficients fall off at the lower heat flux in one study while they still increase at the higher heat flux in the other study. This could be an effect of the heating methods or because of multi-channel vs. single channel test setups. It should be mentioned that well design test system, proper measurement techniques and data reduction methods should carefully considered when conducting experiments. Furthermore, careful analysis of the experimental results against heat transfer mechanisms are also needed.

Harirchian and Garimella [65] conducted experiments of flow boiling with FC-77 in multiple rectangular microscale channel heat sinks. They analysed the effect of the mass flow rate and the channel size on the flow boiling heat transfer characteristics in microscale channels with a constant channel depth of 400 µm and different channel widths ranging from 100 µm to 5850 µm. The mass fluxes ranged from 250 to 1600 kg/ m^{2}s in their tests. Figure 17 shows the mass flux effect on the flow boiling heat transfer characteristics. It can be seen that the heat transfer coefficient increases with increasing the mass flux in the single-phase regime. The heat transfer coefficient becomes independent of mass flux and increases with increasing the heat flux in the boiling region. At higher heat fluxes, the convective boiling is the dominant heat transfer

mechanism, therefore, the heat transfer coefficient increases with increasing the mass flux. From the flow visualizations performed in their study, the suppression phenomena of the bubble nucleation in the microscale channels were observed. This has confirmed the convective boiling dominant heat transfer mechanism which is related to the measured heat transfer characteristics. The experimental results and observations are in consistence with those obtained by Chen and Garimella [77]. With further increasing high heat fluxes, the heat transfer coefficient starts to decrease due to the incipience of dryout in the microscale channels. The partial dryout phenomena on the channel wall has been has confirmed through flow visualization and been explained by Chen and Garimella [77]. Figure 17 shows the effects of microscale channel width on the local heat transfer coefficient as a function of (a) wall heat flux and (b) base heat flux. It is obvious that the heat transfer coefficient is independent of microscale channel width for channels of width 400 µm and larger than 400 µm. Even for the microscale channel width less than 400 µm, the heat transfer coefficient has little dependence on the channel size. For example, for the channel width of 250 µm, the heat transfer coefficients are slightly less than those for the larger channel widths for any wall heat flux as shown in Fig. 17(a). However, for the microscale channel width of 100 µm, the flow boiling heat transfer characteristics are significantly different. The heat transfer coefficients are relatively higher at lower heat fluxes. With increasing the heat flux, the boiling heat transfer curve crosses over and the heat transfer coefficients are is less than those of the larger microscale channel widths. This is mainly due to higher vapor quality at the exit of the microscale channels with the width of the 100 µm and the corresponding flow regime is annular flow. Therefore, the heat transfer coefficients are larger at lower heat fluxes. As shown in Fig. 17 (a), when the width of the microscale channels is larger than 400 µm for a constant channel depth, there is no effect on the heat transfer coefficient at a constant wall heat flux. Fig.

17 (b) shows the variation of the heat transfer coefficient with the base heat flux for different microscale channel widths. At a constant heat flux in the microscale channel heat sink, the heat transfer coefficient increases with increasing the microscale channels width.

Qu and Mudawar [60] conducted experimental study of flow boiling in a water-cooled microscale channel heat sink. Their heat sink was made on a copper substrate and contained 21 parallel channels, each having a 231×713 μm^2 rectangular cross-section. The inlet Reynolds number ranged from 60 to 300. The inlet temperature was maintained constant at either 30^{o}C or 60^{o}C by appropriately adjusting the mass flux and heat flux, in the range of 135-402 kg/m^{2}s and 20-135 W/cm^2, respectively. Their measured saturated flow boiling heat transfer coefficients were measured at two inlet temperatures of 30^{o}C and 60^{o}C. The heat transfer coefficient are be in the range of 22-44 kW/m^{2}K. It seems that the inlet temperature has some effect on the heat transfer coefficient but the knowledge in this aspect is very little in the literature. Contrary to behaviour observed in macroscale channels, the heat transfer coefficient decreased with increasing vapour quality. They attributed the unexpected heat transfer trends to appreciable droplet entrainment at the onset of the annular flow regime. Similar dependence of heat transfer coefficient on vapour quality was reported by Hetsroni et al. [82] for flow boiling of Vertrel XF in a heat sink that had 21 parallel triangular microscale channels each of hydraulic diameter 129 μm. Yen et al. [81] studied flow boiling of water and refrigerant HCFC123 and FC72 in microscale channels respectively. They also observed that the heat transfer coefficient decreases with an increase in vapour quality, in agreement with the results of Qu and Mudawar [60] and Hetsroni et al. [82].

More recently, Charnay et al. [83] conducted experimental study on flow boiling in a 3 mm diameter horizontal circular tube. They investigated the effect of heat flux on the heat transfer

coefficients at mass velocity of 700 kg/m^{2}s and two different saturation temperatures (60 and 80 ^{o}C). At 60 ^{o}C, the heat transfer coefficients are strongly affected by the heat fluxes at low vapour qualities where the flow regime is intermittent flow. The heat flux heat transfer coefficient curves at low and high heat fluxes converge at high vapour qualities where the flow regime is annular flow. At 80 ^{o}C, the heat flux strongly affects the heat transfer coefficients at all vapour qualities before the incipience of dryout. The heat transfer coefficient increases with increasing the vapour quality in annular flow. This is attributed to the enhanced contribution of convective boiling heat transfer with increasing the vapour quality. Considering the heat transfer mechanisms, nucleate boiling is dominant in the intermittent flow regime while nucleate and convective boiling are important in the annular flow regime. They also investigated the mass flux effect on the heat transfer coefficients. Two different trends have been identified as distinguished: the higher the mass velocity, the larger the heat transfer coefficient for 60 ^{o}C and the higher the mass flux, the smaller the heat transfer coefficient at lower vapor qualities while the higher the mass velocity, the larger the heat transfer coefficient at higher vapor qualities 80 ^{o}C. They have found that the heat transfer coefficients are independent of the vapor qualities in the intermittent flow regime and the mass flux effect is less important because the nucleate boiling is the dominant heat transfer mechanism. In the annular flow regime, the heat transfer coefficient increases with increasing the vapor quality except for a mass velocity of 300 kg/m^2 s where the heat transfer coefficient is almost constant over the whole range of vapor quality. Convective boiling is the dominant heat transfer mechanism in this region. At large mass fluxes, the smaller bubbles tend to coalesce to form bigger bubbles. Thus, the bubbles frequency reduction could be used to explain the results.

As mentioned in the fore-going, it is very important to relate the flow regimes and bubble dynamics to the heat transfer coefficient behaviours because they are intrinsically related each other. In particular, for microscale channel, well designed test facility and accurate measurement system are essential for accurate experimental heat transfer coefficient data. The different heat transfer trends may be explained by their respective heat transfer mechanisms and they may also due to many other affecting factors such as the measurement accuracy, channel size and shape, fluid types and physical properties, the test parameter ranges, the data analysis and presentations etc. Different heating methods such as fluid heating and electrical heating, measurement methods and different data reduction methods could results in quite big contradictory results. For instance, local and average heat transfer coefficients may be quite different, depending on how the wall and local saturation temperatures are determined. Furthermore, careful energy balance and validation of the measurement system should be done before performing the flow boiling experiments. Experimental results from the literature can hardly be compared against one or another since there is no accepted benchmark. Furthermore, The issue of the dominant heat transfer mechanisms is not well explored and explained according to the experimental data. In other words, researchers are in somewhat of a 'dilemma' to conclude which is the dominant heat transfer mechanism in their studies as sometimes their proposed heat transfer mechanisms actually do not describe their heat transfer coefficient trends properly.

There is still a debate about the possible governing heat transfer mechanism for microchannel flow boiling, i.e. nucleate boiling dominant or forced convective boiling dominant. Generally, in the nucleate boiling dominant region, the heat transfer coefficient is mainly a function of heat flux and system pressure but is less independent of vapour quality and mass flux. In convective boiling dominant region the heat transfer coefficient largely depends on

vapour quality and mass flux but is not a function of heat flux. On this basis, many researchers have addressed their experimental flow boiling results in microchannel as governed by the nucleate boiling or the convective boiling mechanism, depending on the heat transfer coefficient trend as a function of thermal-hydraulic parameters only. In fact, the current research results are quite diverse. Some anomaly heat transfer trends cannot be explained according to the relevant heat transfer mechanisms as described in the foregoing. For flow boiling in microscale channels, understanding the fundamental heat transfer mechanisms should be relevant to the relevant flow regimes and bubble dynamics in microscale channels, considering the channel size effect on the bubble growth and flow patterns [84-85]. Unfortunately, in most available publications, the flow patterns and flow boiling heat transfer behaviours have been separately investigated. In fact, the flow regimes and heat transfer behaviours are intrinsically related to each other. Both the flow regimes, bubble behaviours and heat transfer should be observed and measured simultaneously in experiments for a better understanding the microchannel flow boiling phenomena and mechanisms. Furthermore, mechanistic prediction methods based on flow regimes and bubble behaviours are needed. There are already several such studies available. For another example, Jacob and Thome [86], Thome et al. [87] and Dupont et al. [88] proposed a evaporation heat transfer model based on elongated bubble flow in microscale channels, with the hypothesis that thin film evaporation is the dominant heat transfer mechanism as opposed to prior interpretations that conventional macroscale nucleate boiling dominance. Their assumption is that microscale flow is reached when the bubble growth diameter reaches the tube internal diameter followed by subsequent detachment from the wall surface. In their heat transfer model, the critical bubble radius is evaluated using the effective nucleation wall superheat. Furthermore, Consolini and Thome [106] and Thome and Cioncolini [107] have recently developed new mechanistic heat

transfer model for annular flow covering both macro- and micro-channels and a flow pattern based flow boiling model for microchannel combining with the three zone model and the annular flow model. This model covers more flow regimes of elongated bubbles and annular flows which are dominant flow regimes in microchannel. Both models have been evaluated with the database in this review. It shows very promising results with the flow pattern based heat transfer model. However, systematic knowledge in this aspect has not yet completely achieved by relating heat transfer model, mechanism and flow patterns due to the effects of fluid types, channel sizes, test conditions and unstable flow boiling in microscale channels. Especially, generalised flow regime transition criteria are needed for developing/improving the heat transfer prediction using mechanistic methods. Therefore, effort should be made to advance well documented knowledge in microchannel flow boiling heat transfer and the heat transfer mechanisms governing the flow boiling processes through well designed experiments on both flow boiling and flow patterns but considering the channel size effect on them in future.

In summary, from the available studies on microscale flow boiling, flow boiling heat transfer mechanisms have been classified by into four different categories: (i) Nucleate boiling dominant because the heat transfer data are heat flux dependent ; (ii) Convective boiling dominant when the heat transfer coefficient depends on mass flux and vapour quality but not heat flux ; (iii) Both nucleate and convective boiling dominant, and (iv) Thin film evaporation of the liquid film around elongated bubble flows as the dominant heat transfer mechanism, which is heat flux dependent via bubble frequency and conduction across the film. (v) Annular flow model for flow boiling in microchannel.

4. Review and evaluation of models and correlations of flow boiling heat transfer in microscale channels

4.1. Classification of flow boiling heat transfer models and correlations

There are a large number of correlations and models available in the literature for flow boiling of saturated liquids in conventional channels. A number of researchers have developed correlations or models for microchannel flow boiling on the basis of these for macroscale channel flow boiling. Most of these consider the contribution of two flow boiling heat transfer mechanisms: nucleate boiling dominant and convective boiling dominant. The heat transfer coefficient correlations can generally be divided into three groups: (i) The summation correlations: The heat transfer coefficient is considered to be the addition of the nucleate and convective boiling contribution such as the Chen correlation [40]:

$$h_{tp} = Eh_l + Sh_{pool} \tag{5}$$

where the liquid phase heat transfer coefficient h_l is and the pool boiling heat transfer coefficient h_{pool}. S is the nucleate boiling suppression factor The convective enhancement factor, E,. (ii) The asymptotic model: The heat transfer coefficient is assumed as one of the two mechanisms to be dominant such as the Steiner and Taborek model [45]:

$$h_{tp} = \left(h_l + h_{pool}\right)^{\frac{1}{n}} \tag{6}$$

where n >1, the heat transfer coefficient h_{tp} asymptotically approaches to the nucleate boiling heat transfer h_{pool} or convective boiling heat transfer h_l. (iii) The flow pattern based model: This

model consists of a flow pattern map and flow pattern specific models and correlation for the heat transfer such as the prediction methods by Kattan et al. [46], Wojtan et al. [32, 32], Cheng et al. [24-26] and Moreno Quibén et al. [35, 36] which are based on the asymptotic model and the relevant flow patterns, the mechanistic heat transfer models for flow boiling heat transfer in microscale channels such as the three zone heat transfer model for flow boiling in microchannels by Thome et al. [87, 88] and annular flow heat transfer model developed by Cioncolini and Thome [106] and Thome and Cioncolini [107].

4.2. Evaluation of correlations and models for flow boiling heat transfer in microscale channels

Over the past years, a number of correlations and models have been developed for microchannel flow boiling heat transfer. These heat transfer prediction methods are either by modifying the Chen correlation [40] or correlating their own experimental data according to dimensionless numbers by a number of researchers. It should be pointed out that may correlations are only based on limited test fluids and conditions. Although various flow boiling heat transfer mechanisms have been proposed in different studies, their corresponding flow patterns and bubble evolution processes have not been observed by using flow visualization technology. Furthermore, these correlations actually based on the two heat transfer mechanisms for conventional channels do not really represent the very complex heat transfer mechanisms in microchannel flow boiling, which have not yet been well understood. Therefore, these correlations can only work for some specific fluids and conditions. In some cases, they cannot predict the heat transfer properly and even give wrong predictions. This is mainly due to the lack of understanding of the physical mechanisms, the limited applicable parameter ranges and

inaccurate measured heat transfer data or wrong heat transfer data caused by the unreasonable test facility, measurement system and improper data reduction methods etc. Table 2 summarizes the selected flow boiling heat transfer models and correlations in microscale channels.

To evaluate these models and correlations for flow boiling heat transfer in micro-scale channels shown, a database has been established by collecting experimental data from the selected studies in the literature. A heat transfer database including 2336 data points extracted from the selected 11 published papers has been compiled from the studies listed in Table 3. Table 4 summarizes the test fluids and parameter ranges of the database. The database covers a wide range of test fluids and experimental parameter ranges: 8 test fluids including R410A, R141b, R134a, R245fa, R12, R123, R22 and N_2, tube diameter: 0.19 - 3.69 mm, mass flux: 20 - 1471.2 kg/m^{2}s, heat flux: 5 – 150 kW/m^2 and both horizontal and vertical arrangements. The database was compared to the 12 flow boiling heat transfer correlation including the correlations of Chen [40], Gungor and Winterton [41] and Liu and Winterton [42] for conventional channels and nine selected models and correlations for microscale channels in Table 1. The statistical analysis is based on relative error ξ_i (the percentage of predicted points within ±30%):

$$\xi_i = \frac{\text{Predicted} - \text{Measured}}{\text{Measured}} \tag{16}$$

Table 5 shows the statistical analysis of the predicted results with the selected flow boiling correlations for each individual fluid and all fluids using the relative error ξ_i within ±30%. The two best correlations for each fluid are in highlighted in table 5. According to the proportions of data falling within the ranges of $\pm 30\%$ error band, comparative results of the two best correlations for each fluid are shown in Figs. 18 to 25. Overall, the Saitoh et al. [61] and the Li

and Wu [58] correlations provide better predictions than other correlations for the whole database. However, the Saitoh et al. correlation only predicted 54.9% of the whole database, and the Li and Wu correlation only predicts 56.7% of the whole database. Although some correlations may work well for certain fluids, e.g. the Saitoh et al. correlation predicts well the R12, R22 and R141b data, they do not work for other fluids while the Saitoh et al. correlation only predicts 3.1% of R410A data. It is interesting that the Chen correlation predicts well the R245fa data better than all other correlations except that the Li and Wu correlation poorly predicted the data. This might be by chance to capture the data for that fluid, or some other reasons such as the R245fa flow boiling might be still in macro-scale channels. It should be realised that the database for developing the Li and Wu correlation concludes R245fa data. The reason why their correlation does not work well for the R245fa data is unclear.

In general, the heat transfer correlations for flow boiling conventional channels do not work for microscale channel flow boiling. It can be concluded that no models and correlations can satisfactorily predict all the experimental data for the tested 8 fluids in the database. It is impossible to reach a conclusion from the comparisons due to the big discrepancies among the experimental data from different researches. Furthermore, another reason is due to the flow boiling mechanisms in micro channels. In fact, simply modifying the heat transfer correlation for conventional channels does not representing the actual heat transfer mechanisms governing the microchannel flow boiling phenomena. Simply referring to the two different heat transfer mechanisms for microscale channel flow boiling, which can in fact simultaneously occur in microscale channels, does not properly representing the actual mechanisms in microscale channels. Furthermore, quite a large number of experiments were conducted in the presence of two phase flow instabilities, which may drastically affect the heat transfer trends. Moreover,

erroneous data regression procedure is frequently adopted to develop a new correlation. Inherent difficulties verified in conventional flow boiling heat transfer measurements are incremented in the case of microscale channels due to the reduced scales involved. The different data reduction methods may be another big factor which affects the experimental results significantly, and thus further affects the prediction method developed based on these data.

4.3. Evaluation the three-zone heat transfer model and the flow pattern based heat transfer model for flow boiling in microscale channels

Several flow pattern-based mechanistic models for two phase flow and heat transfer in microscale channels have been developed over the past decades [87, 105-107]. In particular, various new mechanistic models for flow boiling in microscale channels such as three zone heat transfer model for elongated bubbles in microchannels by Thome et al. [87, 88], recent updated version of three zone model by Costa-Patry and Thome [105] and annular flow heat transfer models covering both macro- and microchannel by Cioncolini and Thome [106] and Thome and Cioncolini [107]. The three-zone heat transfer models and a flow pattern based heat transfer model the three zone model and the annular flow model were evaluated with the database. According to the comparative results, some analysis and future research needs are addressed.

Figure 26 shows the diagram illustrating the three zones: a liquid slug, an elongated bubble and a vapour slug. They proposed this flow boiling heat transfer model, which predicts the local dynamic and the local time-averaged heat transfer coefficient at fixed locations along the channel based on the evaporation of elongated bubbles. As shown in Fig. 26, following the passage of a liquid slug, a bubble is modelled to pass as a confined elongated bubble trapping a thin liquid film against the inner wall. If the liquid film does dry out before the arrival of the next

liquid slug then a vapour slug follows (triplet). If not, then the model assumes the existence of a pair consisting of the liquid slug and the elongated bubble. Therefore, one of the novelties of the model is the fact that it considers a dryout zone and exploits the transient evaporation of the film. The model determines the time-averaged local heat transfer coefficient as follows:

$$h(z) = \frac{t_l}{\tau} h_l(z) + \frac{t_{film}}{\tau} h_{film}(z) + \frac{t_{dry}}{\tau} h_v(z) \tag{17}$$

where $h_l(z)$ and $h_v(z)$ are heat transfer coefficients of the liquid and vapour slugs. They are calculated from their local Nusselt numbers using the respective equivalent lengths of the liquid slug, L_l and dry wall zone L_{dry} as in Fig. 26. The London and Shah correlation for laminar developing flow and the Gnielinski correlation for transition and turbulent developing flow [108]. The mean heat transfer coefficient through the evaporating thin liquid film surrounding the elongated bubble $h_{film}(z)$ is calculated as follows:

$$h_{film}(z) = \frac{k_l}{\delta_0 - \delta_{end}} \ln\left(\frac{\delta_0}{\delta_{end}}\right) \tag{18}$$

$$\delta(z,t) = \delta_0(z) - \frac{q}{\rho_l h_{lv}} t \tag{18a}$$

$$\frac{\delta_0}{d} = C_{\delta_0} \left(\frac{\mu_l}{V_p d}\right)^{0.28} \left[\left(0.07 Bd^{0.41}\right)^{-8} + 0.1^{-8}\right]^{-\frac{1}{8}} \tag{18b}$$

$$V_p = g\left(\frac{x}{\rho_v} + \frac{1-x}{\rho_l}\right) \tag{18c}$$

$$Bd = \frac{\rho_l d}{\sigma} V_p^2 \tag{18d}$$

where t_l is the time for the liquid slug pass a fixed location z , t_{film} is the residence time of the film and t_{dry} is the duration of the local wall dryout, which are calculated as follows:

$$t_l = \frac{\tau}{1 + \frac{\rho_l}{\rho_v}\left(\frac{x}{1-x}\right)} \tag{19}$$

$$t_v = \frac{\tau}{1 + \frac{\rho_v}{\rho_l}\left(\frac{1-x}{x}\right)} \tag{20}$$

$$t_{dry,\,film}(z) = \frac{\rho_l h_{lv}}{q}\left[\delta_0(z) - \delta_{min}\right] \tag{21}$$

$$\delta_{min} = 0.3\ \mu m \tag{21a}$$

$$f = \frac{1}{\tau} = \left(\frac{q}{q_{ref}}\right)^{1.74} \tag{22}$$

where the reference heat flux is a function of the reduced pressure:

$$q_{ref} = 3328\left(\frac{p_{sat}}{p_{crit}}\right)^{1.74} \tag{22a}$$

It should be mentioned here that Costa-Patry and Thome [105] have presented a new flow pattern-based prediction methods in microchannel based on their experimental results and apply an updated three-zone flow boiling model for elongated bubbles for several multimicrochannel

evaporators in silicon and copper and for single-microchannel tubes in stainless steel. They have found the dryout thickness is well represented by setting it equal to the measured channel roughness for the silicon, copper and stainless steel test surfaces in the updated three-zone flow boiling model for elongated bubbles. They have reported that their method predicts the results quite accurately and also captures the trends in the heat transfer coefficients well. Furthermore, they use the Reynolds number of 1500 to distinguish the laminar and turbulent flow and apply different heat transfer correlations for laminar and turbulent flows. However, according to our comparisons of the updated model to the database, it does not show significant different from the original three zone model. The main reason that that heat transfer in the liquid film is the dominated heat transfer mechanism according to the model. In our database, the surface roughness is not known. It is recommended to use the updated three zone model if surface roughness is known.

Cioncolini and Thome [106] proposed a heat transfer model for convective evaporation in annular flow in the absence of wall nucleation and proposed a new algebraic turbulence model for the transport of linear momentum and heat through the annular liquid film. Figure 27 shows their physical model of annular flow. Thome and Cioncolin [107] have recently presented a unified modeling suite for annular flow for two phase flow, convective boiling and condensation in macro- and micro-channels. The annular flow suite currently includes models to predict the void fraction, the entrained liquid fraction, and the wall shear stress and pressure gradient, and a turbulence model for momentum and heat transport inside the annular liquid film. The turbulence model, in particular, allows prediction of the local average liquid film thicknesses and the local heat transfer coefficients during convective evaporation and condensation. Their heat transfer model for microchannels is as follows:

$$\mathrm{Nu} = \frac{\mathrm{h}\delta_{\mathrm{film}}}{\mathrm{k_l}} = 0.0776\left(\delta^*\right)^{0.9}\ \mathrm{Pr_l}^{0.52} \tag{23}$$

$$\delta^* = \frac{\delta}{\mathrm{y}^*} = \frac{\rho_\mathrm{l}\mathrm{V}^*\delta}{\mu_\mathrm{l}} \tag{23a}$$

$$\mathrm{y}^* = \frac{\mu_\mathrm{l}}{\rho_\mathrm{l}\mathrm{V}^*} \tag{23b}$$

$$\mathrm{V}^* = \sqrt{\frac{\tau_\mathrm{w}}{\rho_\mathrm{l}}} \tag{23c}$$

$$\delta^* = \max\left(\sqrt{0.5\,\mathrm{Re_{lf}}}, 0.0165\,\mathrm{Re_{lf}}\right) \tag{23d}$$

$$\mathrm{Re_{lf}} = (1-\mathrm{e})(1-\mathrm{x})\frac{\mathrm{Gd}}{\mu_\mathrm{l}} \tag{23e}$$

$$\mathrm{f_{tp}} = \frac{2\tau_\mathrm{w}}{\rho_\mathrm{c}\mathrm{V_c}^2} = 0.0196\mathrm{We_c}^{-0.372}\,\mathrm{Re_{lf}}^{0.318} \qquad \text{for Bd} \le 4 \text{ (microchannel)} \tag{24}$$

$$\rho_\mathrm{c} = \frac{\mathrm{x} + \mathrm{e}(1-\mathrm{x})}{\frac{\mathrm{x}}{\rho_\mathrm{v}} + \frac{\mathrm{e}(1-\mathrm{x})}{\rho_\mathrm{l}}} \tag{24a}$$

$$\mathrm{J_v} = \frac{\mathrm{xG}}{\rho_\mathrm{v}} \tag{24b}$$

$$\mathrm{V_c} = \frac{\mathrm{J_v}}{\varepsilon} = \frac{\mathrm{xG}}{\varepsilon\rho_\mathrm{v}} \tag{24c}$$

$$We_c = \frac{\rho_c J_v^{\,2} d}{\sigma} \tag{24d}$$

$$Bd = \frac{g(\rho_l - \rho_v)d^2}{\sigma} \tag{24e}$$

$$e = \left(1 + 279.6 We_c^{\,-0.8395}\right)^{-2.209} \qquad \text{for } 10 < We_c < 10^5 \tag{25}$$

$$\varepsilon = \frac{m x^n}{1 + (m-1)x^n} \tag{26}$$

$$m = -2.129 + 3.129\left(\frac{\rho_v}{\rho_l}\right)^{-0.2186} \tag{27a}$$

$$n = 0.3487 + 0.6513\left(\frac{\rho_v}{\rho_l}\right)^{0.515} \tag{27b}$$

Costa-Patry and Thome [105] presented a new flow pattern-based prediction methods in microchannel based on their experimental results and apply an updated three-zone flow boiling model for elongated bubbles and the Cioncoilin-Thome unified annular flow model for convective boiling [106, 107]. The two methods are jointed together into a flow pattern-based method using a new heat flux-dependent flow pattern transition criterion between slug flow and annular flow as follows:

$$x_{CB-AF} = 425\left(\frac{\rho_v}{\rho_l}\right)^{0.1} \frac{Bo^{1.1}}{Co^{0.5}} \tag{28}$$

It should be pointed out that Eq. (28) is only based on several fluids and their test conditions. When applying to other fluids and test conditions, it does not always give proper transition from slug flow to annular flow. In this case, heat transfer behaviour together with corresponding void fraction (> 0.5) is used to distinguish the transition for the slug and annular flows. From below comparison, it works reasonably but it is suggested that further development of a generalised transition criterion for a wide range of fluids and test conditions be conducted in future.

Table 6 shows the statistical analysis of the predicted results with the selected flow boiling correlations for each individual fluid using the relative error ξ_i within ±30%. It can be seen that the three zone model predicts 48.3% of the R134a data within ±30%, 48.7% of R22 data within ±30% and 43.6% of the R141b data within ±30% while for others fluids it does not work well. In the comparisons, it should be realized that the three zone model only predicts 67% of their original database including R11, R12, R113, R123, R134a, R141b and CO_2 [88]. Thus, the predictions for the independent data are quite reasonably. Predictions for some fluids are poor due to these fluids were not in their original database. Furthermore, the model does not cover some test conditions such as heat flux, saturation temperatures and channel sizes. Considering R134a data, the model works very well for some data while it does not predict other data at all. Here just show one example, the model predicts 90.4% of the 365 data points of R134a by Wang et al. [64] within ±30% as shown in Fig. 28. It does not predict the data points of R134a by In and Jeong [63] at all. This may be caused due to the flow pattern difference and also other test parameter ranges. Eqs. (21a), (22) and (22a) actually depend on the database and test conditions. To apply the three zone model to other fluids and conditions, these equations should be modified. It should also be realized that the three zone model sometimes does not capture the

parametric trends of the experimental data and the effect of diameter as shown in Fig. 34 (The diameter effect does not show the increase of heat transfer coefficient with decreasing the channel diameter). Therefore, it is suggested to update the three zone model according the elongated flows only according to relevant flow maps for microchannels and the corresponding heat transfer mechanisms.

Adopting flow pattern based heat transfer model combining the three zone model and the annular flow model together with the corresponding flow patterns gives much better results than the three zone model alone. It can been seen as in Table 6 that the flow pattern based model predicts 69.1% of the R134 data ±30%, 76.3% of the R22 data within ±30%. 68.4% of the R245fa data within ±30%, 66.7% of the R141b data within ±30% and 64.3% of R123 data within ±30%. Figure 29 (a), (b) and (c) shows the comparative results for all data points of R134a, R234fa and R22 respectively. For N_2 and R12, the predictions are much improved as compared to those predicted by the three zone model alone. Overall the flow pattern based heat transfer model predicts 54.4% of the whole database which among the three best prediction methods used in this paper. Furthermore, the model captures the heat transfer trends as shown in Fig. 30 (a), (b), (c) and (d) for R22, R123, R134 and R234fa at the indicated test conditions respectively. It can be seen that the model works well for a wide range of tube diameters from 0.19 mm to 3 mm as in Fig. 30 (a)-(c). As already mentioned in afore-going, the three-zone model does not always capture the heat transfer trends, therefore, this may affect the predictions when combined with the annular flow model. It is also important to consider the nucleate boiling effect at very low vapor quality range as indicated in Fig. 30 (a) and (b) although this region is very narrow. However it will help to understand the heat transfer mechanisms as the heat flux effect becomes significant in this low vapor quality region. All other flow regimes are evolved from the tiny

bubble generation and their growth due to the added heat flux and nucleate boiling process. Therefore, further improvement of the combined model is needed including updating the three zone model for a wide range of parameters such as mass flux, heat flux and saturation temperature, test fluids, channel sizes and proposing new transition criterion for the slug to annular flow regime.

4.4. Flow pattern based phenomenological models for flow boiling heat transfer covering both macroscale and microscale channels

Cheng et al. [24-26] modified the flow pattern based heat transfer model of Wojtan et al. [31, 32] to CO_2 flow boiling covering both macroscale and microscale channels. The modofied model of Cheng et al. predicted the microscale flow boiling heat transfer of CO_2 reasonably well and it relates the heat transfer mechanisms and behaviours to the corresponding flow regimes. In their model, the Kattan-Thome-Favrat [46] general equation for the local flow boiling heat transfer coefficients h_{tp} in a horizontal tube is used as the basic flow boiling expression:

$$h_{tp} = \frac{\theta_{dry} h_V + \left(2\pi - \theta_{dry}\right) h_{wet}}{2\pi} \tag{17}$$

where θ_{dry} is the dry angle defined in Fig. 31. The dry angle θ_{dry} defines the flow structures and the ratio of the tube perimeter in contact with liquid and vapour. h_v and h_{wet} are the heat transfer coefficients for vapour phase and liquid phase respectively. The details of the model and flow map may be found in [24-26]. The main two modifications are: (i) The nucleate boiling heat

transfer coefficient h_{nb} is calculated with the Cheng et al. [24-26] nucleate boiling correlation for CO_2:

$$h_{nb} = 131 p_r^{-0.0063} \left(-\log_{10} p_r\right)^{-0.55} M^{-0.5} q^{0.58} \tag{18}$$

(ii) The Cheng et al. nucleate boiling heat transfer suppression factor S for CO_2 is applied to reduce the nucleate boiling heat transfer contribution due to the thinning of the annular liquid film:

$$\text{If } x < x_{IA},\ S = 1 \tag{19}$$

$$\text{If } x \geq x_{IA},\ S = 1 - 1.14\left(\frac{D_{eq}}{0.00753}\right)^2\left(1 - \frac{\delta}{\delta_{IA}}\right)^{2.2} \tag{20}$$

Furthermore, if $D_{eq} > 7.53$ mm, then set $D_{eq} = 7.53$ mm.

The updated general CO_2 flow boiling heat transfer model by Cheng et al. was compared to an extensive database [25, 26]. Just to show one example here, Figure 32(a) shows the comparison of the predicted flow boiling heat transfer coefficients to the experimental data of Yun et al. [100] and figure 27(b) shows the corresponding flow pattern map. The updated general flow boiling heat transfer model not only captures the heat transfer trends well but also predicts the experimental heat transfer data satisfactorily.

Figure 33 shows simulation of the updated flow pattern map and flow boiling model for CO_2 at the indicated conditions, superimposed on the same graphs by Cheng et al. [104]. The process path for the vapor quality variation from 0.01 to 0.99 is shown as the horizontal broken line (dash-dot line) while the variation in the heat transfer coefficient as it changes vapor quality and flow pattern is depicted by the dashed line. The flow pattern boundaries are in solid lines. The line (dash line with arrows) indicates the calculated heat transfer coefficient at the indicated mass

velocity and vapor quality. Notice the various changes in trends in the heat transfer coefficient as this occurs. For example, when the flow regime passes from annular flow into the dryout regime, there is a sharp inflection in the heat transfer coefficient as the top perimeter of the tube becomes dry. As pointed out in the fore-going, relating heat transfer behaviors to the corresponding flow regimes may be a better way to understand the flow boiling mechanisms and to develop new prediction models for heat transfer. As already mentioned in section 4.3, the mechanistic heat transfer models for both elongated bubbles and annular flow regime for microchannels have shown reasonable good predictions for the database collecting from the literature. This is very encouraging and promising. Further development of generalized heat transfer models is recommended to improve the prediction accuracy.

4.5. Models of flow boiling heat transfer for specific flow regimes in microscale channels

Analytical models for flow boiling heat transfer based on specific flow patterns such as elongated bubbles, bubbly flow and annular flow regimes etc. are needed in understanding the theoretical basis of the flow boiling heat transfer but such models are still needed to be developed so far.

There are several such models for elongated bubble flow and annular flow in the literature [86-88, 95-98]. As already mentioned in the foregoing, Thome et al. [87] developed a micro-scale model that describes the heat transfer processes during the cyclic passage of elongated bubbles in a micro-scale channel. In this model, bubbles are assumed to nucleate and quickly grow to the channel size upstream such that successive elongated bubbles are formed that are confined radially by the tube wall and grow in length, trapping a thin film of liquid between the bubble and the inner tube wall. The thickness of this film plays an important role in heat transfer.

As shown in Fig. 26, at a fixed location, the process proceeds as follows: (i) a liquid slug passes (without any entrained vapor bubbles, contrary to macroscale flows), (ii) an elongated bubble passes (whose liquid film is formed from liquid removed from the liquid slug), and (iii) if the thin evaporating film of the bubble dries out before the arrival of the next liquid slug, then a vapour slug passes. A time-averaged local heat transfer coefficient is obtained during the cyclic passage. Dupont et al. [88] compared the time averaged local heat transfer coefficient to the experimental data taken from seven independent studies covering seven fluids including R-11, R-12, R-113, R-123, R-134a, R-141b and CO_2, covering tube diameters from 0.77 to 3.1 mm, mass velocities from 50 to 564 kg/m^{2}s, saturation pressures from 124 to 5766 kPa, heat fluxes from 5 to 178 kW/m^2, and vapour qualities from 0.01 to 0.99. Their new three zone model predicts 67% of the database to within ±30%. The new model illustrates the importance of the strong cyclic variation in the heat transfer coefficient and the strong dependency of heat transfer on the bubble frequency, the minimum liquid film thickness at dryout and the liquid film formation thickness. It should be mentioned here that quite different flow patterns such as bubbly flow, intermittent flow and annular flow etc. may be relevant to their database. Only based on elongated bubble flow considering the liquid film heat transfer does not really represent the actual mechanisms in the database. In fact, their heat transfer model predicted an increase in heat transfer coefficient with a decrease in diameter for low values of vapour quality and a decrease in heat transfer coefficient for large vapour qualities as shown in Fig. 34. This may be the reason why their model predicts 67% of the database, which is actually quite low. Furthermore, it only captures part of the heat transfer mechanisms for the cases in their study. However, this is a very good starting point to develop theoretical model for microchannel flow boiling. Their model includes a simplified description of the dynamics of the formation and flow of the liquid film and the thin

film evaporation process, taking into account the added mass transfer by breakup of the bridging liquid slugs. Their new model has been confronted against experimental data taken within the coalescing bubble flow mode that have been identified by a diabatic microscale flow pattern map [94]. The comparisons for three different fluids (R-134a, R-236fa and R-245fa) gave encouraging results with 83% of the database predicted within a ±30% error band. Furthermore, they have found that their new model is able to predict a ‘‘nucleate boiling curve” with an exponent of 0.74 typical of numerous micro-channel flow boiling studies, thus suggesting film evaporation as the controlling heat transfer mechanism rather than nucleate boiling. They suggested film evaporation as the controlling heat transfer mechanism rather than nucleate boiling in microchannel flow boiling. However, the experimental data have shown quite complex heat transfer mechanisms. Furthermore, accurate flow pattern map for microchannel flow boiling is needed to use their model. It is actually a big challenge as no universal flow pattern maps are available to predict the flow patterns as pointed out by Cheng et al. [11].

Annular flow is a common flow pattern observed in microscale channel flow boiling. Analytical model for annular flow may be developed from the mass, momentum and energy conservation with the aid of some assumptions and empirical correlations for wall and interfacial shear stress and droplets entrainment and deposition rates such as the study by Cheng [96]. Similarly, annular flow models for microchannel flow boiling have also been investigated by Qu and Mudawar [97] and Kim and Midawaer [98]. These models have some theoretical basis. However, in order to validate these models, a well-documented universal flow pattern map is needed to segment the heat transfer data but a generalized flow pattern map is not yet available [11, 37].

Analytical models for flow boiling in microscale channels are very complex, and the required assumptions to solve these models restrict the ability to capture the real physics of boiling mechanisms. Also, most empirical correlations are not able to predict other experimental data, even under a similar range of operating conditions where the correlations were obtained. The complex nature of flow boiling in microscale channels such as liquid-vapour interactions, bubble growth in the flow as well as in the thin liquid film make analytical or empirical models of the two-phase flow a very difficult task. A serious need was felt to conduct a comprehensive study of phase change phenomena in microscale channels to understand the fundamental mechanisms involved in the boiling process before attempting any modeling. More accurate models for the heat transfer coefficient will be obtained if the modeling efforts are concentrated on each particular flow pattern [99]. Therefore, flow pattern maps with well-developed flow patterns and transition lines may facilitate the modeling efforts but universal flow maps are not available so far. Therefore, it is essential to further conduct systematic experimental research in microchannel flow boiling to obtain the heat transfer and flow pattern data simultaneously to provided good database. Furthermore, new heat transfer mechanisms should be developed based on both heat transfer behaviors and the relevant flow patterns. Effort should be made to develop universal flow boiling heat transfer models in future.

5. Unstable and transient flow boiling heat transfer in microscale channels

It is essential to understand the mechanisms of the unstable and transient flow boiling heat transfer in microscale channels. Flow boiling and two phase instability in macrochannels are divided into dynamic and static instabilities. For dynamic instability, it is related to pressure,

mass flux and temperature. It is commonly recognized that three types of oscillations exist in two phase flow and flow boiling in a macroscale channels: pressure drop oscillation, density wave oscillation and thermal oscillation [109, 110]. These unstable behaviors may even cause deterioration of heat transfer and thus cause dryout and boiling crisis which may occur in subcooled conditions. In recent years, a great deal of attention has been paid to the investigation of dynamic flow boiling instability in microchannel [48, 111-115]. These include both single and parallel microchannels. Hetsroni et al. [113, 114] found that small pressure fluctuations in their experiments of water boiling in 21 silicon triangular microchannels of a hydraulic diameter of 0.129 mm and observed periodic annular flow and periodic dry steam flow in the microchannel. In fact, these unstable flow boiling phenomena are caused due to the confined flow regimes changes, back flow and non-uniform flow and so on. For instance, Qu and Mudawar [47] observed backflow as shown in Fig. 8. The inlet/outlet configuration may have a significant effect of the unstable flow. Wang et al. [48] carried out simultaneous visualisation and measurement study on the effects of inlet/outlet configuration on flow boiling instabilities in parallel microchannel of a length of 30 mm and a hydraulic diameter of 0.186 mm. They found fluctuation of temperature and oscillations in the microchannels which correspond to the unstable flow regime and flow regime transition. Huang et al. [116] recently conducted experimental on the thermal response of multi-microchannels during flow boiling of R236fa and R245fa under transient heat loads with flow visualization. They investigated the base temperature response of multi-microchannel evaporators under transient heat loads, including cold startups and periodic step variations in heat flux using two different test sections for a wide variety of flow conditions. The effects on the base temperature behavior of the test section, heat flux magnitude, mass flux, inlet subcooling, outlet saturation temperature, and fluid were investigated. The transient base

temperature response, monitored by an infrared (IR) camera, was recorded simultaneously with the flow regime acquired by a high-speed video camera. For cold startups, it was found that reducing the inlet orifice width, heat flux magnitude, inlet subcooling, and outlet saturation temperature but increasing the mass flux decreased the maximum base temperature. Meanwhile, the time required to initiate boiling increased with the inlet orifice width, mass flux, inlet subcooling, and outlet saturation temperature but decreased with the heat flux magnitude. For periodic variations in heat flux, the resulting base temperature was found to oscillate and then damp out along the flow direction. Furthermore, the effects of mass flux and heat flux pulsation period were insignificant. Figure 35 shows the effect of heat flux magnitudes on the thermal response of micro-evaporators: (a) test section 1 and (b) test section 2. It is found that the maximum base temperature increases with increasing heat flux from 14 to 30 W/cm^2 for test section 1. Similar results are found for test section 2. Furthermore, the onset of flow boiling occurred earlier for higher heat flux magnitude. According to their study, for transient cases with a periodic variation in heat flux, the effects of mass flux and heat flux pulse period on the base temperature response are shown to be insignificant within the current testing range. Independent of the mass flux and heat flux pulse width, the temperature variation resulted from the periodic change in heat flux was damped along the distance downstream. It should be mentioned here that transient flow boiling heat transfer, as a special important topic, has not yet been well understood. Therefore, systematic experimental, analytical and modelling studies of transient flow boiling in microchannels are needed.

6. Concluding remarks and future Research recommendations

A large number of studies on microchannel flow boiling heat transfer have been conducted over the past years. Various heat transfer behaviours trends are available, which have been mostly explained with the two flow boiling heat transfer mechanisms by different researchers. However, the actual heat transfer mechanisms are much more complex than the two mechanisms and should be well understood. Furthermore, a number of heat transfer models and correlations have also been developed based on microchannel flow boiling experimental data. From the analysis and comparison of the experimental data from different studies, it can be concluded that well performed and documented experimental studies on microchannel flow boiling are still needed. The channel size effect on the flow boiling heat transfer behaviours and mechanisms have not yet well been understood. In general, the available heat transfer correlations and models poorly predict the experimental database collected from the literature. No universal prediction methods are available for microscale channel flow boiling heat transfer so far. Furthermore, the available heat transfer correlations and models lack the heat transfer mechanism basis. The below main issues have been identified in the available studies as:

(i) Big discrepancies among experimental results from different studies at similar conditions have been found. Quite different heat transfer trends have been identified.

(ii) The two main flow boiling heat transfer mechanisms in conventional channels are generally used to explain the experimental results in microscale channels but some anomaly trends cannot be reasonably explained.

(iii) The existing correlations and models poorly predict the independent microchannel flow boiling heat transfer data. The current prediction methods lack the heat transfer mechanism basis. Reliable universal prediction methods are not available so far.

(iv) The flow pattern based heat transfer model for flow boiling in microchannel predict the database reasonably well. However, mechanistic prediction methods and models are needed to be well developed and improved.

(v) Relating the heat transfer behaviours to the corresponding flow regimes is a promising methods to understand the heat transfer mechanisms and to develop new prediction models for flow boiling covering both macroscale and microscale channels.

(vi) Systematic experimental, analytical and modelling studies of unstable and transient flow boiling phenomena in microchannels should be focused on.

Therefore, as a priority, well performed and documented experimental studies on microscale channel flow boiling are needed in future. Furthermore, experiments on two-phase flow and flow boiling at a wide range of conditions should be conducted by considering the effect of channel size on both heat transfer coefficients and the relevant flow patterns. Furthermore, flow pattern visualization and transition criteria of two-phase flow and flow boiling of microscale channels should be systematically investigated, which should be related to the flow boiling heat transfer behaviors and mechanisms. Generalized heat transfer models should be targeted by incorporating the flow boiling mechanisms, flow patterns, channel sizes and fluid properties etc. Development of the theory of two-phase flow and flow boiling of microscale channels should also be focused on by analyzing the heat transfer model for specific flow patterns as a starting point. This should include a detailed study of the mechanisms of mass, momentum and heat transfer under conditions of interaction of hydrodynamic and thermal effects and phase changes in microscale channels. It is envisaged that a systematic research on two-phase flow and flow boiling in

microscale channels will bring advancement of knowledge and new theory of two-phase flow and flow boiling in microscale channels and meet the practical requirements in various industrial applications. However, it is still a challenge to in microscale channel flow boiling field due to the complexity and difficulty of two phase flow and flow boiling phenomena involved in microscale channels. Efforts should be made to contribute to both experimental and theoretical studies in the future. Furthermore, systematic studies of unstable and transient flow boiling phenomena in microchannels should be conducted to provide comprehensive knowledge, theory and models in this aspect.

Nomenclature

Acs cross sectional area, m^2

Bd Bond number, defined by Eq. (4a), Eq. (18d) and Eq. (24e)

Bo boiling number, $[q/(Gi_{fg})]$

C constant

Co confinement number

c_p specific heat at constant pressure, J/kgK

D characteristic number, defined by Eq. (4b)

D_{eq} equivalent diameter, m

D_h internal tube hydraulic diameter, m

d diameter, m

d_b bubble diameter, m

E convective boiling heat transfer enhancement factor

E' convective boiling heat transfer enhancement factor

e entrained liquid droplet mass fraction

Fr Froude number, $[G^2/(\rho_L^2 g D_h)]$

G total gas and liquid two-phase mass velocity, kg/m^2s

g gravitational acceleration, 9.81 m/s^2

h heat transfer coefficient, W/m^2K

i_{fg} latent heat of evaporation, J/kg

J superficial velocity, m/s

k thermal conductivity, W/mK

L Laplace number, defined by Eq. (1)

M Molecular weight

m parameter defined by Eq. (27a)

Nu Nusselt number defined by Eq. (23)

n parameter defined by Eq. (27b)

p pressure, N/m^2

p_r redcued pressure $[p/p_{crit}]$

Pr_l prandtl number, $[\mu_l c_{pl}/k_l]$

q heat flux, W/m^2

Re Renolds number

Re_{lo} Reynolds number considering the total gas-liquid two phase flow as liquid flow $[GD_h/(\mu_l)]$

Re_l Reynolds number considering only liquid phase flow $[G(1-x)D_h/(\mu_l)]$

S nucleate suppression factor

T temperature, K

T_{sat} saturation temperature, K

t time, s

V velocity, m/s

V* dimensionless velocity

We_l liquid Weber number considering the total vapor-liquid flow as liquid flow $[G^2 D_h/(\rho_l \sigma)]$

We_g gas phase Weber number $[G^2 x^2 D_h/(\rho_g \sigma)]$

We_c gas phase Weber number $[\rho_v J_v^2 d/\sigma]$

X_{tt} Martinelli number, $\{[(1-x)/x)]^{0.9}[\rho_g/\rho_l]^{0.5}[\mu_l/\mu_g]^{0.1}\}$

x vapor quality

y* dimenisonless length

z location

Greek symbols

δ film thickness, m

ε void fraction

δ* dimensionless film thickness

ϕ^2 two phase friction multiplier

μ dynamic viscosity, Ns/m^2

ρ density, kg/m^3

θ_{dry} dry angle, rad

σ surface tension, N/m

τ time, s, shear stress Pa

ξ_i relative error defined by Eq. (16)

Subscripts

b bubble

CB-AF confined bubble to annular flow regime

c core flow

crit critical

cs cross sectiona

dry dry perimeter

end end

F fluid

f frequency, Hz

fg, lv latent

film liquid film

g gas phase

IA intermittent flow to annular flow transition

l liquid phase

lf liquid film

lo considering the total gas-liquid two phase flow as liquid flow

min minimum

nb nucleate boiling

p constant pressure, pair

pool pool boiling

ref reference

sat saturation

tp two phase

v vapor phase

w tube wall

wet wetted perimeter

δ_0 initial film thickness

0 initial

References

[1] L. Cheng, Microscale and nanoscale thermal and fluid transport phenomena: Rapidly developing research fields, Int. J. Microscale Nanoscale Thermal Fluid Transport Phenomena 1 (2010) 3-6.

[2] J.R. Thome, The new frontier in heat transfer: microscale and nanoscale technologies, Heat Transfer Eng. 27(9) (2006) 1-3.

[3] S.G. Kandlikar, Fundamental issues related to flow boiling in minichannels and microchannels, Exp. Therm. Fluid Sci. 26 (2002) 389-407.

[4] J.R. Thome, State-of-the art overview of boiling and two-phase flows in microschannels, Heat Transfer Enging 27(9) (2006) 4-19.

[5] L. Cheng, Fundamental issues of critical heat flux phenomena during flow boiling in microscale-channels and nucleate pool boiling in confined spaces, Heat Transfer Engineering 34 (2013) 1011-1043.

[6] J.R. Thome, Boiling in microchannels: A review of experiment and theory, Int. J. Heat Fluid flow 25 (2004) 128-139.

[7] G. Ribatski, L. Wojtan, J.R. Thome, An analysis of experimental data and prediction methods for two-phase frictional pressure drop and flow boiling heat transfer in micro-scale channels, Exp. Therm. Fluid Sci. 31 (2006) 1-19.

[8] S.K. Suha, G. Zummo, G.P. Celata, Review on Flow Boiling in Microchannels Int. J. Microscale Nanoscale Thermal Fluid Transport Phenomena, 1 (2010) 111-178.

[9] L. Cheng, E. P. Bandarra Filho, J.R. Thome, Nanofluid two-phase flow and thermal physics: a new research frontier of nanotechnology and its challenges, J. Nanosci. Nanotech. 8 (2008) 3315-3332.

[10] L. Cheng, L. Liu, Boiling and two phase flow phenomena of refrigerant-based nanofluids: fundamentals, applications and challenges, Int. J. Refrigeration 36 (2013), pp. 421-446.

[11] L. Cheng, G. Ribatski, J.R. Thome, Gas-liquid two-phase flow patterns and flow pattern maps: fundamentals and applications, ASME Appl. Mech. Rev. 61 (2008) 050802.

[12] L. Cheng, D. Mewes, Review of two-phase flow and flow boiling of mixtures in small and mini channels, Int. J. Multiphase Flow 32 (2006) 183-207.

[13] L. Cheng, Critical Heat flux in microscale channels and confined Spaces: A review on experimental studies and prediction methods, Russian J. General Chemistry, 82 (12) (2012) 2116-2131.

[14] B. Agostini, M. Fabbri, J. E. Park, L. Wojtan, J. R. Thome and B. Michel. State of the art of high heat flux cooling technologies, Heat Transfer Eng. 28 (2007) 258-281.

[15] Schmidt, R. R., and Notohardjono, B. D., High-End Server Low-Temperature Cooling, IBM J. Res. & Dev., 46 (6) (2002) 739–751.

[16] L. Cheng, J.R. Thome, Cooling of microprocessors using flow boiling of CO_2 in a micro-evaporator: preliminary analysis and performance comparison, Appl. Therm. Eng. 29 (2009) 2426-2432.

[17] R.K., Shah, Classification of Heat Exchangers. In: Heat Exchangers: Thermal Hydraulic Fundamentals and Design (Eidted by Kakac S., Bergles A.E., Mayinger F.), Hemisphere Publishing Corp., Washington DC, 1986, pp 9-46.

[18] S.S. Mehendale, A.M. Jacobi, R.K. Shah, Fluid flow and heat transfer at micro- and meso-scales with application to heat exchanger design. Applied Mech. Revs. 53 (2000) 175-193.

[19] K.A. Triplett, S.M. Ghiaasiaan, S.I. Abdel-Khalik, D.L. Sadowski, Gas-liquid two-phase flow in microchannels. Part I: Two-phase flow patterns, Int. J. Multiphase Flow 25 (1999) 377-394.

[20] P.A. Kew, K. Cornwell, Correlations for the prediction of boiling heat transfer in small-diameter channels, Appl. Thermal Eng., 17 (1997) 705-715.

[21] N. Brauner, D. Moalem-Maron, Identification of the range of small diameter conduits regarding two-phase flow pattern transitions, Int. Comm. Heat Mass Transfer 19 (1992) 29-39.

[22] T. Harirchian, S.V. Garimella, A comprehensive flow regime map for microchannel flow boiling with quantitative transition criteria, Int. J. Heat Mass Transfer 53 (2010) 2694–2702.

[23] C.L. Ong, J.R. Thome, Macro-to-microchannel transition in two-phase flow: Part 1 – Two-phase flow patterns and film thickness measurements, Exp. Therm. Fluid Sci. 35 (2011) 37–47.

[24] L. Cheng, G. Ribatski, L. Wojtan, J.R. Thome, New flow boiling heat transfer model and flow pattern map for carbon dioxide evaporating inside horizontal tubes, Int. J. Heat Mass Transfer 49 (2006) 4082-4094.

[25] L. Cheng, G. Ribatski, J., Quibén Moreno, J.R. Thome, New prediction methods for CO_2 evaporation inside tubes: Part I – A two-phase flow pattern map and a flow pattern based phenomenological model for two-phase flow frictional pressure drops, Int. J. Heat Mass Transfer 51 (2008) 111-124.

[26] L. Cheng, G. Ribatski, J.R. Thome, New prediction methods for CO_2 evaporation inside tubes: Part II – An updated general flow boiling heat transfer model based on flow patterns, Int. J. Heat Mass Transfer 51 (2008) 125-135.

[27] J.L. Gasche, Carbon doxide evaporation in a single micro-channel, J. Brazil Soc. Mech. Sci. Eng. 28 (1) (2006) 69–83.

[28] C.B. Tibiriçá, G. Ribatski, An Experimental study on flow boiling heat transfer of R134a in a 2.3 mm Tube, Int. J. Microscale Nanoscale Thermal Fluid Transport Phenomena, 1 (2010) 37-58

[29] L. Cheng, L. Liu, Analysis and evaluation of gas-liquid two-phase frictional pressure drop prediction methods for microscale channels, Int. J. Microscale Nanoscale Thermal Fluid Transport Phenomena, 2 (2011) 259-280.

[30] L. Cheng, H. Zou, Evaluation of flow boiling heat transfer correlations with experimental data of R134a, R22, R410A and R245fa in microscale channels, Int. J. Microscale Nanoscale Thermal Fluid Transport Phenomena 1 (2010) 363-380.

[31] L. Wojtan, T. Ursenbacher, J.R. Thome, Investigation of flow boiling in horizontal tubes: Part I – A new diabatic two-phase flow pattern map, Int. J. Heat Mass Transfer 48 (2005) 2955-2969.

[32] L. Wojtan, T. Ursenbacher, J.R. Thome, Investigation of flow boiling in horizontal tubes: Part II – development of a new heat transfer model for stratified-wavy, dryout and mist flow regimes, Int. J. Heat Mass Transfer, 48 (2005). 2970-2985.

[33] S-M. Kim and I. Mudawar, Review of databases and predictive methods for heat transfer in condensing and boiling mini/micro-channel flows, Int. J. Heat and Mass Transfer 77 (2014) 627–652.

[34] L. Cheng, D. Mewes, A. Luke, Boiling phenomena with surfactants and polymeric additives: a state-of-the-art review, Int. J. Heat Mass Transfer 50 (2007) 2744-2771.

[35] J. Moreno Quibén, L. Cheng, R.J. da Silva Lima, J.R. Thome, Flow boiling in horizontal flattened tubes: part I — two-phase frictional pressure drop results and model, Int. J. Heat Mass Transfer 52 (2009) 3634-3644.

[36] J. Moreno Quibén, L. Cheng, R.J. da Silva Lima, J.R. Thome, Flow boiling in horizontal flattened tubes: part II — flow boiling heat transfer results and model, Int. J. Heat Mass Transfer 52 (2009) 3645-3653.

[37] L. Cheng, Microscale Flow Patterns and Bubble Growth in Microchannels, Chapter 3, in Microchannel Phase Change Heat Transfer, First Edition, Editor: Sujoy Kumar Saha, Elsevier Publisher, 2015, pp.91-140.

[38] L. Cheng, Flow Boiling Heat Transfer with Models in Microchannels, Chapter 4, in Microchannel Phase Change Heat Transfer, First Edition, Editor: Sujoy Kumar Saha, Elsevier Publisher, 2015, pp.141-191.

[39] L. Cheng, T. Chen, Study of flow boiling heat transfer in a tube with axial microgrooves, Exp. Heat Transfer 14 (1) (2001) 59-73.

[40] J.C. Chen, Correlation for boiling heat transfer to saturated fluids in convective flow, Industrial and Engineering Chemistry – Process Design and Development 5 (3) (1966) 322 -329

[41] K.E. Gungor, R.H.S. Winterton, A general correlation for flow boiling in tubes and annuli, Int. J. Heat Mass Transfer 29 (3) (1986) 351-358.

[42] Z. Liu, R.H.S. Winterton, A general correlation for saturated and subcooled flow boiling in tubes and annuli, based on a nucleate pool boiling equation, Int. J. Heat Mass Transfer 34 (11) (1991) 2759-2766.

[43] S.G. Kandlikar, A general correlation for two-phase flow boiling heat transfer coefficient inside horizontal and vertical tubes, J. Heat Transfer 102 (1990) 219–228.

[44] S.G. Kandlikar, A model for predicting the two-phase flow boiling heat transfer coefficient in augmented tube and compact heat exchanger geometries, J. Heat Transfer 113 (1991) 966–972.

[45] D. Steiner and J. Taborek, Flow boiling heat transfer in vertical tubes correlated by an asymptotic model, Heat Transfer Eng., 13 (2) (1992) 43–69.

[46] N. Kattan, J. R. Thome and D. Favrat, Flow boiling in horizontal tubes: Part-3: Development of a new heat transfer model based on flow patterns, ASME J. Heat Transfer 120 (1998) 156-165.

[47] W. Qu and I. Mudawar, Measurement and correlation of critical heat flux in two-phase micro-channel heat sinks, International Journal of Heat and Mass Transfer 47 (2004) 2045 - 2059.

[48] G. Wang, P. Cheng, A.E. Bergles, Effects of inlet/outlet configurations on flow boiling instability in parallel microchannels, Int. J. Heat and Mass Transfer 51 (2008) 2267–2281.

[49] G.M. Lazarek, S.H. Black, Evaporative heat transfer, pressure drop and critical heat flux in a small vertical tube with R-113, Int. J. Heat Mass Transfer 25 (7) (1982) 945-960.

[50] Z.Y. Bao, D.F. Fletcher, B.S. Haynes, Flow boiling heat transfer of Freon R11 and HCFC123 in narrow passages, Int. J. Heat Mass Transfer 43 (2000) 3347-3358.

[51] G.R. Warrier, V.K. Dhir, L.A. Momoda, Heat transfer and pressure drop in marrow rectangular channels, Exp. Ther. Fluid Sci. 26 (2002) 53-64.

[52] W. Zhang, T. Hibiki, K. Mishima, Correlation for flow boiling heat transfer in mini-channels, Int. J. Heat Mass Transfer 47 (2004) 5749-5763.

[53] J. Lee, I. Mudawar, Two-phase flow in high-heat-flux micro-channel heat sink for refrigeration cooling applications: Part II-heat transfer characteristics, Int. J. Heat Mass Transfer 48 (2005) 941-955.

[54] A.S. Pamitran, K. Choi, J.Oh, H. Oh, Forced convective boiling heat transfer of R-410A in horizontal minichannels, Int. J. of Refrigeration 30 (2007) 155-165.

[55] S.S. Bertsch, E.A. Groll, S.V. Garimella, A composite heat transfer correlation for saturated flow boiling in small channels, Int. J. Heat Mass Transfer 52 (2009) 2110-2118.

[56] C.L. Ong, J.R. Thome, Flow boiling heat transfer of R134a, R236a and R245fa in a horizontal 1.030 mm circular channel, Exp. Ther. Fluid Sci. 33 (2009) 651-663.

[57] L. Sun, K. Mishima, An evaluation of prediction methods for saturated methods for saturated flow boiling heat transfer, Int. J. Heat Mass Transfer 52 (2009) 5323-5329.

[58] W. Li, Z. Wu, A general correlation for evaporative heat transfer in micro/mini-channels, Int. J. Heat Mass Transfer (2010) 53 1778-1787.

[59] Tibirica, G. Ribatski, Flow boiling heat transfer of R134a and R245fa in a 2.3 mm tube, Int. J. Heat Mass Transfer 53 (2010) 2459-2468.

[60] W. Qu, I. Mudawar, Flow boiling heat transfer in two-phase micro-channels heat sinks – I. Experimental investigation and assessment of correlation methods, Int. J. Heat Mass Transfer 46 (2003) 2755-2271.

[61] S. Saitoh, H. Daiguji, E. Hihara, Effect of tube diameter on boiling heat transfer of R-134a in horizontal small-diameter tubes, Int. J. Heat Mass Transfer 48 (2005) 4973-4984.

[62] S.S. Bertsch, E.A. Groll, S.V. Garimella, Refrigerant flow boiling heat transfer in parallel microchannels as a function of local vapor quality, Int. J. Heat Mass Transfer 51 (2008) 3724-3735.

[63] S. In, S. Jeong, Flow boiling heat transfer of R134a, R236fa and R245fa in a horizontal 1.03mm circular channel, Exp. Ther. Fluid Sci. 33 (2009) 651-663.

[64] L. Wang, M. Chen, M. Groll, Flow boiling heat transfer characteristics of R134a in a horizontal mini tube, J. Chem. Eng. Data 54 (2009) 2638-2645.

[65] Harirchian and Garimella, Microchannel size effects on local flow boiling heat transfer to a dielectric fluid, Int. J. Heat Mass Transfer 51 (2008) 3724–3735.

[66] K.H. Bang, W.H. Choo, Flow boiling in minichannels of copper, brass, and aluminum round tubes, in: Proceedings of 2nd International Conference on Microchannels and Minichannels, Rochester, USA, 2004, pp. 559–564.

[67] N.H. Kim, Y.S. Sim, C.K. Min, Convective boiling of R22 in a flat extruded aluminum multi-port tube, in: Proceedings of 2nd International Conference on Microchannels and Minichannels, Rochester, USA, 2004, pp. 507–514.

[68] R. Yun, J. Heo, Y. Kim, J.T. Chung, Convective boiling heat transfer characteristics of R410A in microchannels, in: Proceedings of 10th International Refrigeration and Air Conditioning Conference at Purdue, West Lafayette, USA, 2004.

[69] K. Choi, A.S. Pamitran, C.Y. Oh, J.T. Oh, Boiling heat transfer of R-22, R-134a, and CO_2 in horizontal smooth minichannels, Int. J. Refrigeration 30 (2007) 1336-1346.

[70] T.N. Tran, M.W. Wambsganss, D.M. France, Small circular and rectangular channel boiling with two refrigerants. Int. J. Multiphase Flow 22 (1996) 485–498.

[71] W. Owhaib, C. Martin-Callizo, B. Palm, Evaporative heat transfer in vertical circular microchannels, Appl. Therm. Eng. 24 (2004) 1241-1253.

[72] X. Huo, L. Chen, Y.S. Tian, T.G. Karayiannis, Flow boiling and flow regimes in small diameter tubes, Appl. Therm. Eng. 24 (2004) 1225-1239.

[73] Y.Y. Yan, T.F. Lin, Evaporation heat transfer and pressure drop of refrigerant R134a in a small pipe, Int. J. Heat Mass Transfer 41 (1998) 4183-4194.

[74] C. Huh; M.H. Kim,Two-phase pressure drop and boiling heat transfer in a single horizontal microchannel, Proceedings of the 4th Int. Conf. Nanochannels, Microchannels and Minichannels, ICNMM2006 2006 B, 1097-1104.

[75] S. Lin, P.A. Kew, K. Cornwell, Flow boiling of refrigerant R141b in small tubes, Chem. Eng. Res. Des. 79 (4) (2001) 417–424.

[76] T. Harirchian, S.V. Garimella, Effects of channel dimension, heat flux, and mass flux on flow boiling regimes in microchannels, Int. J. Multiphase Flow 35 (2009) 349–362.

[77] T. Chen, S.V. Garimella, Measurements and high-speed visualization of flow boiling of a dielectric fluid in a silicon microchannel heat sink, International Journal of Multiphase Flow 32 (8) (2006) 957–971.

[78] D. Liu, S.V. Garimella, Flow boiling heat transfer in microchannels, Journal of Heat Transfer 129 (10) (2007) 1321–1332.

[79] T. Chen, S.V. Garimella, Flow boiling heat transfer to a dielectric coolant in a microchannel heat sink, IEEE Transactions on Components and Packaging Technologies 30 (1) (2006) 24–31.

[80] L. Zhang, E.N. Wang, K.E. Goodson, T.W. Kenny, Phase change phenomena in silicon microchannels, Int. J. Heat Mass Transfer 48 (2005) 1572–1582.

[81] T.-H. Yen, M. Shoji, F. Takemura, Y. Suzuki, N. Kasagi, Visualization of convective boiling heat transfer in single microchannels with different shaped cross-sections, Int. J. Heat Mass Transfer 49 (2006) 3884–3894.

[82] G. Hetsroni, A. Mosyak, Z. Segal, G. Ziskind, A uniform temperature heat sink for cooling of electronic devices, Int. J. Heat Mass Transfer 45 (2002) 3275-3286.

[83] R. Charnay, R.Revellin, J. Bonjour, Flow boiling characteristics of R-245fa in a minichannel at medium saturation temperatures, Exp. Therm. Fluid Sci. 59 (2014) 184–194.

[84] L. Jiang, M. Wong, Y. Zohar, Phase change in microchannel heat sinks with integrated temperature sensors, J. Microelectromech. Syst. 8 (1999) 358-365.

[85] L. Zhang, E.N. Wang, K.E. Goodson, T.W. Kenny, Phase change phenomena in silicon microchannels, Int. J. Heat Mass Transfer 48 (2005) 1572-1582.

[86] A.M. Jacobi, J.R. Thome, Heat transfer model for evaporation of elongated bubble flows in microchannels, J. Heat Transfer 124 (2002) 1131–1136.

[87] J.R. Thome, V. Dupont, A.M. Jacobi, Heat transfer model for evaporation in microchannels. Part I: Presentation of the model, Int. J. Heat Mass Transfer 47 (2004) 3375–3385.

[88] V. Dupont, J.R. Thome, A.M. Jacobi, Heat transfer model for evaporation in microchannels. Part II: Comparison with the database, Int. J. Heat Mass Transfer 47 (2004) 3387–3401.

[89] C. Vlasie, H. Macchi, J. Guilpart, B. Agostini, Flow boiling in small diameter channels, Int. J. refrigeration 27 (2004) 191-201.

[90] B. Agostini, A. Bontemps, Vertical flow boiling of refrigerant R134a in small channels, Int. J. Heat and Fluid Flow 26 (2005) 296-306.

[91] R. Yun, J.H. Heo, Y. Kim, Evaporative heat transfer and pressure drop of R410A in microchannels, Int. J. Refrigeration 29 (2006) 92-100.

[92] S.L. Qi, P. Zhang, L.X. Xu, Flow boiling of liquid nitrogen in micro-tubes: Part II – Heat transfer characteristics and critical heat flux, Int. J. Heat Mass Transfer 50 (2007) 5017-5030.

[93] D. Shiferaw, T.G. Karayiannis, D.B.R. Kenning, Flow boiling in a 1.1 mm tube with R134a: Experimental results and comparison with model, Int. J. Thermal Sci. 48 (2009) 331-341.

[94] R. Revellin, J.R. Thome A new type of diabatic flow pattern map for boiling heat transfer in microchannels, J.Micromechanics Microengineering 17 (2006) 788–796.

[95] L. Consolini, J.R. Thome, A heat transfer model for evaporation of coalescing bubble in micro-channel flow, Int. J. Heat Fluid Flow 31 (2010) 115–125.

[96] L. Cheng, Modelling of heat transfer of upward annular flow in vertical tubes, Chem. Eng.

Comm. 194 (2007) 975-993.

[97] W. Qu, I. Mudawar, Flow boiling heat transfer in two-phase micro-channel heat sinks—II. Annular two-phase flow model, Int. J. Heat Mass Transfer 46 (2003) 2773–2784.

[98] S.-M. Kim, I. Mudawar, Theoretical model for local heat transfer coefficient for annular flow boiling in circular mini/micro-channels, Int. J. Heat Mass Transfer 73 (2014) 731–742.

[99] S. M. Magnini, J.R. Thome, Proposed models, ongoing experiments, and latest numerical simulations of microchannel two-phase flow boiling, Int. J. Multiphase Flow 59 (2014) 84–101.

[100] R. Yun, Y. Kim, M.S. Kim Convective boiling heat transfer characteristics of CO_2 in microchannels, Int. J. Heat Mass Transfer 48 (2005) 235-242.

[101] J. Pettersen, Flow vaporization of CO_2 in microchannel tubes, Exp. Thermal and Fluid Sci. 28 (2004) 111-121.

[102] S. Koyama, K. Kuwahara, E. Shinmura, S. Ikeda, Experimental study on flow boiling of carbon dioxide in a horizontal small diameter tube. IIR Commission B1 Meeting, Paderborn, Germany, 2001, pp. 526-533.

[103] R. Yun, Y. Kim, M.S. Kim, Flow boiling heat transfer of carbon dioxide in horizontal mini tubes, Int. J. Heat Fluid Flow 26 (2005) 801-809.

[104] L. Cheng, G. Ribatski and J.R. Thome, On the prediction of flow boiling heat transfer of CO_2, The 22nd IIR Int. Congr. Refrig., Beijing, P.R. China, August 21-26, 2007.

[105] E. Costa-Patry, J.R. Thome, Flow pattern based flow boiling heat transfer model for microchannel, Int. J. Refrigeration 36 (2013) 414-420.

[106] A. Cioncolini, J.R. Thome, Algebraic Turbulence Modeling in Adiabatic and Evaporating Annular Two- Phase Flow, Int. J. Heat Fluid Flow 32 (2011) 805–817.

[107] J.R. Thome, A. Cioncolini, Unified model suite for two phase flow, convective boiling and condensation in macro- and microchannel, Heat Transfer Eng. 37 (2016) 1148-1157.

[108] VDI-Warmeatlas, Springer-Verlag, Berlin, Heidelberg, 1997.

[109] J.A. Bore, A.E. Bergles, L.S. Tong, review of two phase flow instability, Nucl. Eng. Des. 25 (1973) 165-192;

[110] H. Yuncu, O.T. Yildirim, S. Kakac, Two phase flow instabilities a in a horizontal single boiling channel, Appl. Sci. res. 48 (1991) 83-104.

[111] G. Wang, P. Cheng, H. Wu, Unstable and stable flow boiling in parallel microchannel and in a single microchannel, Int. J. Heat Mass Transfer 50 (2007) 4297-4310.

[112] G. Wang, P. Cheng, An experimental study of flow boiling instability in a single microchannel, Int. Comm. Heat Mass Transfer 35 (2008) 1229-1234.

[113] G. Hetsroni, A. Mosyak, Z. Segal, G. Ziskind, A uniform temperature heat sink for cooling of electric devices, Int. J. Heat mass Transfer 45 (2002) 3275-3286.

[114] G. Hetsroni, A. Mosyak, Z. Segal, Nonuniform temperature distribution in electric device cooled by flow in parallel microchannel, IEEE Trans. Compon. Pack. technol. 24 (2001) 17-23 heat sink for cooling of electric devices, Int. J. Heat mass Transfer 45 (2002) 3275-3286.

[115] H.Y. Wu, P. Cheng, Visualization and measurements of periodic boiling in silicon microchannel heat sinks, Int. J. Heat Mass transfer 46 (2003)2603-2614

[116] H. Huang, N. Borhani and J.R. Thome, Thermal response of multi-microchannel evaporators during flow boiling of refrigerants under transient heat loads with flow visualization, J. Electronic Packaging 128 (2016) 031004-1.

List of table captions

List of table captions

Fig. 1. (a) Cross-section of computer chips with an evaporator by Schmidt and Notohardjono [15]. (b) Schematic diagram of a silicon multi-microchannel evaporator used for chips cooling by Cheng and Thome [16].

Fig. 2. Schematic of refrigeration components for electronic chips cooling by Schmidt and Notohardjono [15].

Fig. 3. Comparisons of simulation results of base temperature of CO2 and R236fa at the indicated conditions for chips cooling. [16].

Fig. 4. Comparison of various definitions of threshold diameters for micro-scale channels: (a) Water, (b) CO_2, by Cheng and Mewes [12].

Fig. 5. Transition from confined flow to unconfined flow using flow behaviours defined by Harirchian and Garimella [22].

Fig. 6. Heat transfer coefficient h versus vapour quality x behaviours identified in the literature [7].

Fig. 7. (a) Comparison of the experimental results of Bang and Choo [66] and Kim et al. [67]; (b) Comparison of the experimental results of Pamitran and Choi [58] and Yun et al. [68] illustrated by Ribatski et al. in their review paper [7].

Fig. 8. Schematic representation of observed vapour backflow at high heat flux by Qu and Mudawar [47].

Fig. 9. Arrangement of 8 parallel microchannels having the same length and identical trapezoidal cross-sectional area and etched in a silicon substrate by Wang et al. [48].

Fig. 10. Photographs and sketch of flow patterns in steady bubbly/slug flow boiling regime in parallel microchannels (D_h = 186 µm) with the Type-C connection at q = 364.68 kW/m^2, G = 124.03 kg/m^2 s and Tin = 35°C (i.e., x_e = 0.359) by Wang et al. [48].

Fig. 11. Photos of steady flow boiling patterns near outlet section of parallel microchannels (D_h = 186 µm) with the Type-C connection at q = 364.68 kW/m^2 and T_{in} = 35°C: (a) G = 682.11 kg/m^2 s (i.e., x_e = -0.034), (b) G = 471.32 kg/m^2 s (i.e., x_e = 0.005), (c) G = 156.04 kg/m^2 s (i.e., x_e = 0.26), by Wang et al. [48].

Fig. 12. Schematic of flow patterns and the corresponding heat transfer mechanisms and qualitative variation of the heat transfer coefficients for flow boiling in a horizontal tube [33].

Fig. 13. Flow boiling data plotted versus vapour quality, Huo et al. [72].

Fig. 14. Effect of heat flux (q) and mass flux (G) on heat transfer coefficient for three different diameter tubes: (a) 3.1-mm-ID; (b) 1.12-mm-ID and (c) 0.51-mm-ID [61].

Fig. 15. The experimental heat transfer coefficients in the same literature showing different results with a very little change of hydraulic diameters from 1.53 mm to 1.54 mm (Solid symbols showing the experimental results of Yun et al. [100]: D_h = 1.53 mm, G = 300 kg/m^{2}s, T_{sat} = 5 °C and q = 20 W/m^2 and hollow symbols showing the experimental results of Yun et al. al.: D_h = 1.54 mm, G = 300 kg/m^{2}s, T_{sat} = 5 °C and q =20 W/m^2.).

Fig. 16. The experimental heat transfer coefficients in the literature showing opposite behaviour of heat transfer (Solid symbols showing the experimental results of Pettersen [101]: D_h = 0.8 mm, G = 190 kg/m^{2}s, T_{sat} = 0 °C and q = 10 W/m^2 and hollow symbols showing the experimental results of Koyama et al. al. [102]: D_h = 1.8 mm, G = 260 kg/m^{2}s, T_{sat} = 0.26 °C and q =32.06 W/m^2.).

Fig. 17. Effect of microchannel width on local heat transfer coefficient as a function of (a) wall heat flux and (b) base heat flux. [65].

Fig. 18. Comparison of N_2 heat transfer coefficient data with the best predictive correlation (A) Tran et al. [70]; (B) Li and Wu [58].

Fig. 19. Comparison of R12 heat transfer coefficient data with the best predictive correlation (A) Saitoh et al. [61]; (B) Sun and Mishima [57].

Fig. 20. Comparison of R22 heat transfer coefficient data with the best predictive correlation (A) Saitoh et al. [61]; (B) Kew and Cornwell [22].

Fig. 21. Comparison of of R134a heat transfer coefficient data to the best two correlations: (A) Li and Wu [58]; (B) Sun and Mishima [57].

Fig. 22. Comparison of R141b heat transfer coefficient data with the best predictive correlation (A) Saitoch et al. [61] ; (B) Sun and Mishima [57].

Fig. 23. Comparison of of R245fa heat transfer coefficient data to the best two correlations: (A) Li and Wu [58]; (B) Chen [40].

Fig. 24. Comparison of R123 heat transfer coefficient data with the best predictive correlation: (A) Zhang et al. [52]; (B) Li and Wu [58].

Fig. 25. Comparison ofR410A heat transfer coefficient data to the best two correlations: (A) Kew and Cornwell [20]; (B) Lazarek and Black [49].

Fig. 26. The Three-zone heat transfer model for elongated bubble flow regime in microscale channels: diagram illustrating a triplet comprised of a liquid slug, an elongated bubble and a vapour slug [87].

Fig. 27. Annular flow model in tubes [106].

Fig. 28. Comparison of R134a heat transfer coefficient data by Wang et al. [64] to the Thome et al. three zone heat transfer model [87]: 90.4% of the data are predicted by the model with ±30%.

Fig. 29(a) Comparison of the whole R134a heat transfer coefficient data to the flow pattern based model combining the three zone heat transfer model [87] with the unified annular flow heat transfer model [106, 107].

Fig. 29(b) Comparison of the whole R234fa heat transfer coefficient data to the flow pattern based heat transfer model combining the three zone heat transfer model [87] with the unified annular flow heat transfer model [106, 107].

Fig. 29(c) Comparison of the whole R22 heat transfer coefficient data to the flow pattern based heat transfer model combining the three zone heat transfer model [87] with the unified annular flow heat transfer model [106, 107].

Fig. 30(a) Comparison of the R22 heat transfer coefficient data to the flow pattern based heat transfer model combining the three zone heat transfer model [87] with the unified annular flow heat transfer model [106, 107] at the conditions: mass flux G = 500 kg/m^{2}s, heat flux q = 30 kW/m^2, saturation temperature T_{sat} = 10°C and tube diameter D = 3 mm.

Fig. 30(b) Comparison of the R123 heat transfer coefficient data to the flow pattern based heat transfer model combining the three zone heat transfer model [87] with the unified annular flow heat transfer model [106, 107] at the conditions: mass flux G = 314 kg/m^{2}s, heat flux q = 15 kW/m^2, saturation temperature T_{sat} = 49.3°C and tube diameter D = 0.19 mm.

Fig. 30(c) Comparison of the R134 heat transfer coefficient data to the flow pattern based heat transfer model combining the three zone heat transfer model [87] with the unified annular flow heat transfer model [106, 107] at the conditions: mass flux G = 676 kg/m^{2}s, heat flux q = 35.1 kW/m^2, saturation temperature T_{sat} = 24.6°C and tube diameter D = 1.3 mm.

Fig. 30(d) Comparison of the R234fa heat transfer coefficient data to the flow pattern based heat transfer model combining the three zone heat transfer model [87] with the unified annular flow heat transfer model [106, 107] at the conditions: mass flux G = 300 kg/m^{2}s, heat flux q = 10 kW/m^2, saturation temperature T_{sat} = 31°C and tube diameter D = 2.3 mm.

Fig. 31. Schematic diagram of dry angle and physical model for flow boiling.

Fig. 32. (a) Comparison of the predicted heat transfer coefficients to the experimental data of Yun et al. [103] at the test conditions: D_{eq} = 2 mm, q = 30 kW/m^2, T_{sat} = 5°C and G = 1500 kg/m^{2}s; (b) The corresponding flow pattern map at the same test conditions.

Fig. 33. Simulation of flow boiling model and flow pattern map by Cheng et al. [104]: (a) For 1.15 mm channel at the conditions: q = 11 kW/m^2, T_{sat} = 10°C and G = 300 kg/m^{2}s with

indicated value at x = 0.30; (b) For 3 mm channel at the conditions: q = 20 kW/m^2, T_{sat} = 10°C and G = 390 kg/m^{2}s with indicated value at x = 0.70.

Fig. 34. The predicted flow boiling heat transfer coefficient with the three-zone heat transfer model versus vapor quality for different diameters (increment of 0.166 mm) [88].

Fig. 35 The Effect of heat flux magnitudes on the thermal response of micro-evaporators: (a) test section 1 and (b) test section 2 by Huang et al. [116].

Table 1 Selected studies on flow boiling heat transfer and mechanisms in microscale channels in the literature.

Reference	Fluid, Parameter ranges G (kg/m^2s), q (kW/m^2), T (^oC)/P (bar)	Channel size D_h (mm), Substrate, Geometry,)	Remarks
Lazarek and Black [49]	R-113, G=125-750, q=14-380, P=1.3-4.1	D_h = 3.1 mm, Stainless steel, circular, Vertical	Nucleate boiling was dominant. Heat transfer coefficient was strongly dependent on heat flux and independent of mass flux and vapor quality.
Bao et al. [50]	R11/HCFC123, G=50-1800, q=5-200, P=20-50	D_h = 1.95 mm, copper, circular. horizontal	Nucleate boiling was dominant. Heat transfer coefficient was a strong function of heat flux and system pressure, less effects of mass flux and vapor quality.
Warrier et al. [51]	FC-84, G=557-1600, q=0-59.9, T=26, 40, 60	D_h = 0.75 mm, G-10 fibre glass, 5 parallel rectangular, horizontal	Heat transfer coefficient was correlated as a function of Boiling number alone.
Qu and Mudawar [60]	Water, G=135-402, T=30, 60	D_h = 0.349 mm, Parallel rectangular , horizontal 0.13 × 0.71 mm	Convective boiling was dominant. Heat transfer coefficient was dependent of mass flux and vapor quality but independent of heat flux.
Lee and Mudawar [53]	R-134a, G=127-654, q=159-938, T=-18.1-24.7	D_h = 0.35, copper, parallel rectangular 231µm ×713 µm, horizontal	A correlation with vapor quality x in 3 regions: $x < 0.05$, $0.05 < x < 0.55$ and $x > 0.55$ was developed.
Saitoh et al. [61]	R-134a, G=150-450, q=5-39, T=5, 10, 15	D_h = 0.51, 1.12, 3.1, circular, horizontal	Forced convective heat transfer decreases with decreasing D_h.

Pamitran et al. [54]	R-410A, G=300-600, q=10-30, T=10	D_h = 1.5 and 3.0 mm, stainless steel, circular, horizontal,	Nucleate boiling dominates at low x region.
Bertsch et al. [55, 62]	R-134a, G=20.3-81, q=0-200, P=4-7.5	D_h = 1.09 mm, copper, 17 parallel rectangular, horizontal	Heat tansfer coefficient varies with x but not with P_{sat}.
In and Jeong [63]	R-134a, R123 G=314-470, q=10-20, P=1.58-2.08, 9-11	D_h = 0.19 mm, stainless steel, circular, horizontal	Nucleate boiling dominates for R-134a until its suppression at high vapor quality.
Ong and Thome [56]	R134a, R236a, R245fa, G=200-1600, q=2.3-250, T=31	D_h = 1.03 mm, stainless steel, circular, horizontal,	Heat tarnsfer coefficient has a strong function of heat flux and mass flux. Convection dominates at high vapor quality in the annular regime.
Wang et al. [64]	R134a, G=310-860, q=21-50, P=0.65-0.75	D_h = 1.3 mm, stainless steel, circular, horizontal	It demonstrates the dependences of heat transfer coefficient on mass flux, heat flux, saturation pressure and vapor quality.
Tibirica and Ribatski [59]	R134a, R245fa G=50-700, q=5-55, T=22, 31, 41	D_h = 2.3 mm, stainless steel, circular, horizontal	Heat transfer coefficient is a function of heat flux, mass flux and vapor quality and generally increases with increasing saturation temperature.

Table 2 Selected flow boiling heat transfer models and correlations for microscale channels in the literature.

Lazarek and Black [49]	$h_{tp} = 30\,Re_{lo}^{0.857}\,Bo^{0.714}\,\frac{k_l}{D_h}$	(7)
Kew and Cornwell [20]	$h_{tp} = 30\,Re_{lo}^{0.857}\,Bo^{0.714}(1-x)^{-0.143}\,\frac{k_l}{D_h}$	(8)
Tran et al. [70]	$h_{tp} = 8.4\times10^{-5}\,Bo^{0.6}We_l^{0.3}\left(\frac{\rho_l}{\rho_g}\right)^{-0.4}$	(9)
	$We_l = \frac{G^2 D_h}{\sigma\rho_l}$	(9a)
Warrier et al. [51]	$h_{tp} = \left(1+6Bo^{1/16}+f(Bo)x^{0.65}\right)h_{lo}$	(10)
	$f(Bo) = -5.3(1-855Bo)$	(10a)
Zhang et al. [52]	$h_{tp} = Sh_{pool} + Fh_{sp}$	(11)
	h_{sp} is referred to the paper	
	$S = \frac{1}{1+2.53\times10^{-6}\,Re_l^{1.17}}$	(11a)
	$E = MAX(E',\,1)$	(11b)
	$E' = 0.64\left(1+\frac{C}{X_{tt}}+\frac{1}{X_{tt}^2}\right)^{0.5}$	(11c)
Pamitran et al. [54]	$h_{tp} = Sh_{pool} + Fh_l$	(12)
	$S = 9.4626(\phi^2)^{-0.2747}Bo^{0.1285}$	(12a)
	$E = 0.062\phi^2 + 0.938$	(12b)
Saitoh et al. [61]	$h_{tp} = Sh_{pool} + Eh_l$	(13)
	$E = 1+\frac{X_{tt}^{-1.05}}{1+We_g^{-0.4}}$	(13a)
	$We_g = \frac{G^2 x^2 D_h}{\sigma\rho_g}$	(13b)
	$S = \frac{1}{1+0.4\left(Re_{tp}\times10^{-4}\right)^{1.4}}$	(13c)
	$h_{pool} = 207\frac{k_l}{d_b}\left(\frac{qd_b}{k_lT_l}\right)^{0.745}\left(\frac{\rho_g}{\rho_l}\right)^{0.581}Pr_l^{0.533}$	(13d)
	$d_b = 0.51\left[\frac{2\sigma}{g(\rho_l-\rho_g)}\right]^{0.5}$	(13e)
Sun and Mishima [57]	$h_{tp} = \frac{6\,Re_{lo}^{1.05}\,Bo^{0.54}}{We_l^{0.191}(\rho_l/\rho_g)^{0.142}}\frac{k_l}{D_h}$	(14)
Li and Wu [58]	$h_{tp} = 334Bo^{0.3}\left(Bd\,Re_l^{0.36}\right)^{0.4}\frac{k_l}{D_h}$	(15)

Table 3 Summary of the microscale channel flow boiling heat transfer database in the literature.

Reference	Fluid, Parameter ranges: G (kg/m^2s), q (kW/m^2), T (^oC) or P (kPa)	Channel size D_h (mm), Horizontally (unless otherwise stated)	Data Points
Pamitran et al. [54]	R-410A, G=300-600, q=10-30, T=10	D_h=1.5, 3.0,	147
Tibirica and Ribatski [59]	R134a, R245fa G=100-700, q=5-35, T=22, 31, 41	D_h=2.3	136
Vlasie et al. [89]	R134a, R12, R141b G=63.1-212, q=5-90, T=5-32	D_h=2.0, 2.46, 3.69,	166
Agostini and Bontemps [90]	R134a G=219, q=29.049, P= 452, 557, 608	D_h=2.01, Vertically	66
Yun et al. [91]	R410A G=200-400, q=10-20, T=0, 5, 10	D_h=1.36,44	113
Choi et al. [69]	R-22, R134a, G=200-600, q=10-40, T=10	D_h=1.5 3.0	335
Qi et al. [92]	N_2 G=448.4-1471.2, q=82.5-133.5, P=188-735.9	D_h=0.531, 0.834, 1.042, 1.931	284
Bertsch et al. [62]	R134a, R245fa G=20-350, q=0-220, T=8-30	D_h=0.54,1.09	183
In and Jeong [63]	R123, R134a, G=314, 392, 470, q=10-20, T=158-1100	D_h=0.19	217

Shiferaw et al. [93]	R134a, G=100-600, q=16-150, P=600-1200	D_h=1.1	324
Wang et al. [64]	R134a, G=310-860, q=21-50, P=650-750	D_h=1.3	365

Table 4 Test fluids and parameter ranges of the database.

Data points number	2336
Test fluids	R410A, R141b, R134a, R245fa, R12, R123, R22 and N_2
Channel diameter	0.19 - 3.69 mm
Mass flux	20 - 1471.2 kg/m^{2}s
Heat flux	5 – 150 kW/m^2
Orientation	Horizontal and vertical

Table 5 Statistical analysis of the selected flow boiling heat transfer correlations for each individual fluid and all fluids (relative error ξ_i within ±30%).

Correlation\Fluid	R134a	R245fa	R12	R22	R123	R141b	R410A	N_2	Total
Chen [40]	40.5%	**72.7%**	57.4%	41.6%	36.6%	35.9%	4.6%	15.9%	35.2%
Lazark and Black [49]	48.6%	0.8%	92.6%	69.0%	6.3%	66.7%	**52.5%**	2.5%	40.9%
Kew and Cornwell [20]	55.5%	0.8%	92.6%	**83.2%**	16.1%	59.0%	**56.8%**	2.5%	46.3%
Gungor-Winterton [41]	64.0%	71.1%	61.1%	25.7%	4.5%	7.7%	10.8%	5.6%	44.8%
Liu-Winterton [42]	28.5%	39.7%	48.2%	70.8%	33.9%	71.8%	5.8%	44.7%	32.2%
Tran et al. [70]	18.2%	0.8%	55.6%	24.8%	0.0%	76.9%	21.6%	**45.8%**	22.5%
Warrier et al. [51]	12.8%	5.8%	0.0%	31.9%	24.1%	48.7%	6.6%	39.4%	16.9%
Zhang et al. [52]	41.5%	66.1%	57.4%	42.5%	**55.4%**	43.6%	3.9%	14.8%	36.2%
Pamitran et al. [54]	48.9%	43.8%	35.2%	0.0%	7.1%	0.0%	48.3%	0.7%	36.7%
Saitoh et al.[61]	63.0%	65.3%	**98.2%**	**87.6%**	52.7%	**87.2%**	3.1%	37.0%	**54.9%**
Sun and Mishima [57]	**67.4%**	0.8%	**94.4%**	76.1%	18.8%	**79.5%**	27.0%	4.6%	50.0%
Li andWu [58]	**66.0%**	**76.0%**	24.1%	35.4%	**85.7%**	7.7%	1.2%	**68.3%**	**56.7%**

Table 6 Statistical analysis of the two mechanistic heat transfer models for each individual fluid (relative error ξ_i within ±30%).

Model\Fluid	R134a	R245fa	R12	R22	R123	R141b	R410A	N_2
Three zone heat transfer model [87]	**48.3%**	35.5%	27.8%	**48.7%**	0%	**43.6%**	1.2%	14.1%
Flow pattern based heat transfer model combining the three zone model and the annular flow model [106, 107]	**69.1%**	68.4%	44.4%	**76.3%**	64.3%	**66.7%**	5.4%	41.2%

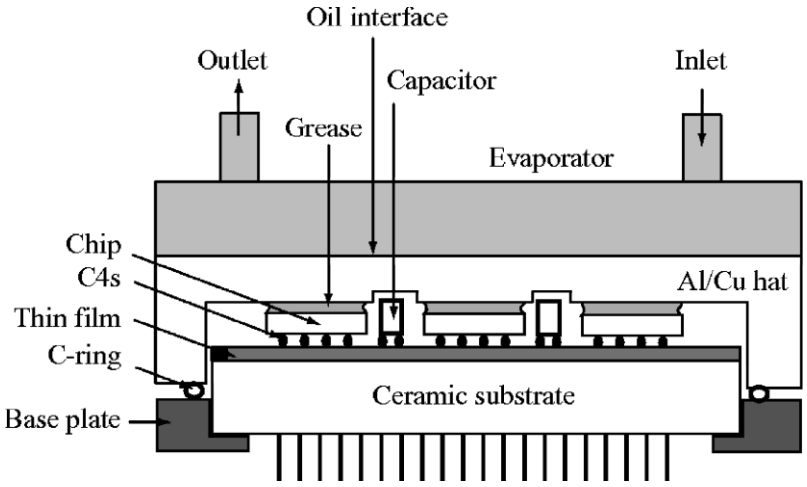

(a)

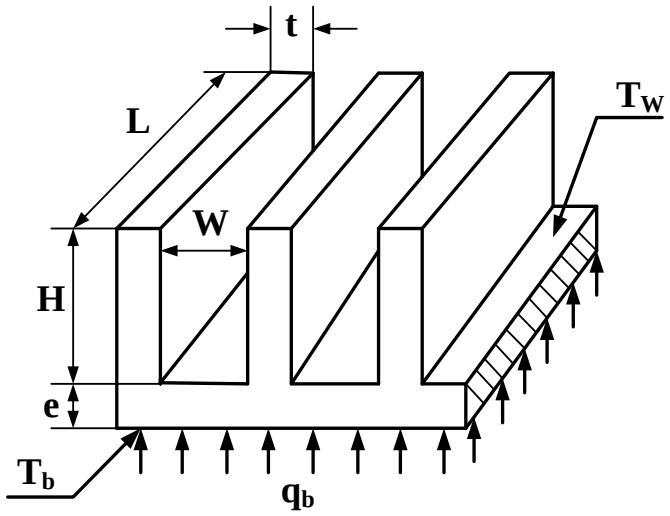

(b)

Fig. 1.(a) Cross-section of computer chips with an evaporator by Schmidt and Notohardjono [15]. (b) Schematic diagram of a silicon multi-microchannel evaporator used for chips cooling by Cheng and Thome [16].

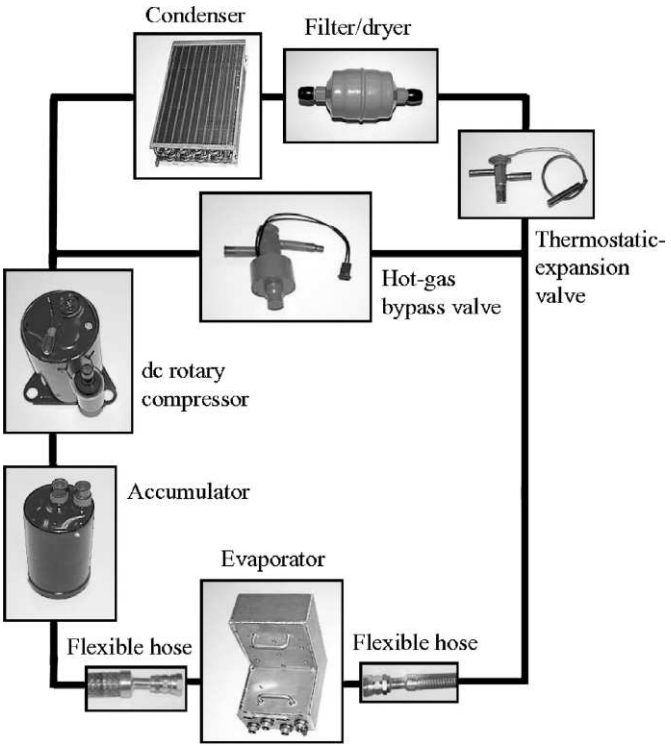

Fig. 2. Schematic of refrigeration components for electronic chips cooling by Schmidt and Notohardjono [15].

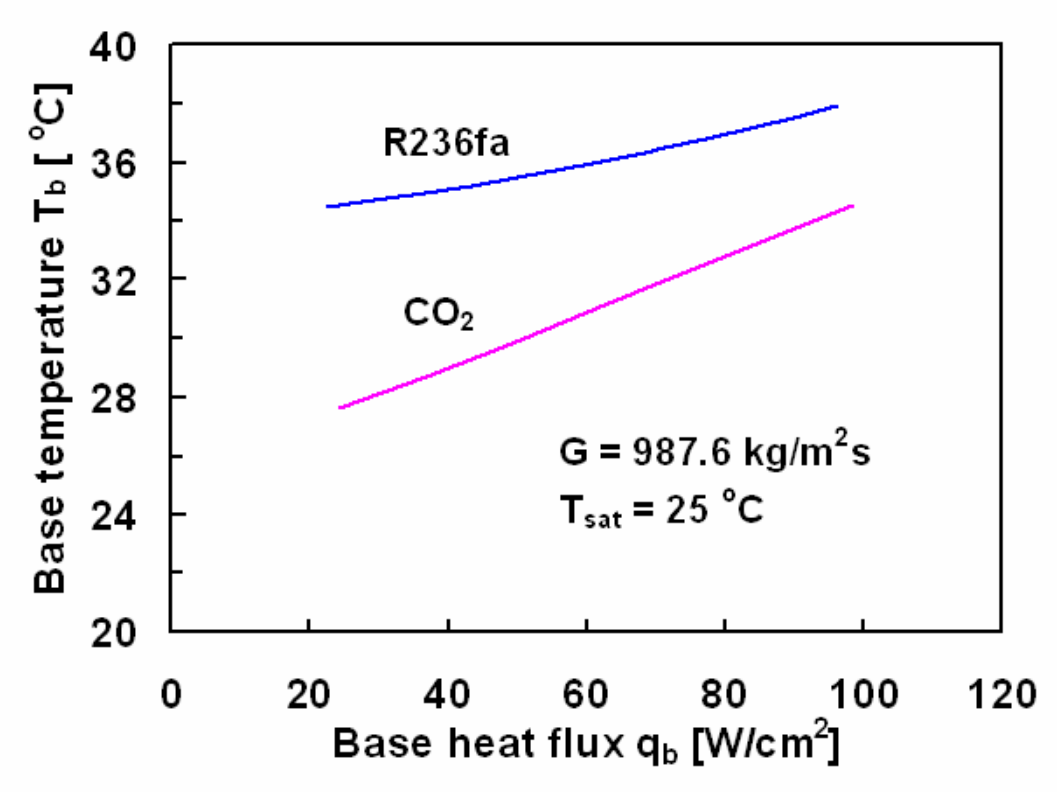

Fig. 3. Comparisons of simulation results of base temperature of CO2 and R236fa at the indicated conditions for chips cooling. [16].

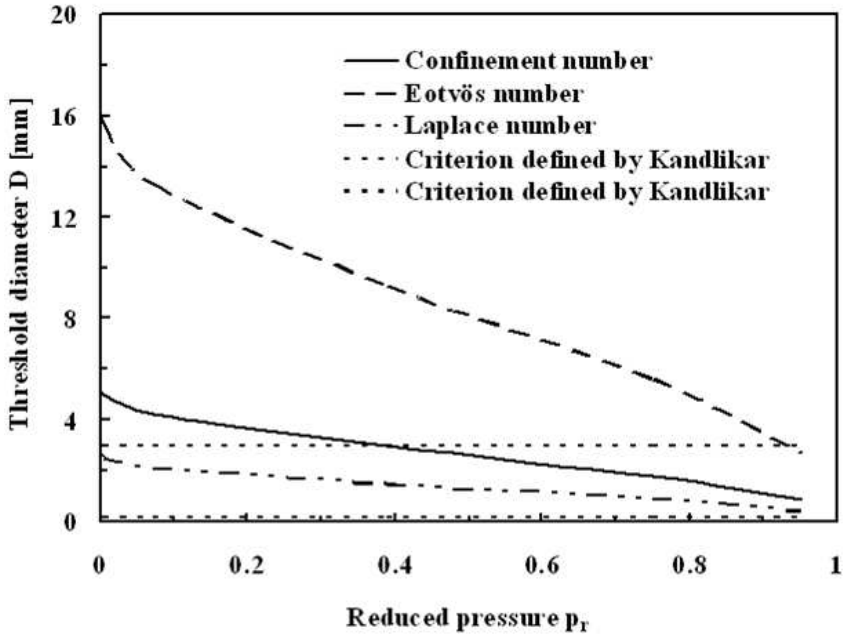

(a)

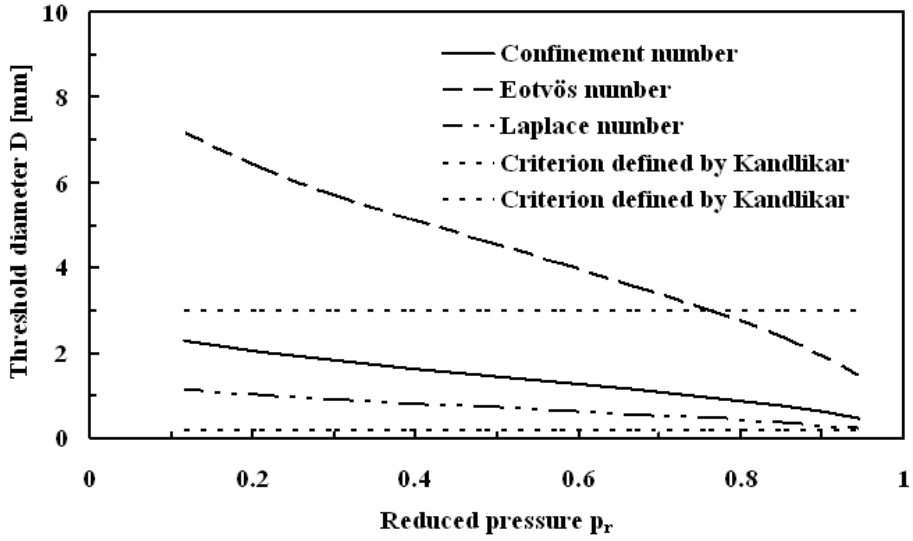

(b)

Fig. 4. Comparison of various definitions of threshold diameters for micro-scale channels: (a) Water, (b) CO_2, by Cheng and Mewes [12].

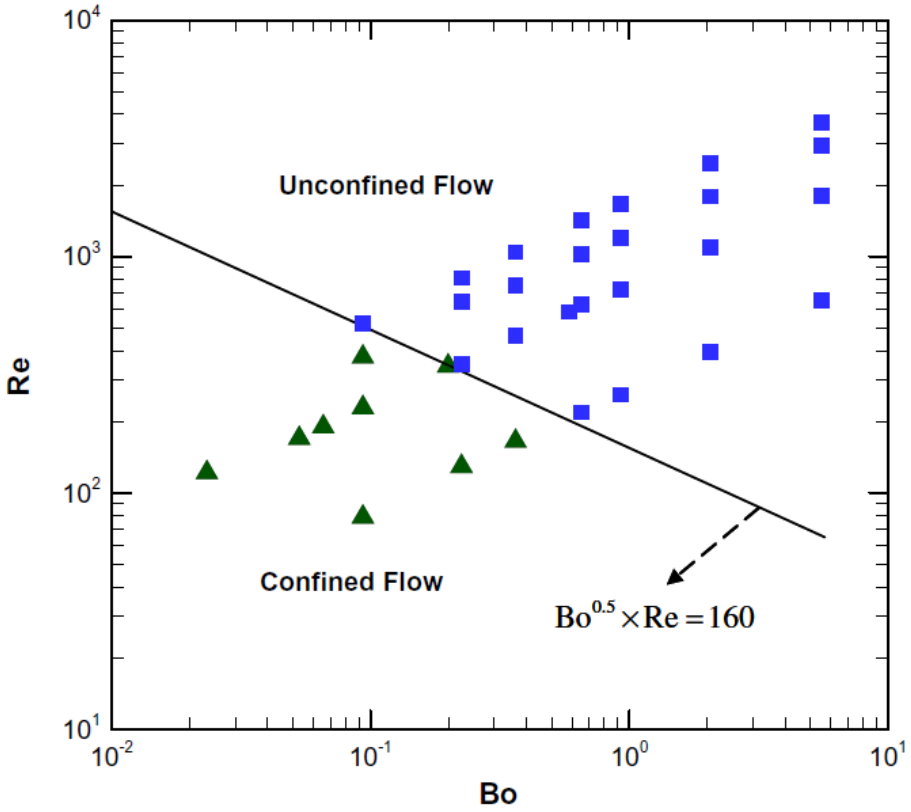

Fig. 5. Transition from confined flow to unconfined flow using flow behaviours defined by Harirchian and Garimella [22].

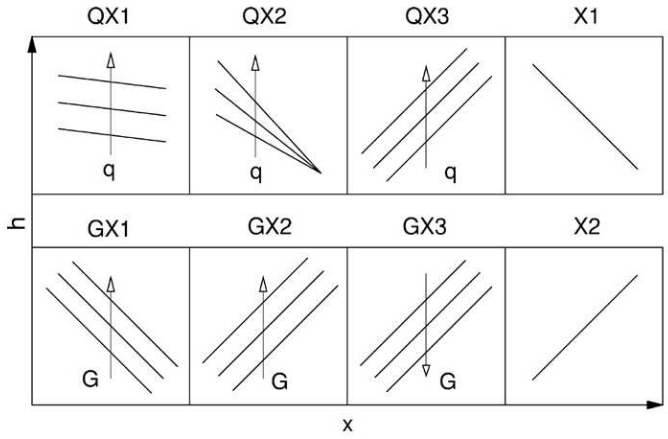

Fig. 6. Heat transfer coefficient h versus vapour quality x behaviours identified in the literature [7].

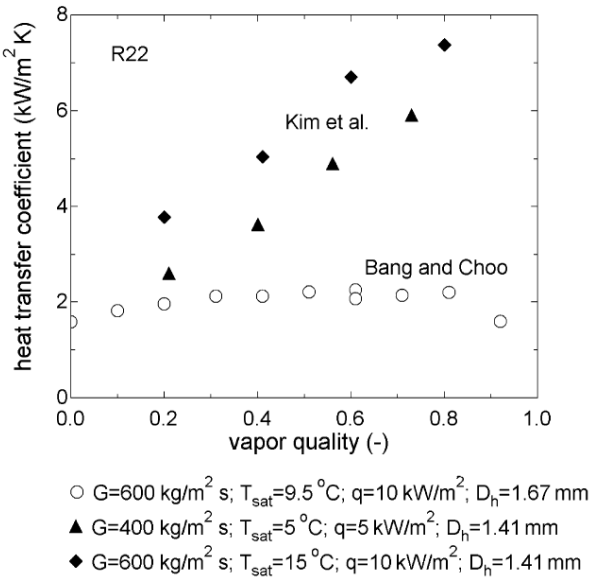

(a)

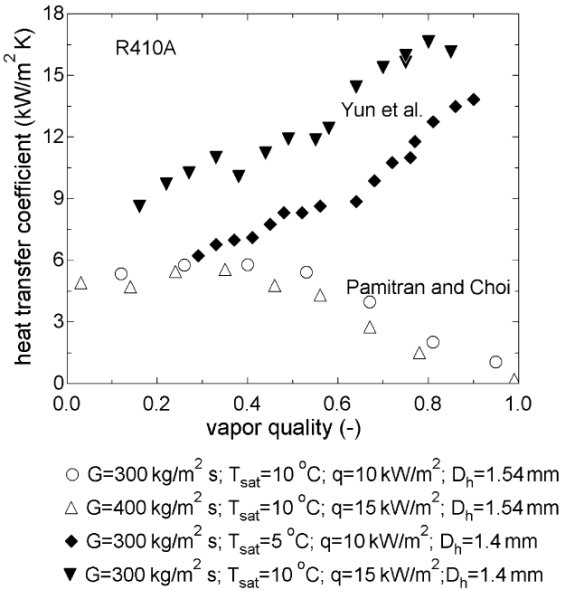

(b)

Fig. 7. (a) Comparison of the experimental results of Bang and Choo [66] and Kim et al. [67]; (b) Comparison of the experimental results of Pamitran and Choi [54] and Yun et al. [68] illustrated by Ribatski et al. in their review paper [7].

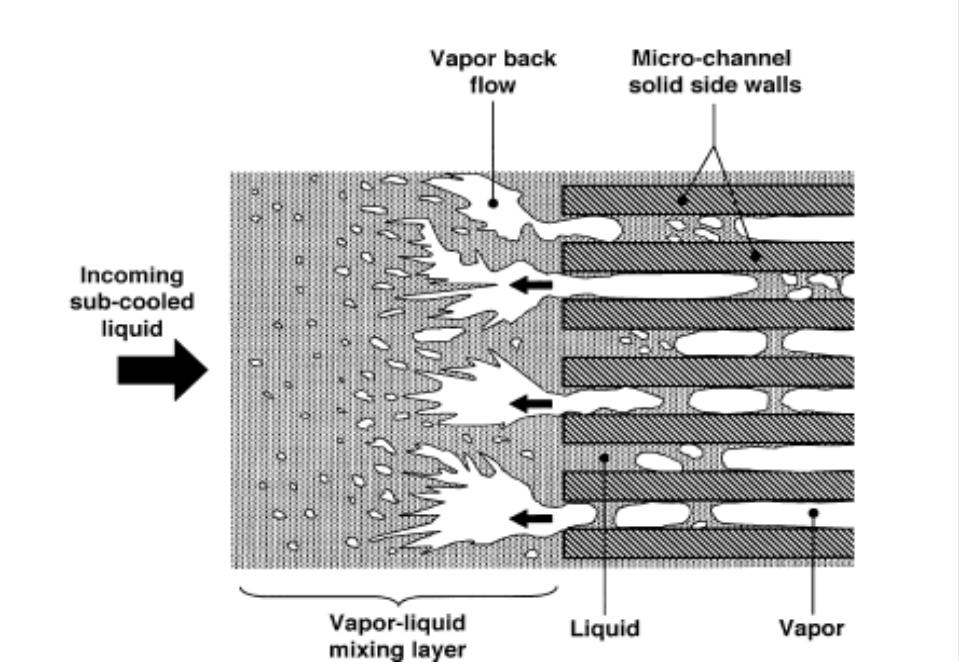

Fig. 8. Schematic representation of observed vapour backflow at high heat flux by Qu and Mudawar [47].

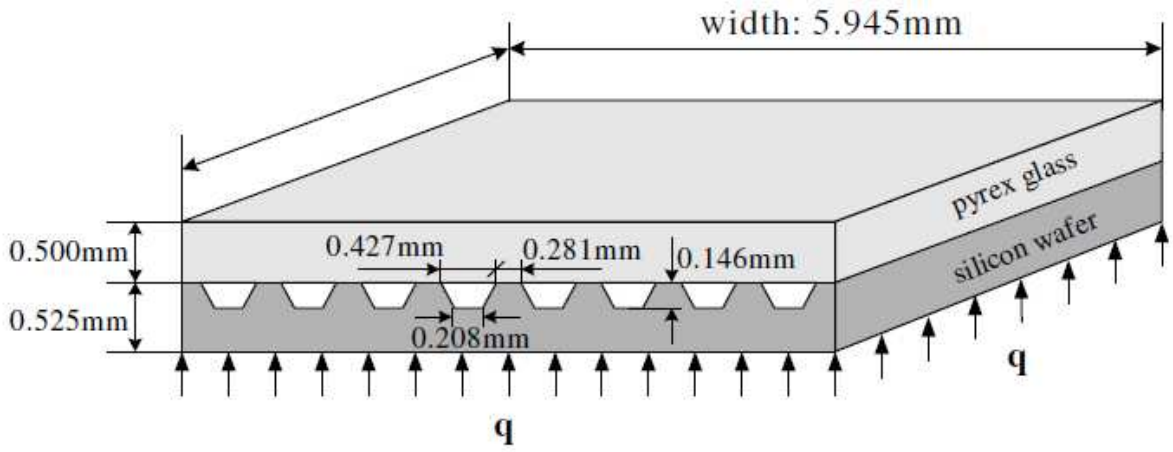

Fig. 9. Arrangement of 8 parallel microchannels having the same length and identical trapezoidal cross-sectional area and etched in a silicon substrate by Wang et al. [48].

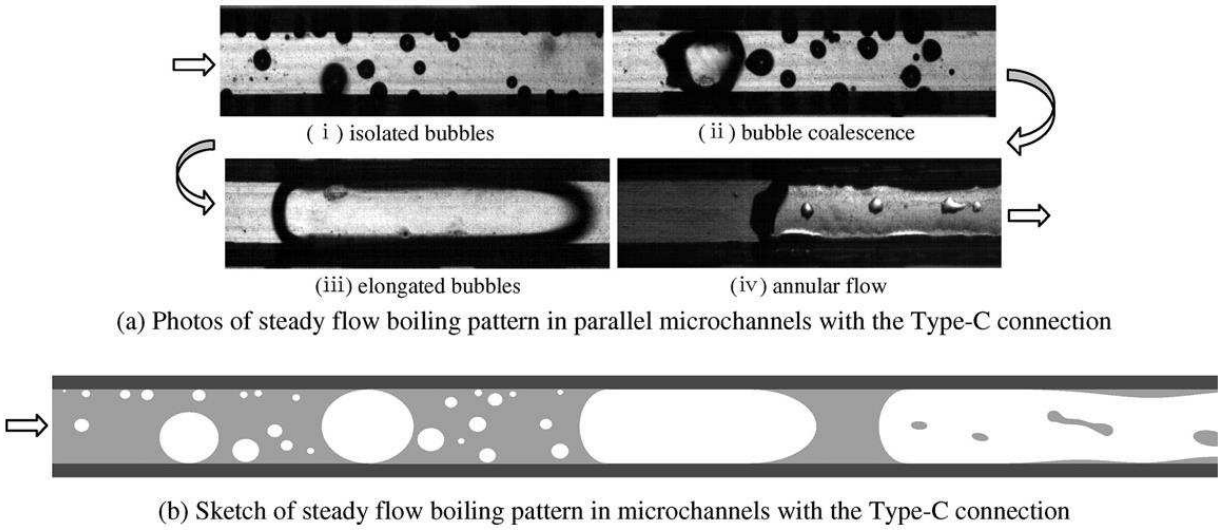

Fig. 10. Photographs and sketch of flow patterns in steady bubbly/slug flow boiling regime in parallel microchannels (D_h = 186 μm) with the Type-C connection at q = 364.68 kW/m^2, G = 124.03 kg/m^2 s and Tin = 35°C (i.e., x_e = 0.359) by Wang et al. [48].

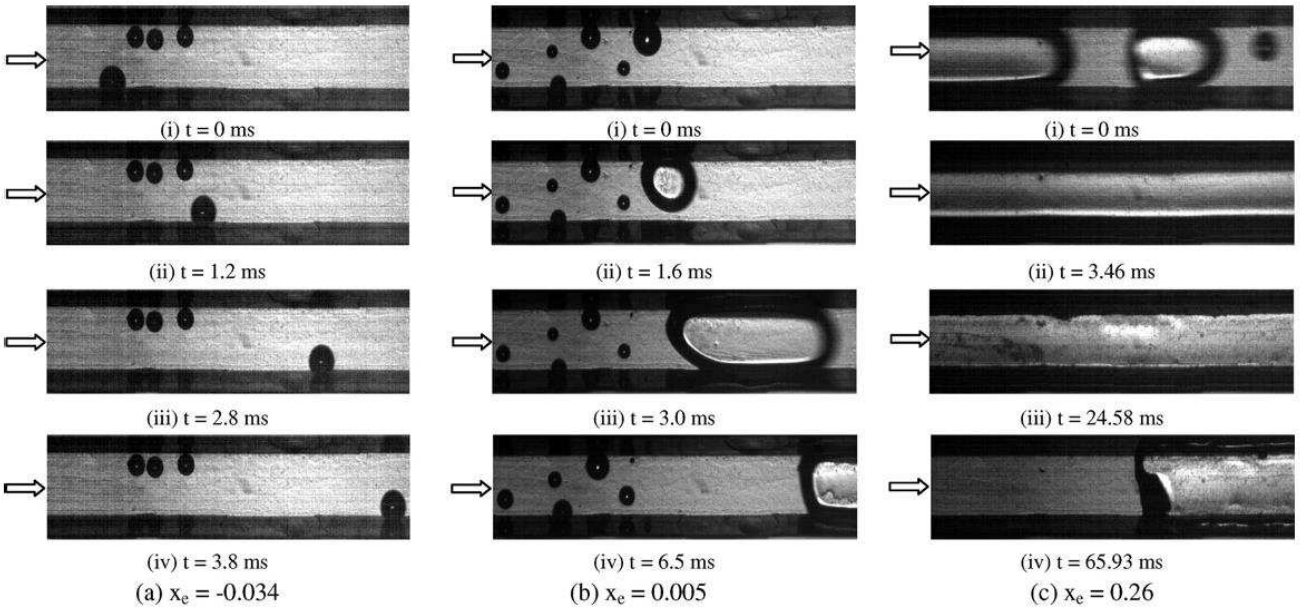

Fig. 11. Photos of steady flow boiling patterns near outlet section of parallel microchannels (D_h = 186 µm) with the Type-C connection at q = 364.68 kW/m^2 and T_{in} = 35°C: (a) G = 682.11 kg/m^2 s (i.e., x_e = -0.034), (b) G = 471.32 kg/m^2 s (i.e., x_e = 0.005), (c) G = 156.04 kg/m^2 s (i.e., x_e = 0.26), by Wang et al. [48].

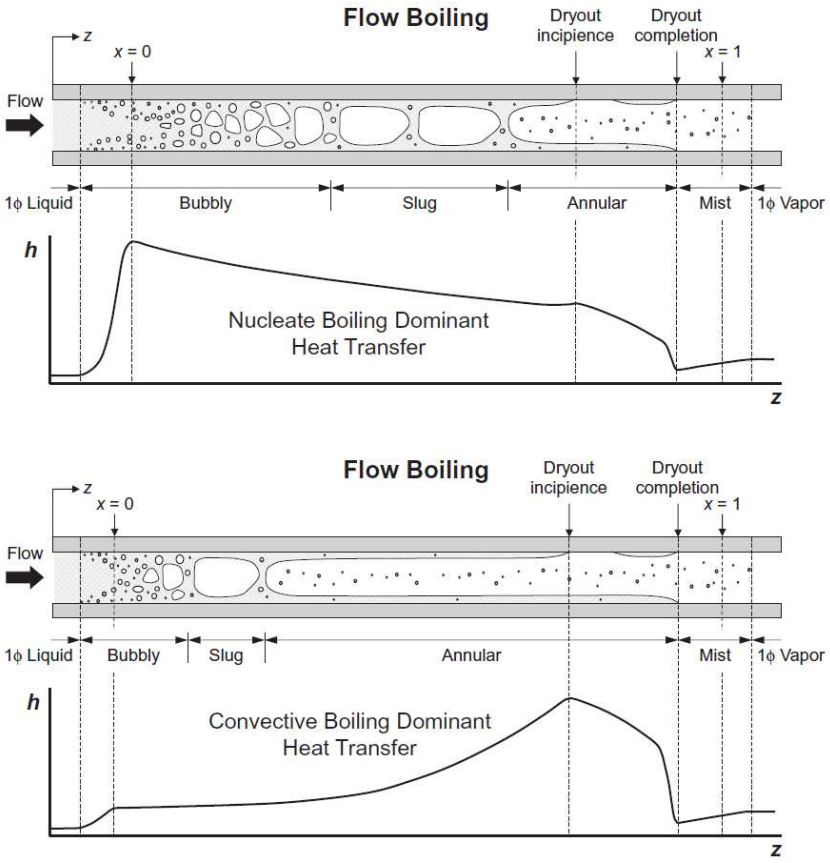

Fig. 12. Schematic of flow patterns and the corresponding heat transfer mechanisms and qualitative variation of the heat transfer coefficients for flow boiling in a horizontal tube [33].

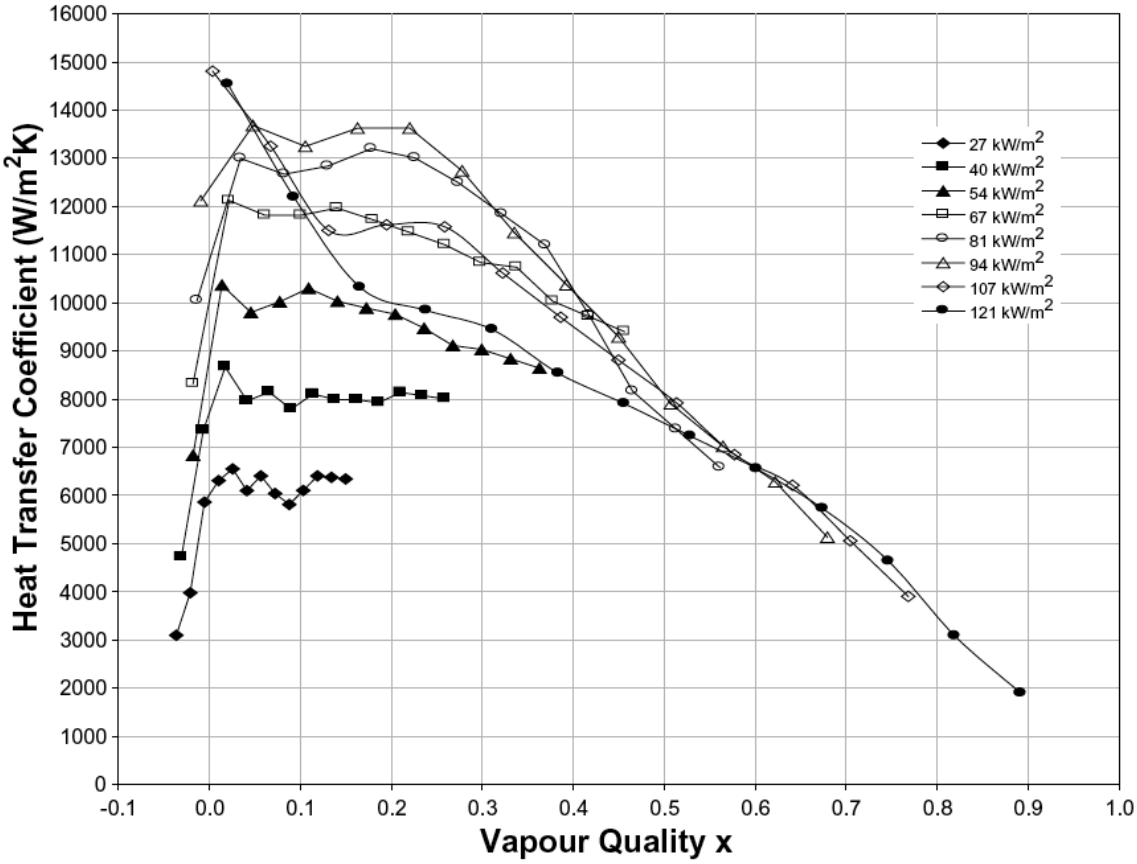

Fig. 13. Flow boiling data plotted versus vapour quality, Huo et al. [72].

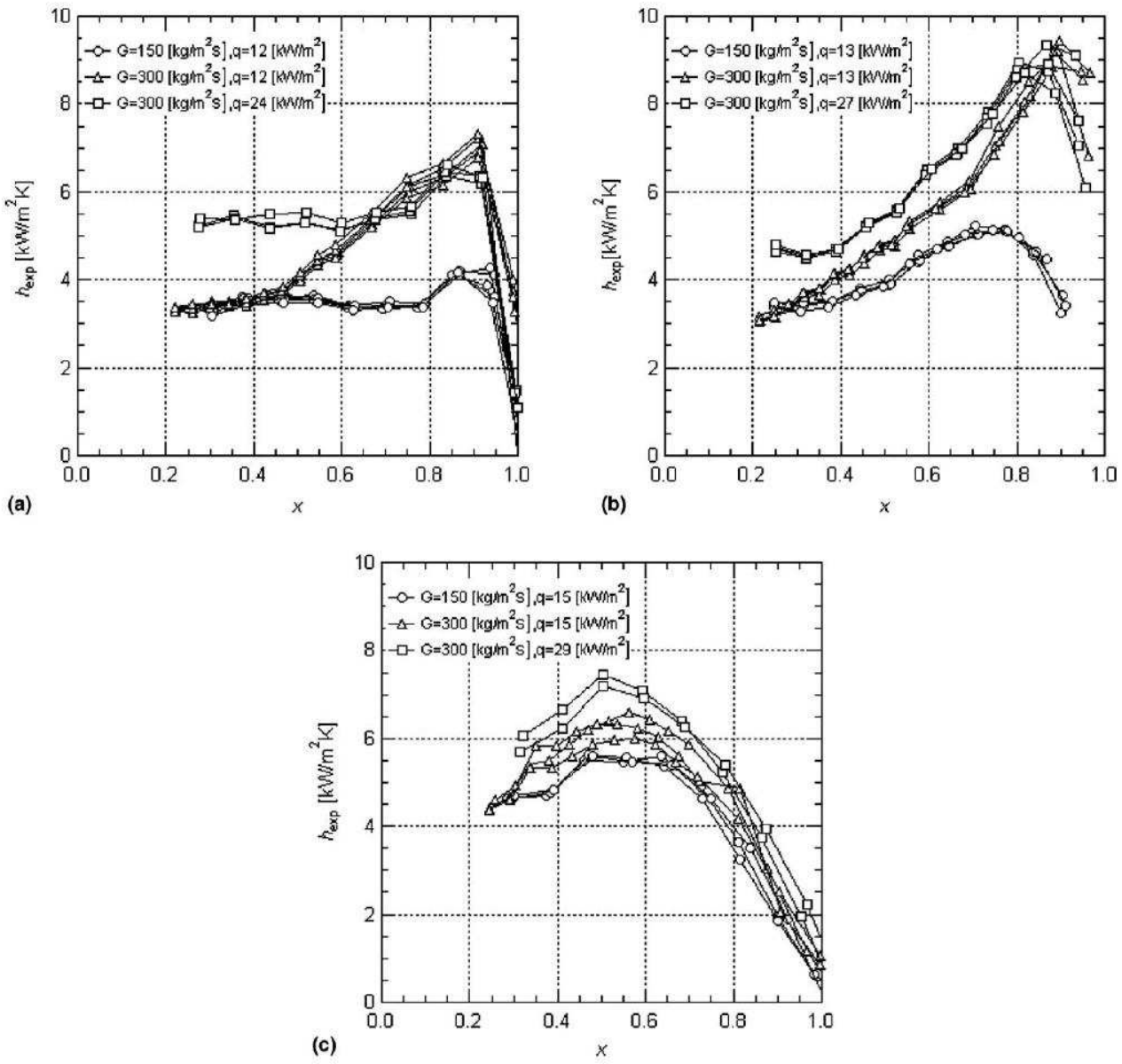

Fig. 14. Effect of heat flux (q) and mass flux (G) on heat transfer coefficient for three different diameter tubes: (a) 3.1-mm-ID; (b) 1.12-mm-ID and (c) 0.51-mm-ID [61].

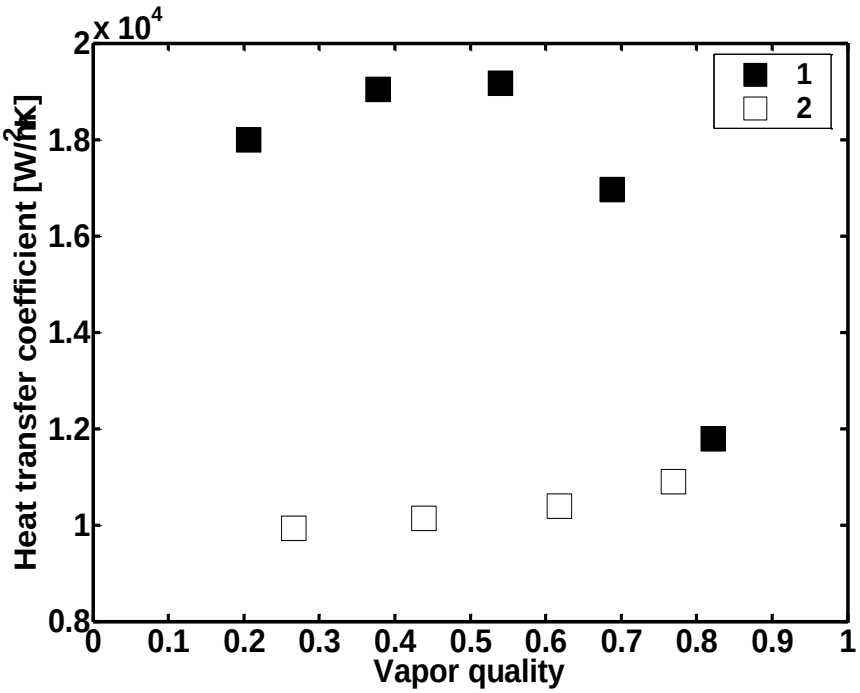

Fig. 15. The experimental heat transfer coefficients in the same literature showing different results with a very little change of hydraulic diameters from 1.53 mm to 1.54 mm (Solid symbols showing the experimental results of Yun et al. [100]: D_h = 1.53 mm, G = 300 kg/m^{2}s, T_{sat} = 5 °C and q = 20 W/m^2 and hollow symbols showing the experimental results of Yun et al. al.: D_h = 1.54 mm, G = 300 kg/m^{2}s, T_{sat} = 5 °C and q =20 W/m^2.).

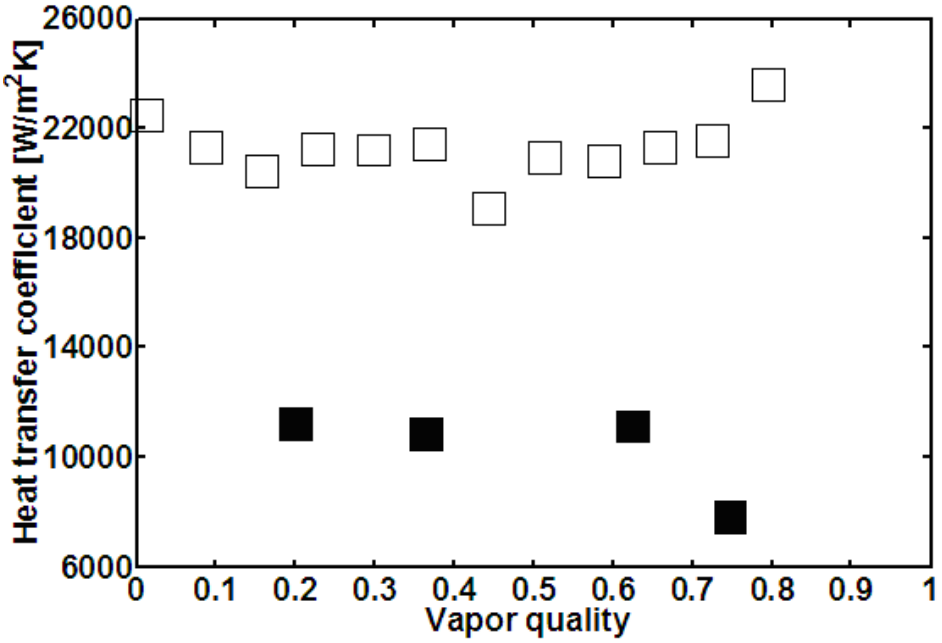

Fig. 16. The experimental heat transfer coefficients in the literature showing opposite behaviour of heat transfer (Solid symbols showing the experimental results of Pettersen [101]: D_h = 0.8 mm, G = 190 kg/m^{2}s, T_{sat} = 0 °C and q = 10 W/m^2 and hollow symbols showing the experimental results of Koyama et al. al. [102]: D_h = 1.8 mm, G = 260 kg/m^{2}s, T_{sat} = 0.26 °C and q =32.06 W/m^2.).

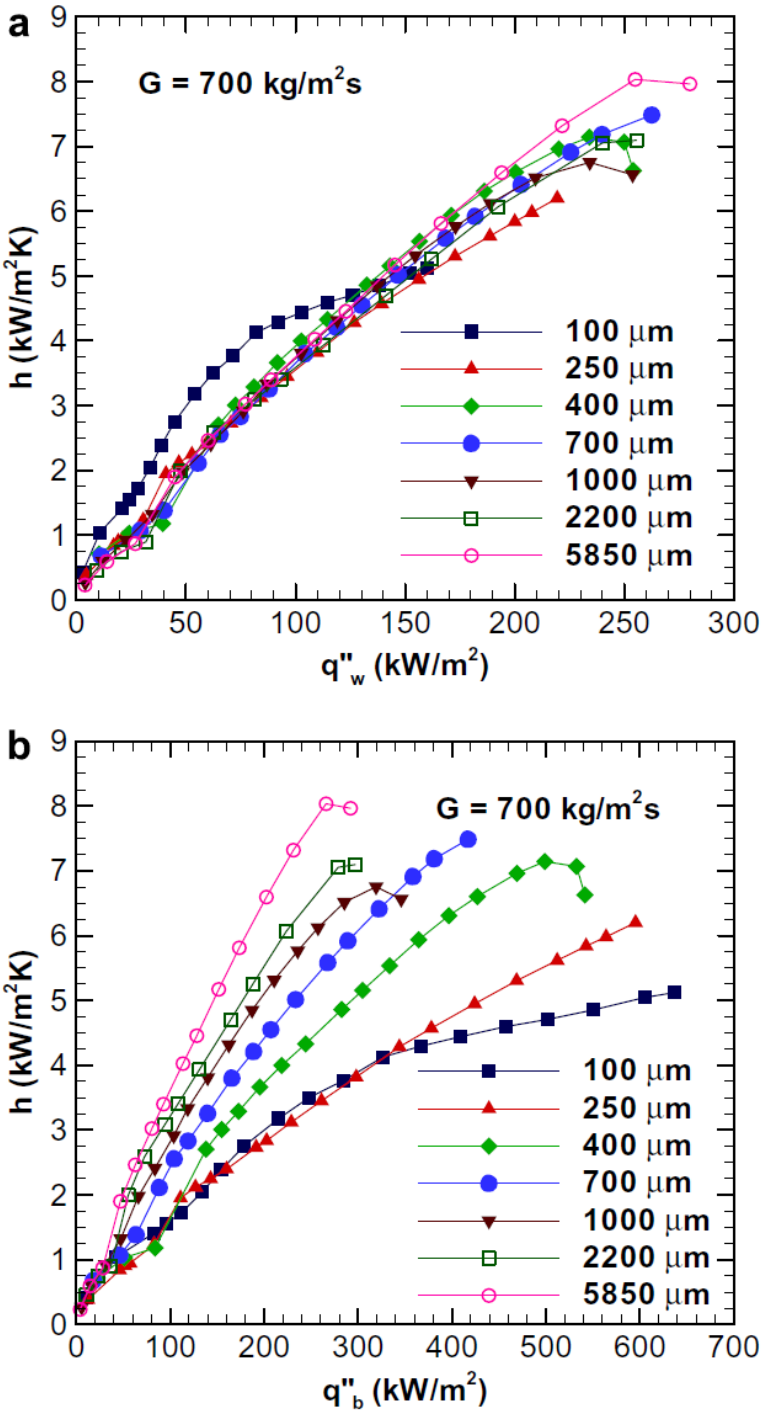

Fig. 17. Effect of microchannel width on local heat transfer coefficient as a function of (a) wall heat flux and (b) base heat flux. [65].

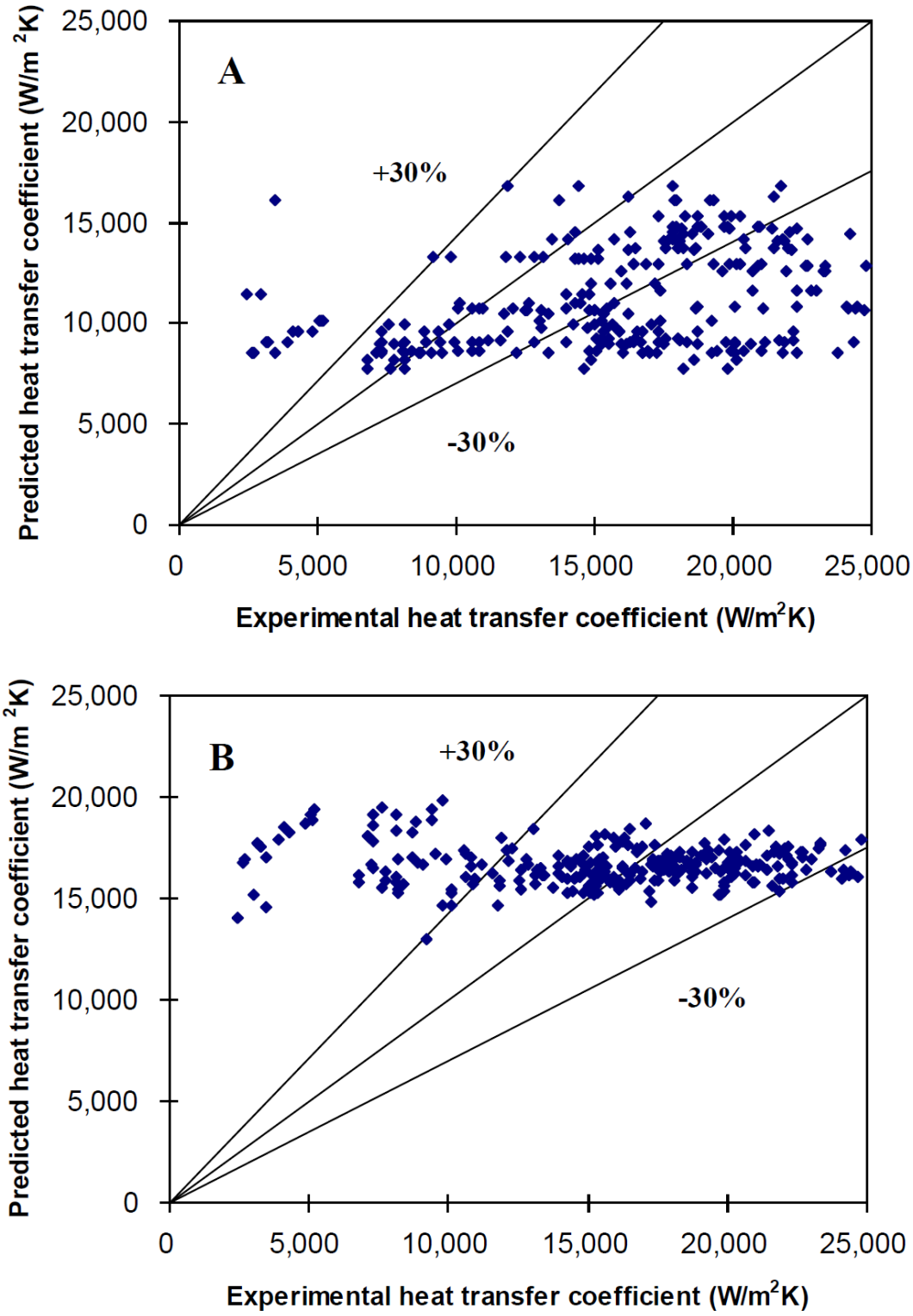

Fig. 18. Comparison of N_2 heat transfer coefficient data with the best predictive correlation (A) Tran et al. [70]; (B) Li and Wu [58].

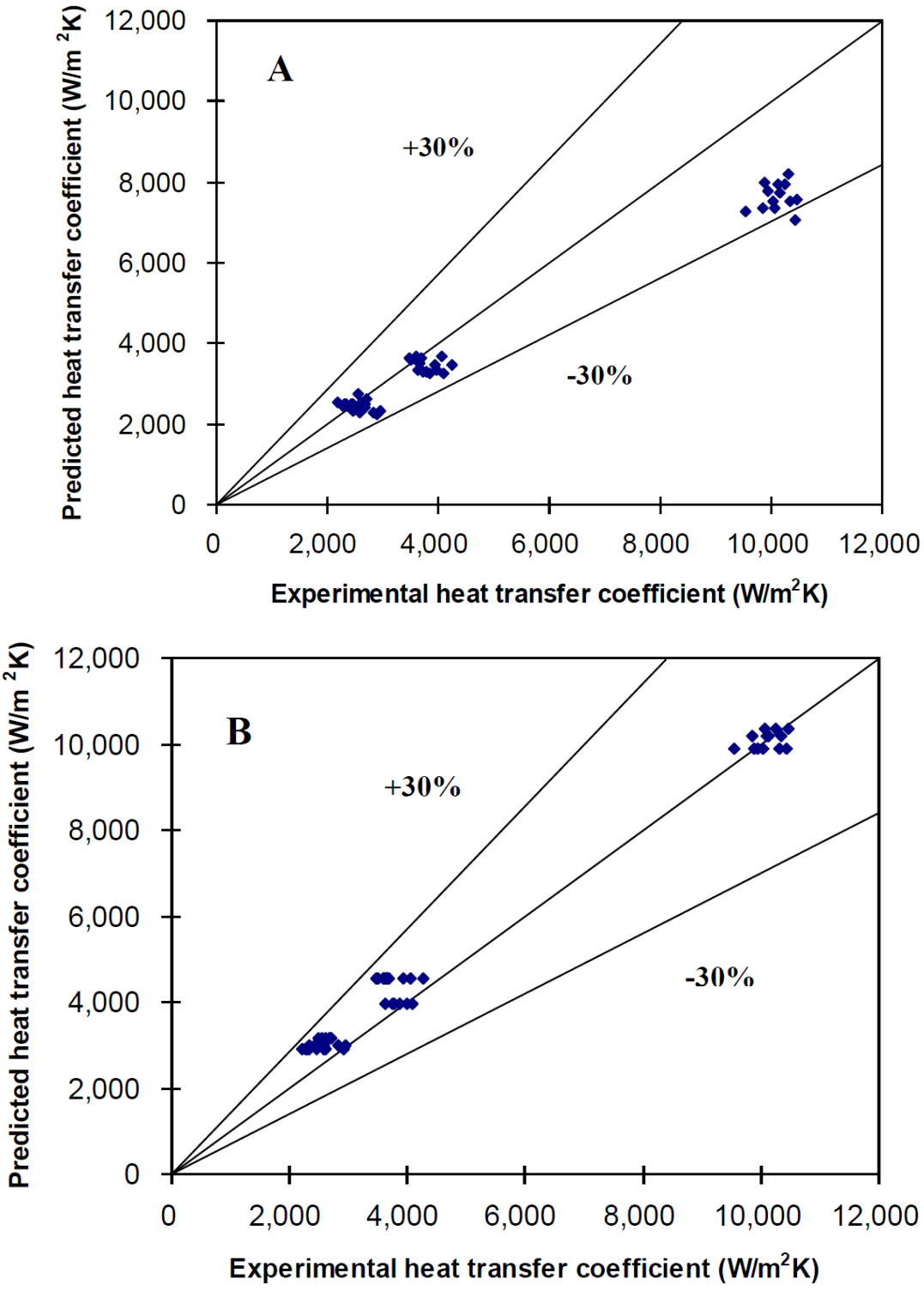

Fig. 19. Comparison of R12 heat transfer coefficient data with the best predictive correlation (A) Saitoh et al. [61]; (B) Sun and Mishima [57].

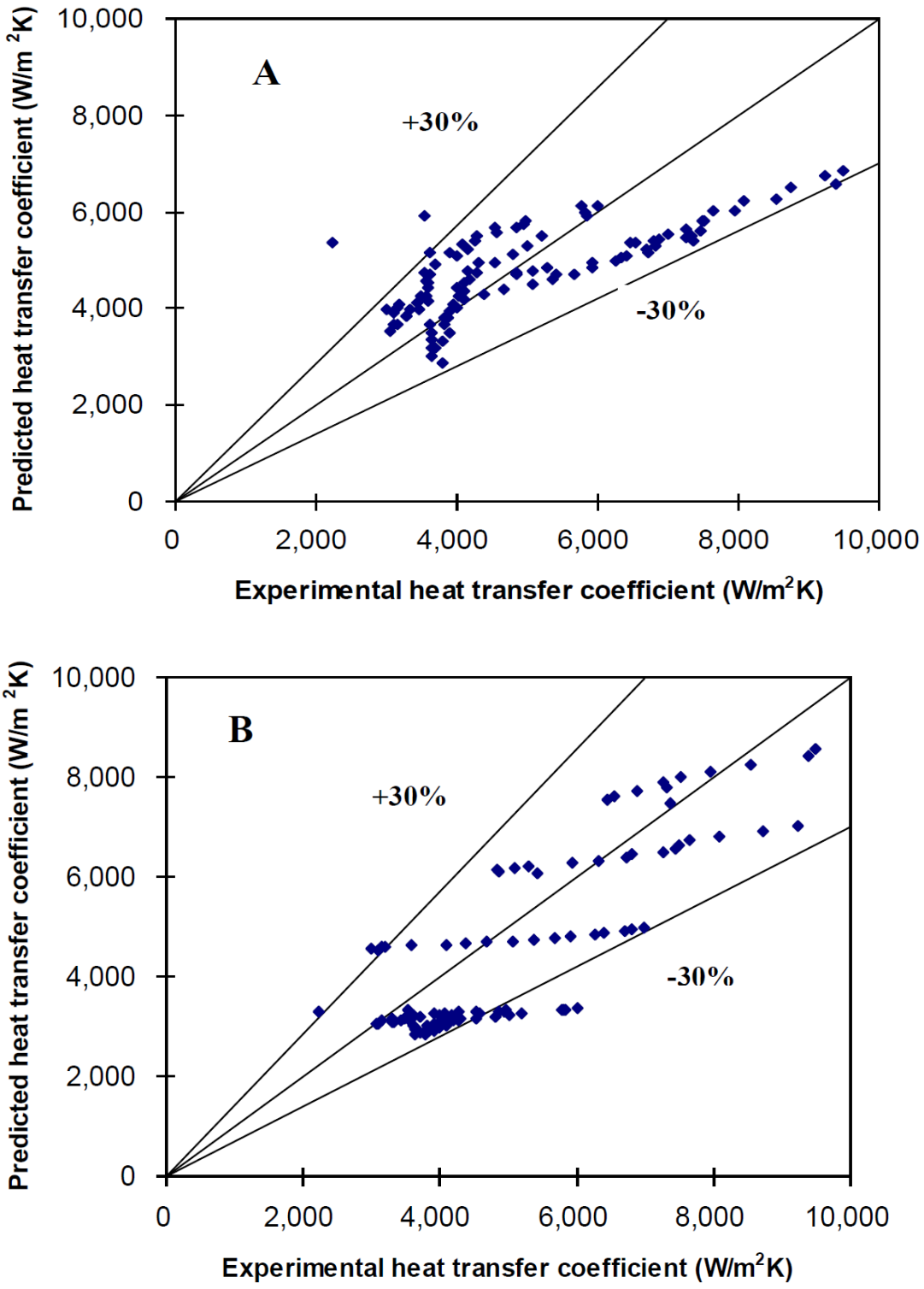

Fig. 20. Comparison of R22 heat transfer coefficient data with the best predictive correlation (A) Saitoh et al. [61]; (B) Kew and Cornwell [20].

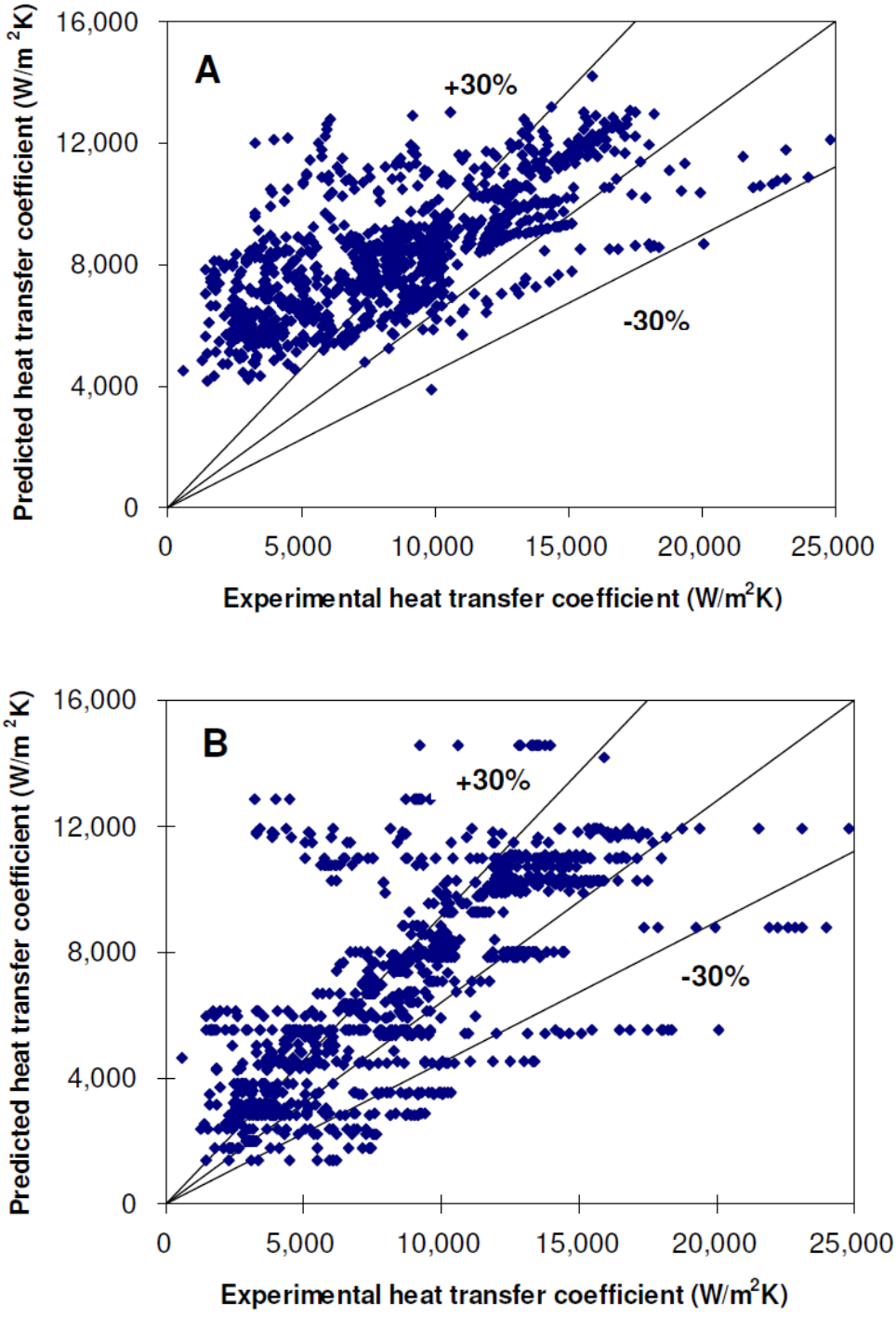

Fig. 21. Comparison of R134a heat transfer coefficient data to the best two correlations: (A) Li and Wu [58]; (B) Sun and Mishima [57].

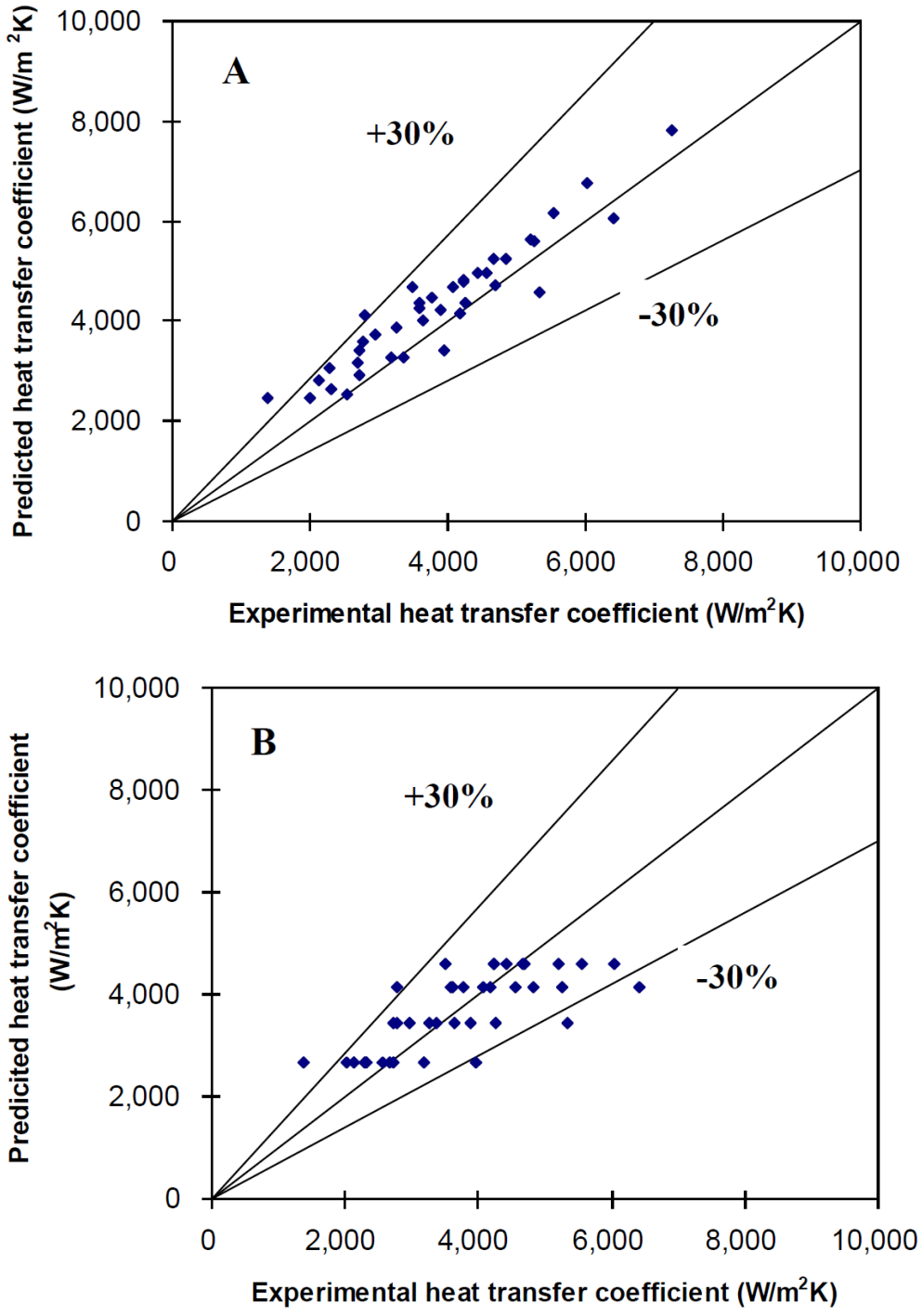

Fig. 22. Comparison of R141b heat transfer coefficient data with the best predictive correlation (A) Saitoch et al. [61] ; (B) Sun and Mishima [57].

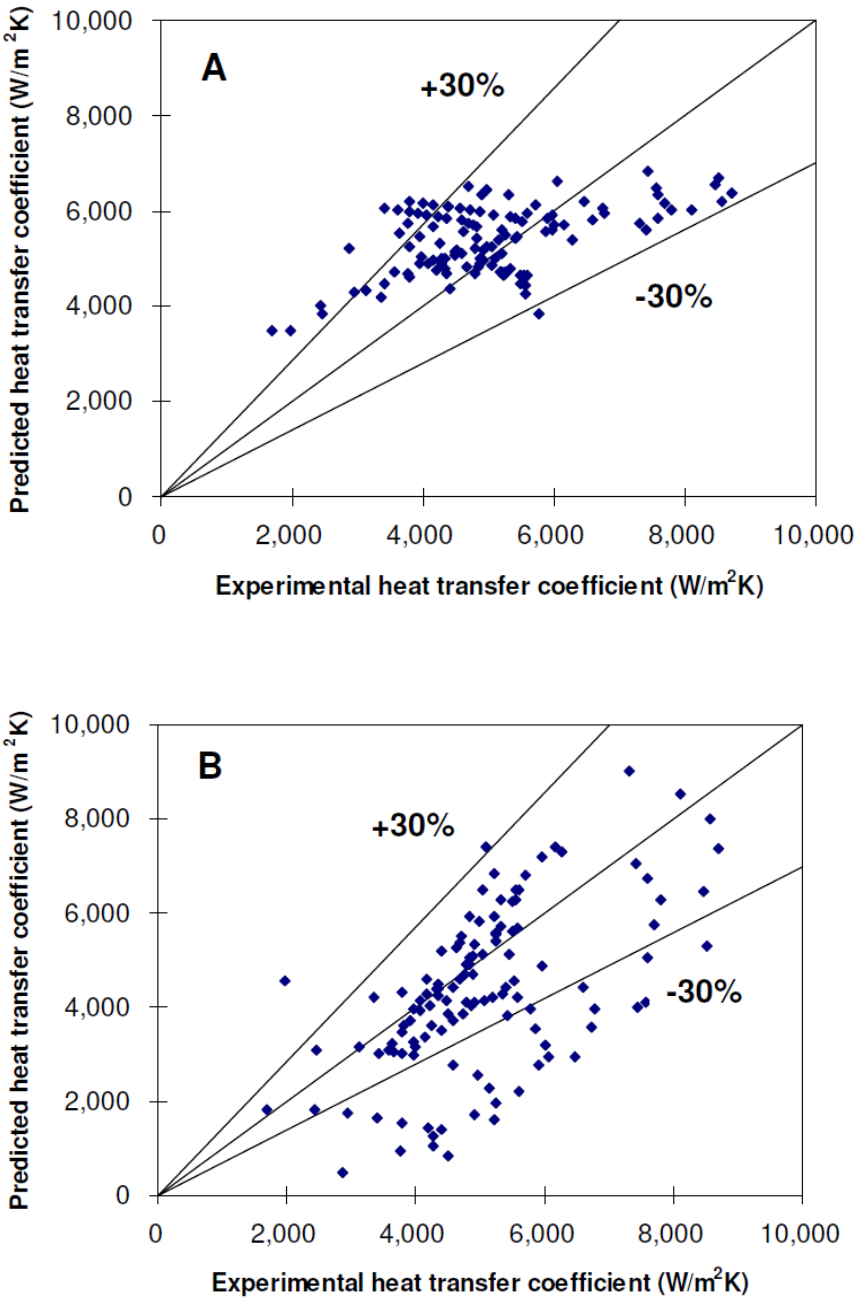

Fig. 23. Comparison of R245fa heat transfer coefficient data to the best two correlations: (A) Li and Wu [58]; (B) Chen [20].

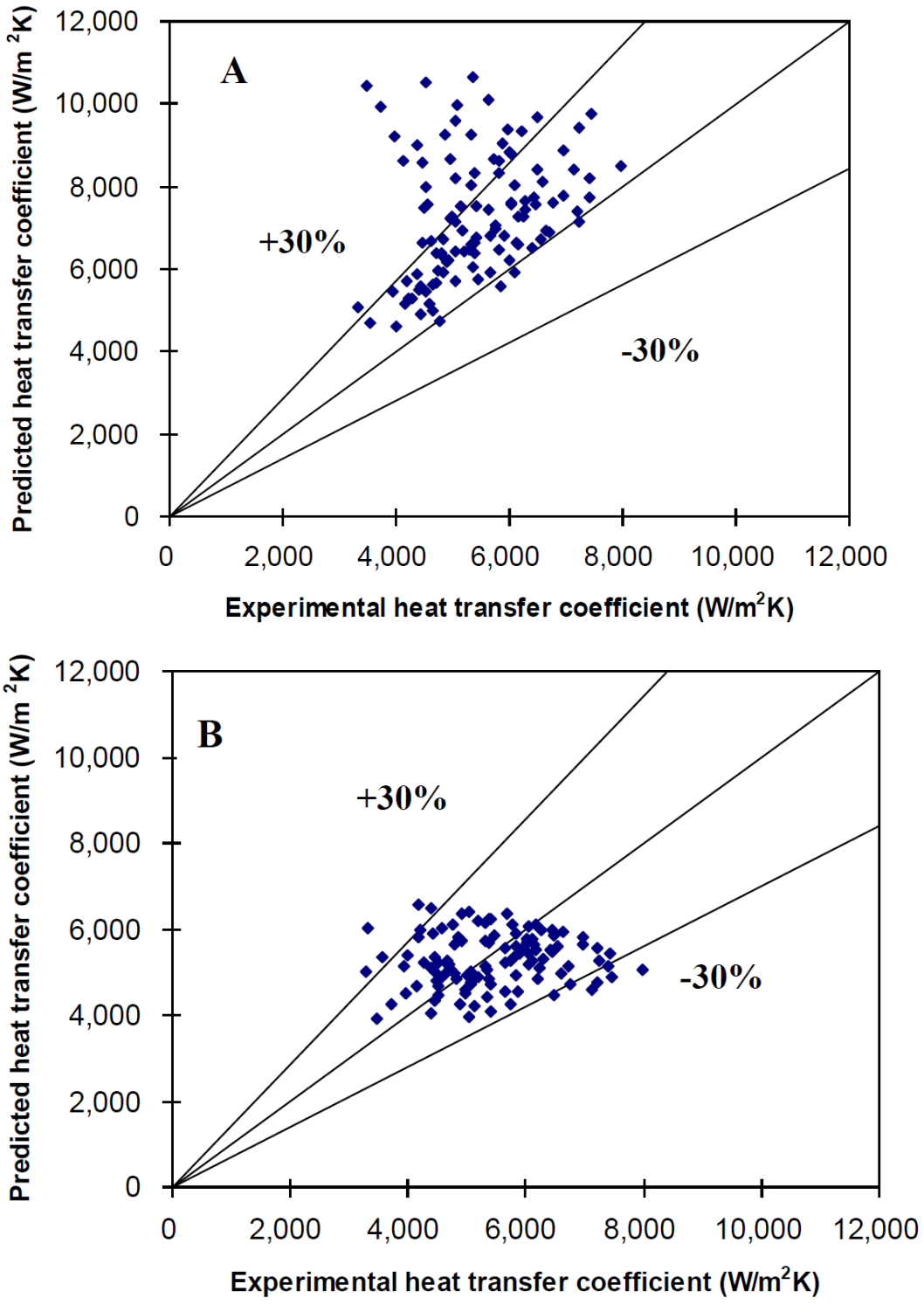

Fig. 24. Comparison of R123 heat transfer coefficient data with the best predictive correlation: (A) Zhang et al. [52]; (B) Li and Wu [58].

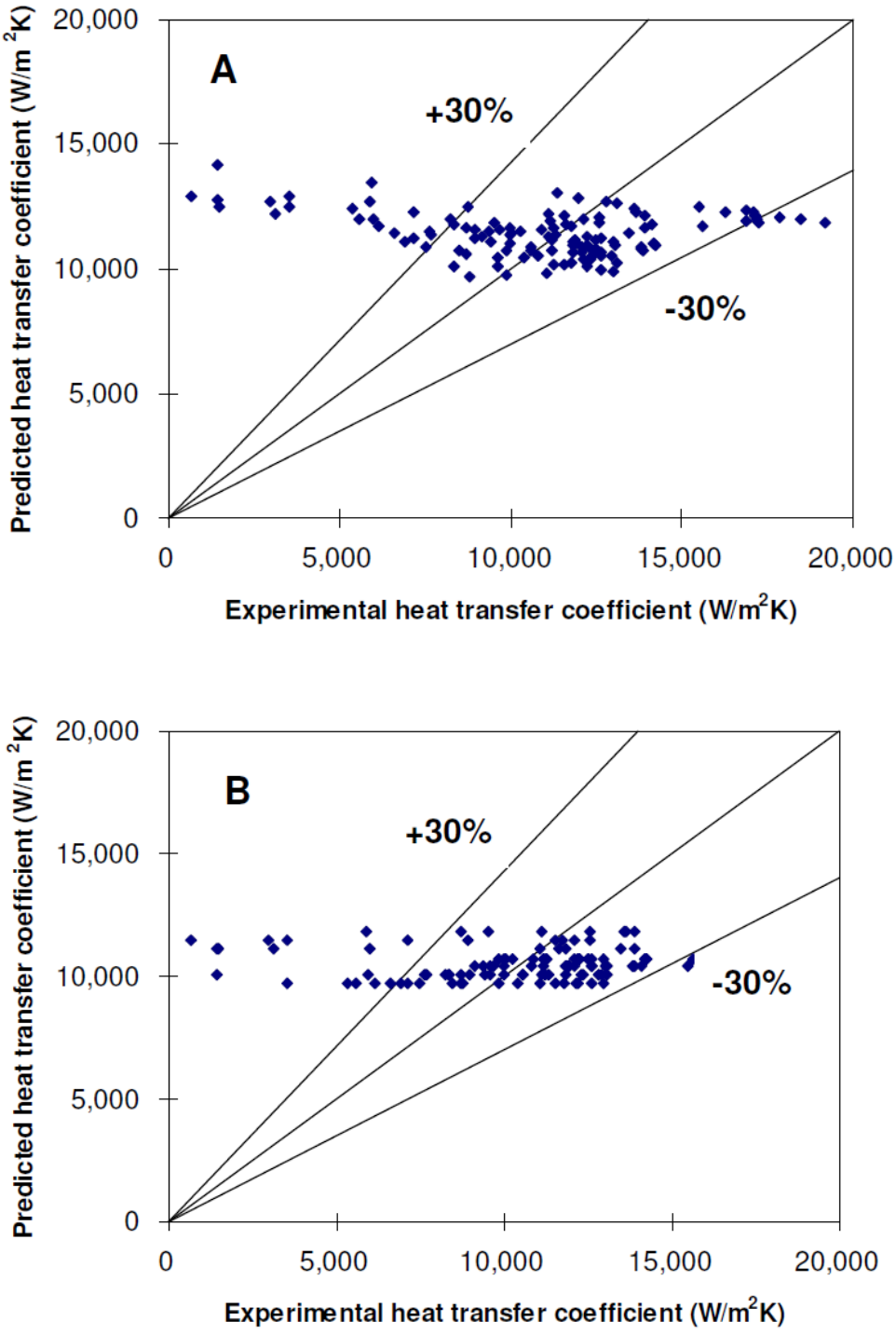

Fig. 25. Comparison of R410A heat transfer coefficient data to the best two correlations: (A) Kew and Cornwell [20]; (B) Lazarek and Black [49].

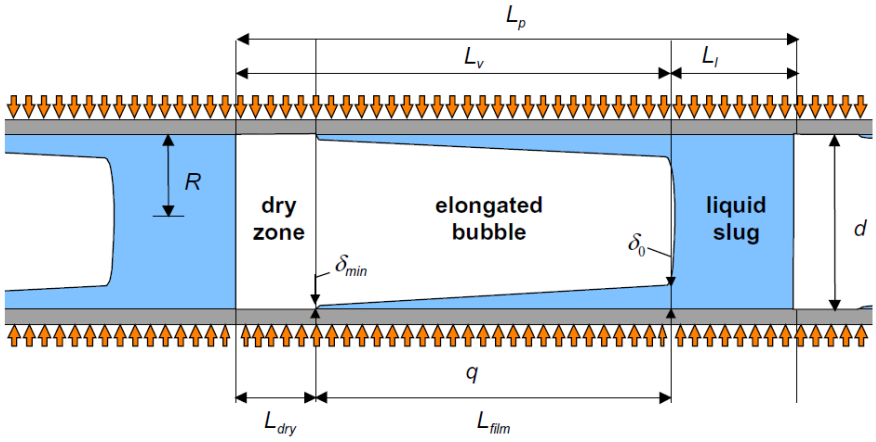

Fig. 26. The Three-zone heat transfer model for elongated bubble flow regime in microscale channels: diagram illustrating a triplet comprised of a liquid slug, an elongated bubble and a vapour slug [87].

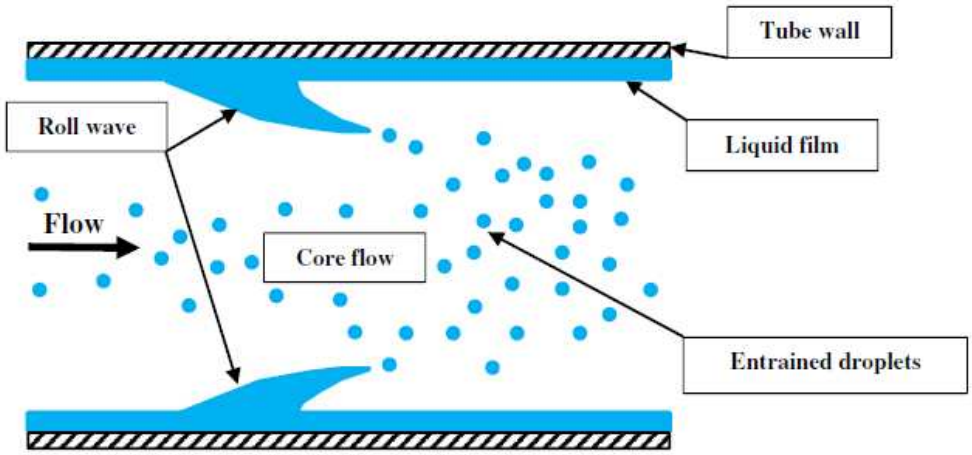

Fig. 27. Annular flow model in tubes [105].

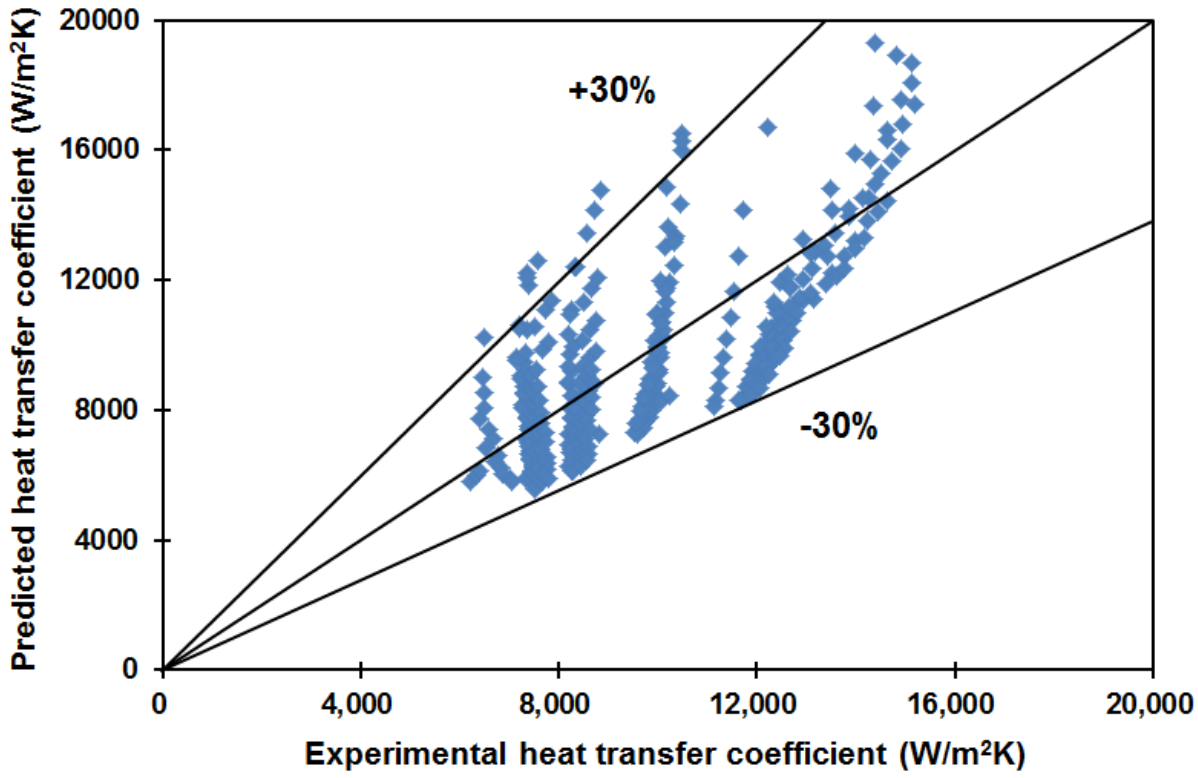

Fig. 28. Comparison of R134a heat transfer coefficient data by Wang et al. [64] to the Thome et al. three zone heat transfer model [87]: 90.4% of the data are predicted by the model with ±30%.

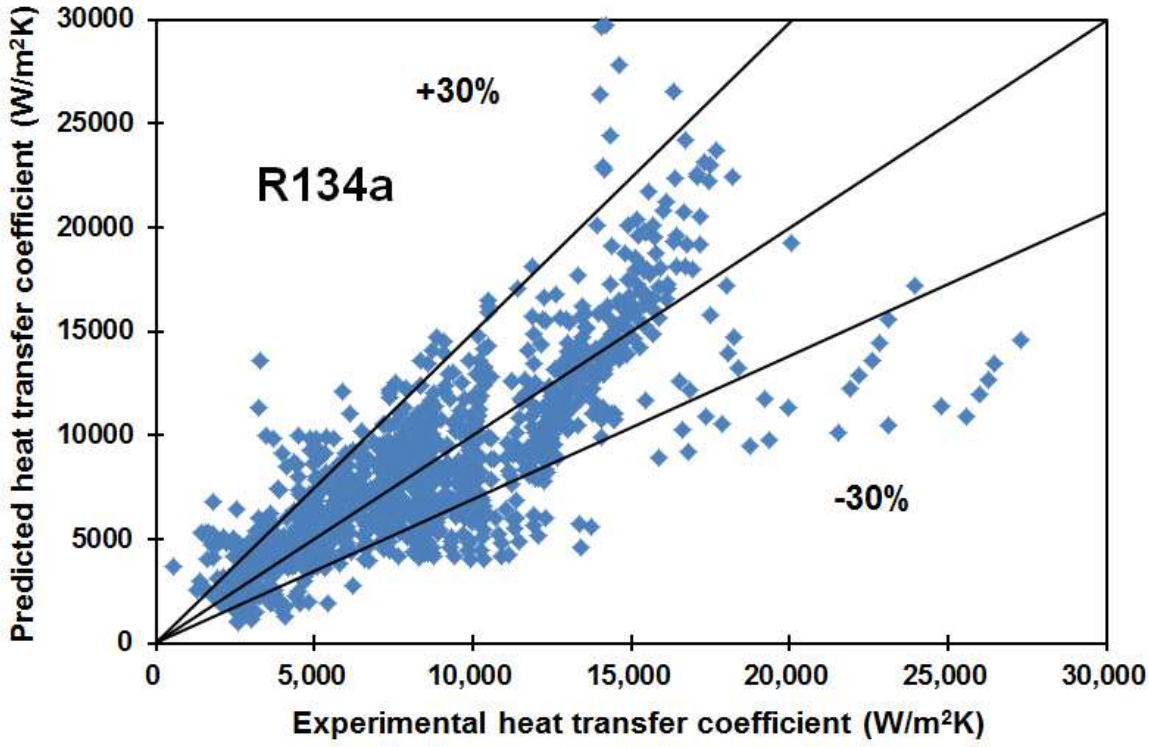

Fig. 29(a) Comparison of the whole R134a heat transfer coefficient data to the flow pattern based heat transfer model combining the three zone heat transfer model [87] and the unified annular flow heat transfer model [105, 106].

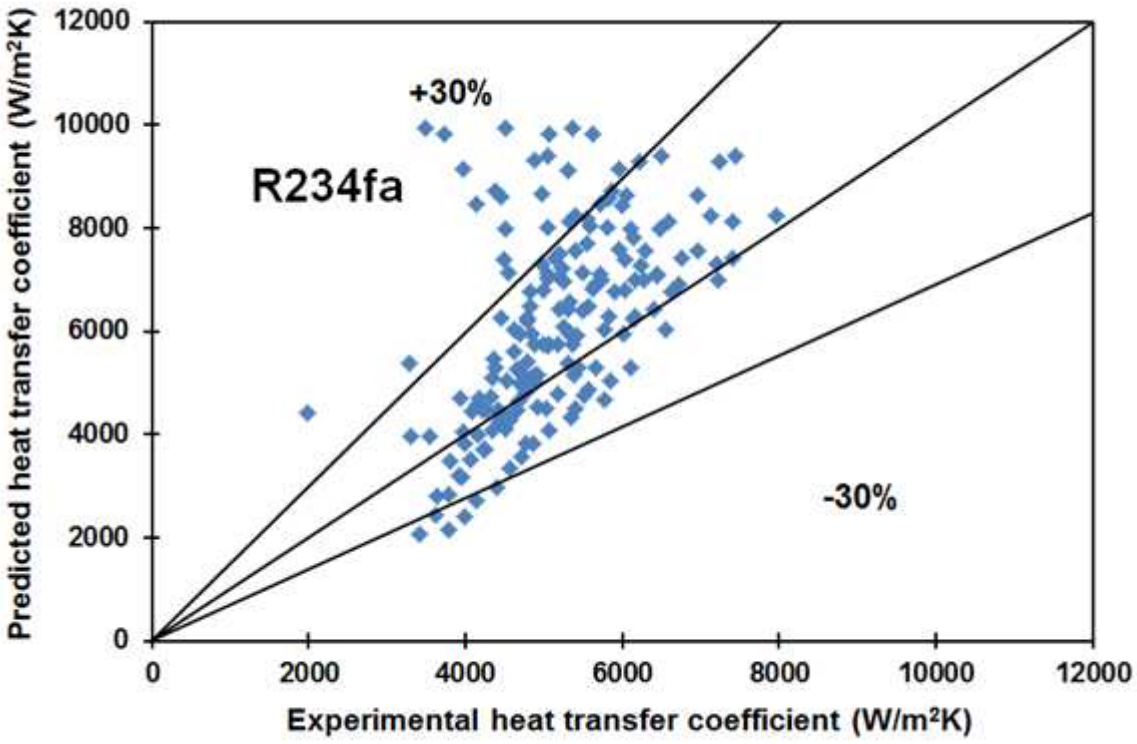

Fig. 29(b) Comparison of the whole R234fa heat transfer coefficient data to the flow pattern based heat transfer model combining the three zone heat transfer model [87] and the unified annular flow heat transfer model [105, 106].

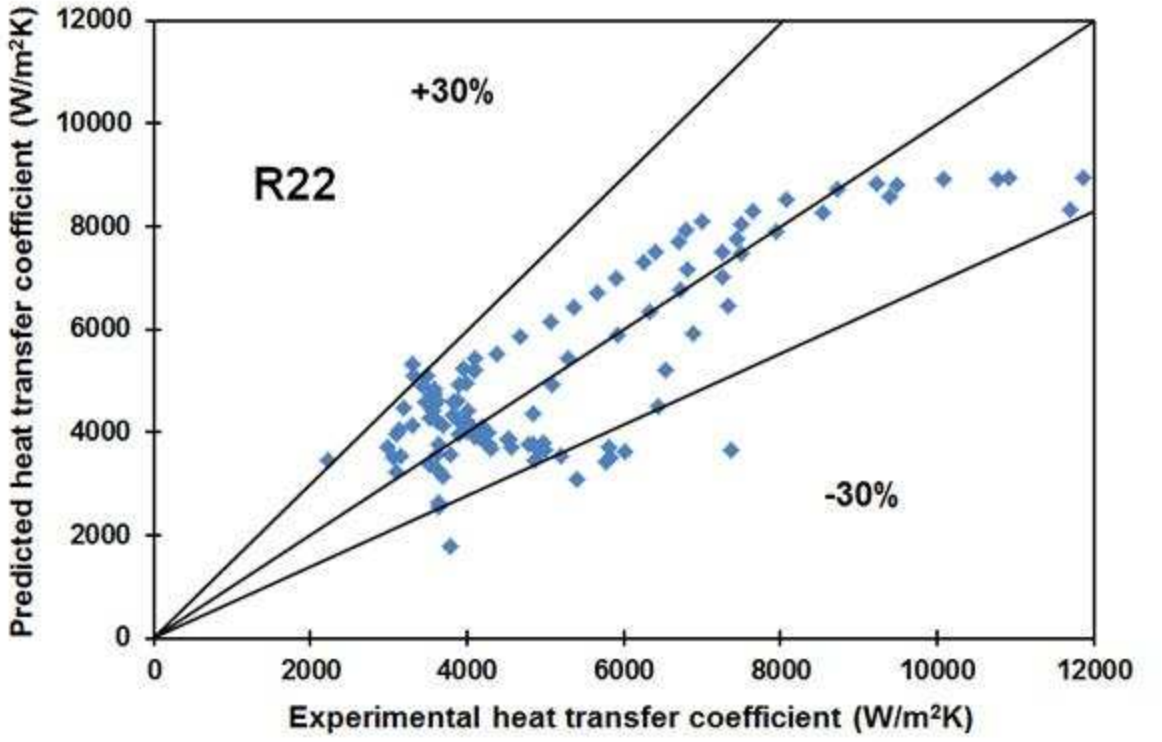

Fig. 29(c) Comparison of the whole R22 heat transfer coefficient data to the flow pattern based heat transfer model combining the three zone heat transfer model [87] and the unified annular flow heat transfer model [105, 106].

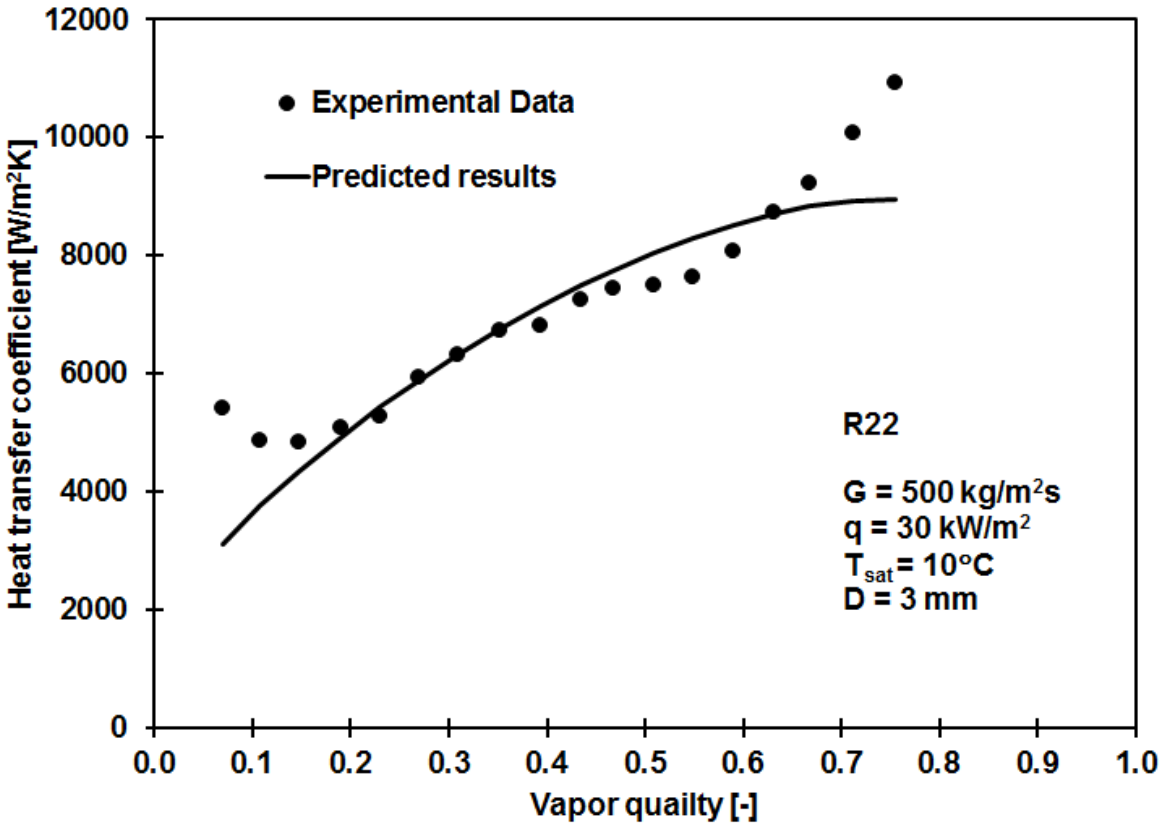

Fig. 30(a) Comparison of the R22 heat transfer coefficient data to the flow pattern based heat transfer model combining the three zone heat transfer model [87] and the unified annular flow heat transfer model [105, 106] at the conditions: mass flux G = 500 kg/m^{2}s, heat flux q = 30 kW/m^2, saturation temperature T_{sat} = 10°C and tube diameter D = 3 mm.

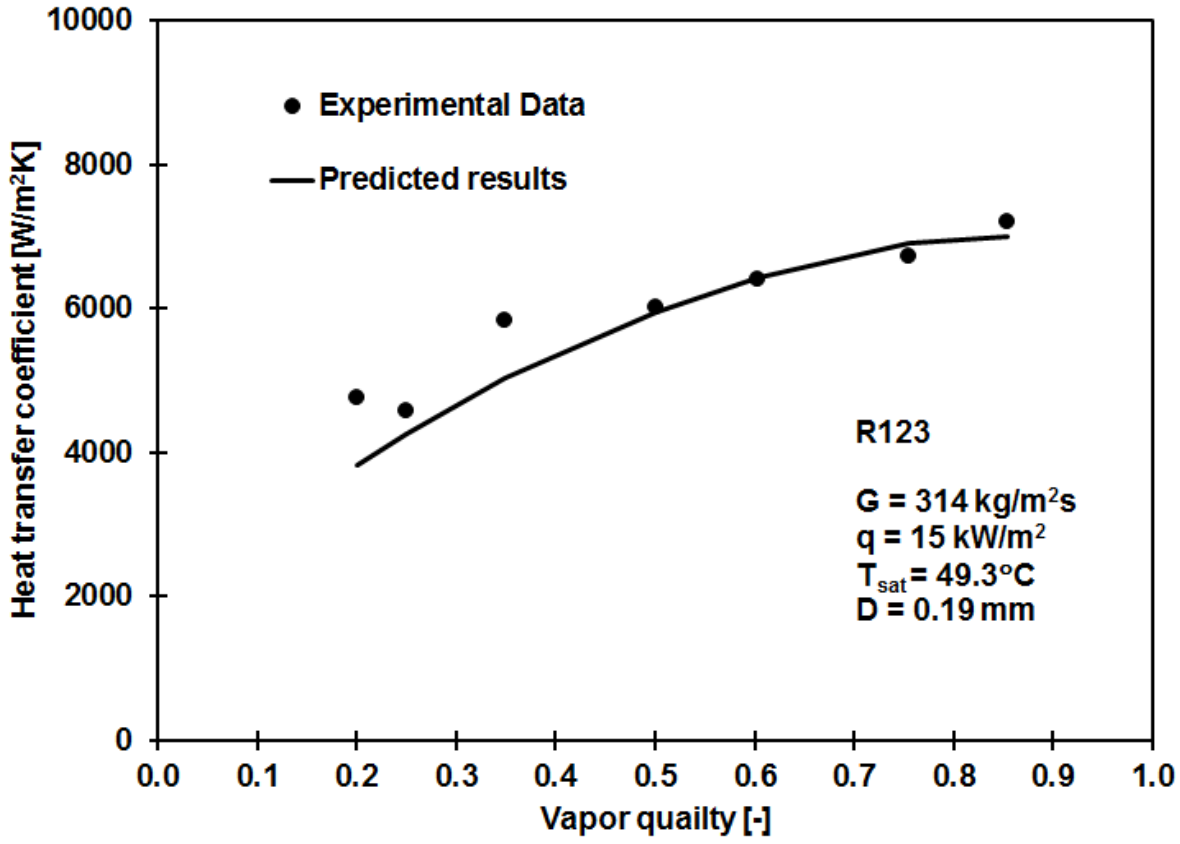

Fig. 30(b) Comparison of the R123 heat transfer coefficient data to the flow pattern based heat transfer model combining the three zone heat transfer model [87] and the unified annular flow heat transfer model [105, 106] at the conditions: mass flux G = 314 kg/m^{2}s, heat flux q = 15 kW/m^2, saturation temperature T_{sat} = 49.3°C and tube diameter D = 0.19 mm.

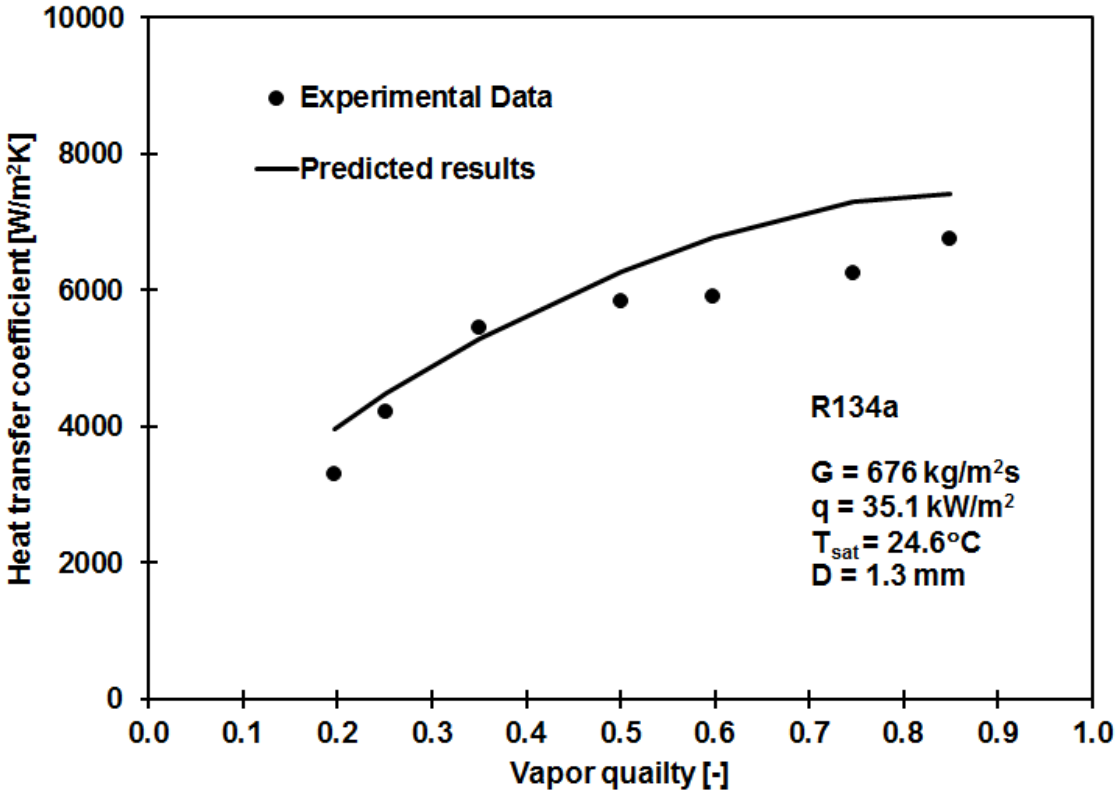

Fig. 30(c) Comparison of the R134 heat transfer coefficient data to the flow pattern based heat transfer model combining the three zone heat transfer model [87] and the unified annular flow heat transfer model [105, 106] at the conditions: mass flux G = 676 kg/m^{2}s, heat flux q = 35.1 kW/m^2, saturation temperature T_{sat} = 24.6°C and tube diameter D = 1.3 mm.

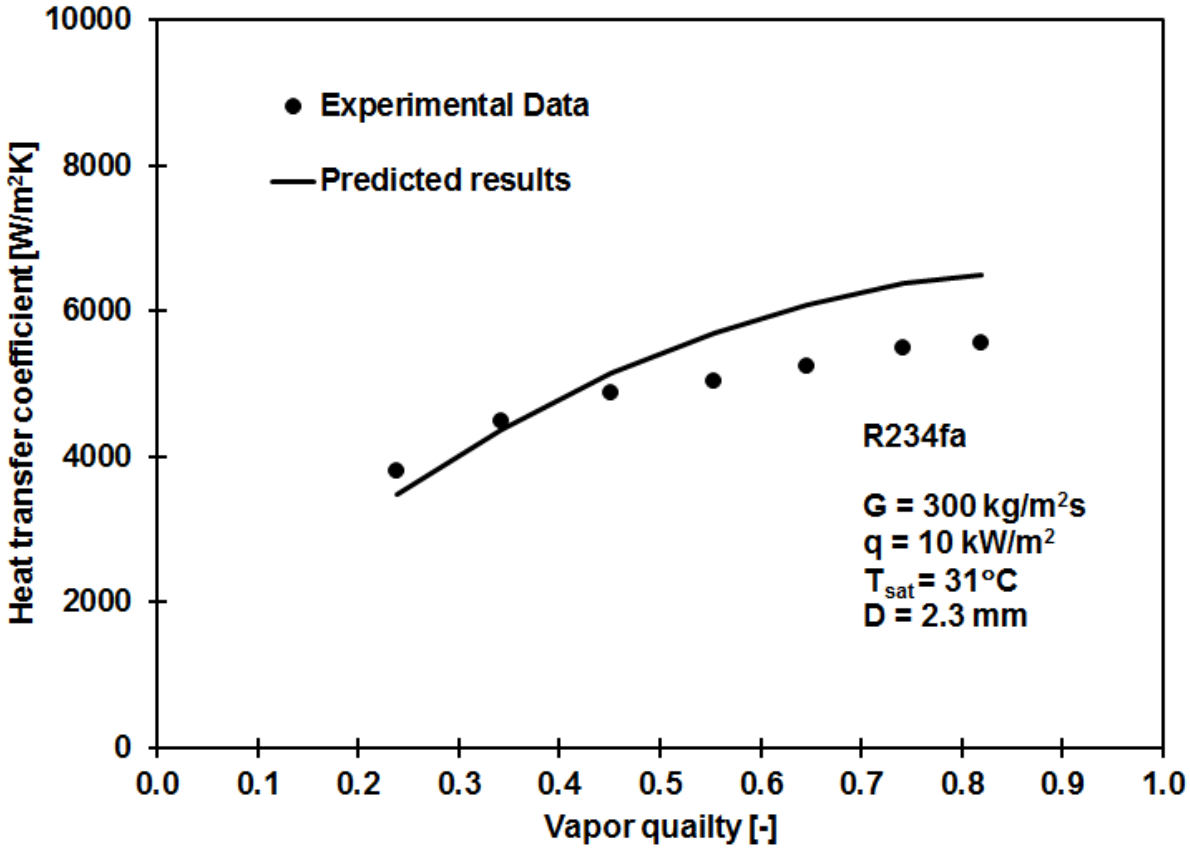

Fig. 30(d) Comparison of the R234fa heat transfer coefficient data to the flow pattern based heat transfer model combining the three zone heat transfer model [87] and the unified annular flow heat transfer model [105, 106] at the conditions: mass flux G = 300 kg/m^{2}s, heat flux q = 10 kW/m^2, saturation temperature T_{sat} = 31°C and tube diameter D = 2.3 mm.

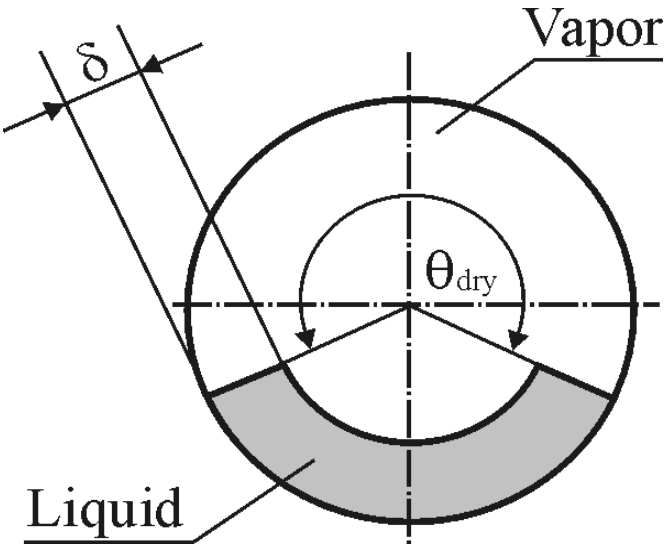

Fig. 31. Schematic diagram of dry angle and physical model for flow boiling.

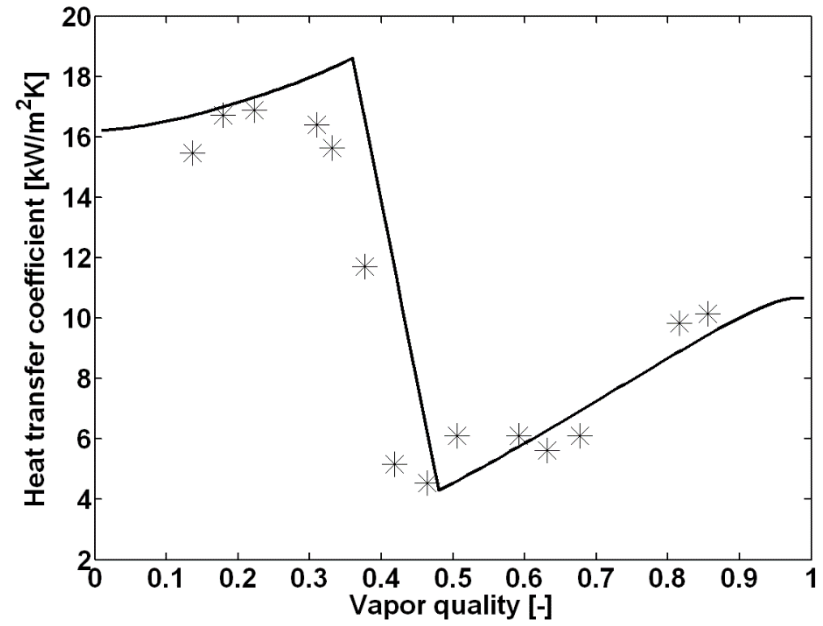

(a)

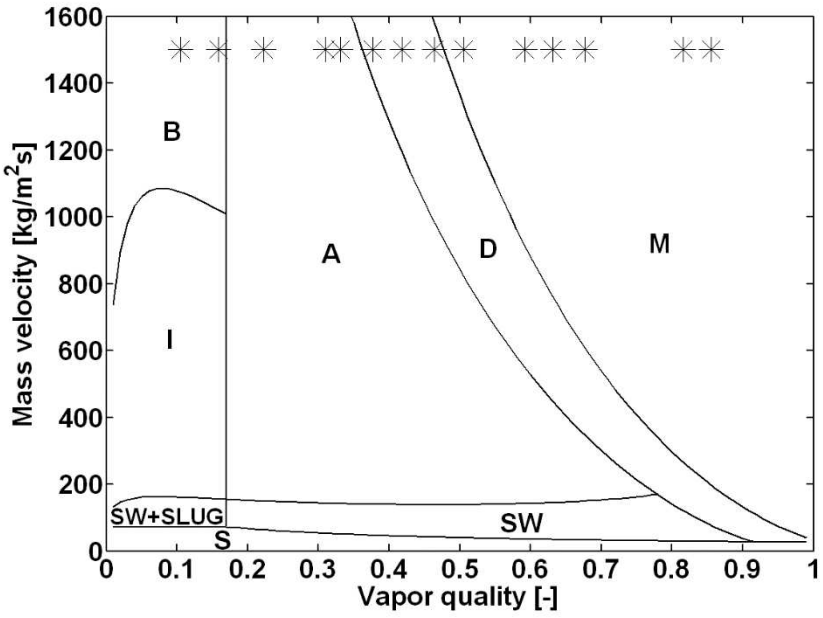

(b)

Fig. 32. (a) Comparison of the predicted heat transfer coefficients to the experimental data of Yun et al. [103] at the test conditions: D_{eq} = 2 mm, q = 30 kW/m^2, T_{sat} = 5°C and G = 1500 kg/m^{2}s; (b) The corresponding flow pattern map at the same test conditions.

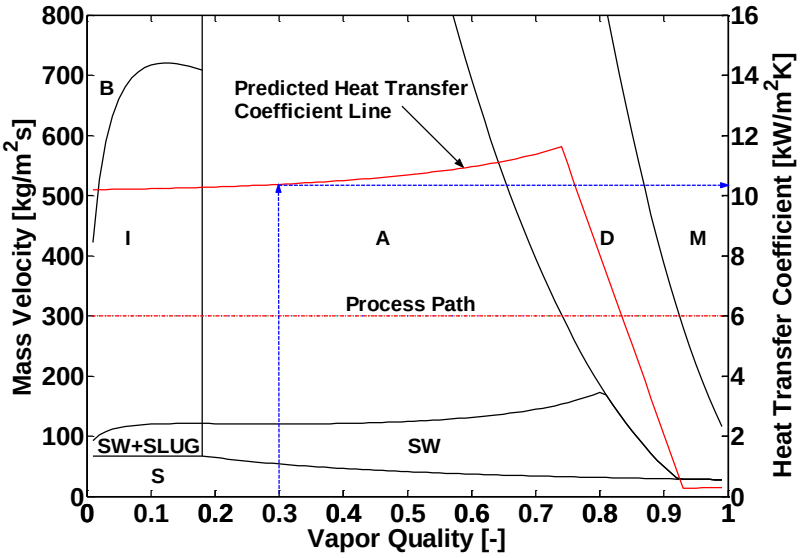

(a)

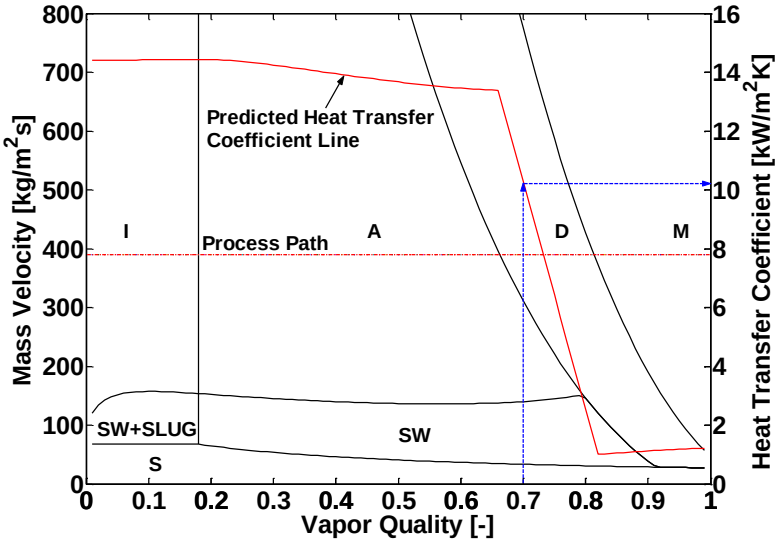

(b)

Fig. 33. Simulation of flow boiling model and flow pattern map by Cheng et al. [104]: (a) For 1.15 mm channel at the conditions: q = 11 kW/m^2, T_{sat} = 10°C and G = 300 kg/m^{2}s with indicated value at x = 0.30; (b) For 3 mm channel at the conditions: q = 20 kW/m^2, T_{sat} = 10°C and G = 390 kg/m^{2}s with indicated value at x = 0.70.

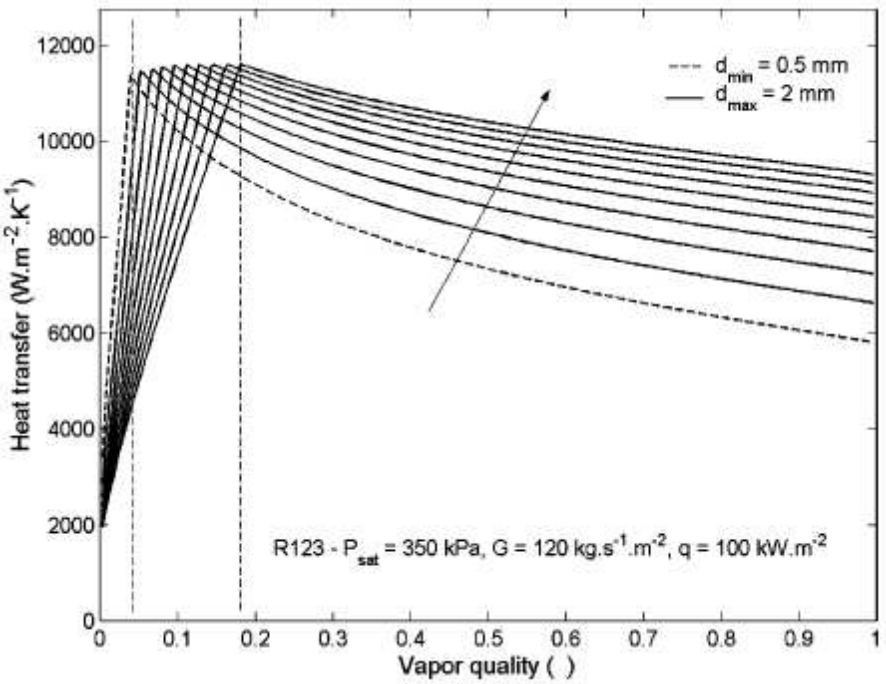

Fig. 34. The predicted flow boiling heat transfer coefficient with the three-zone heat transfer model versus vapor quality for different diameters (increment of 0.166 mm) [88].

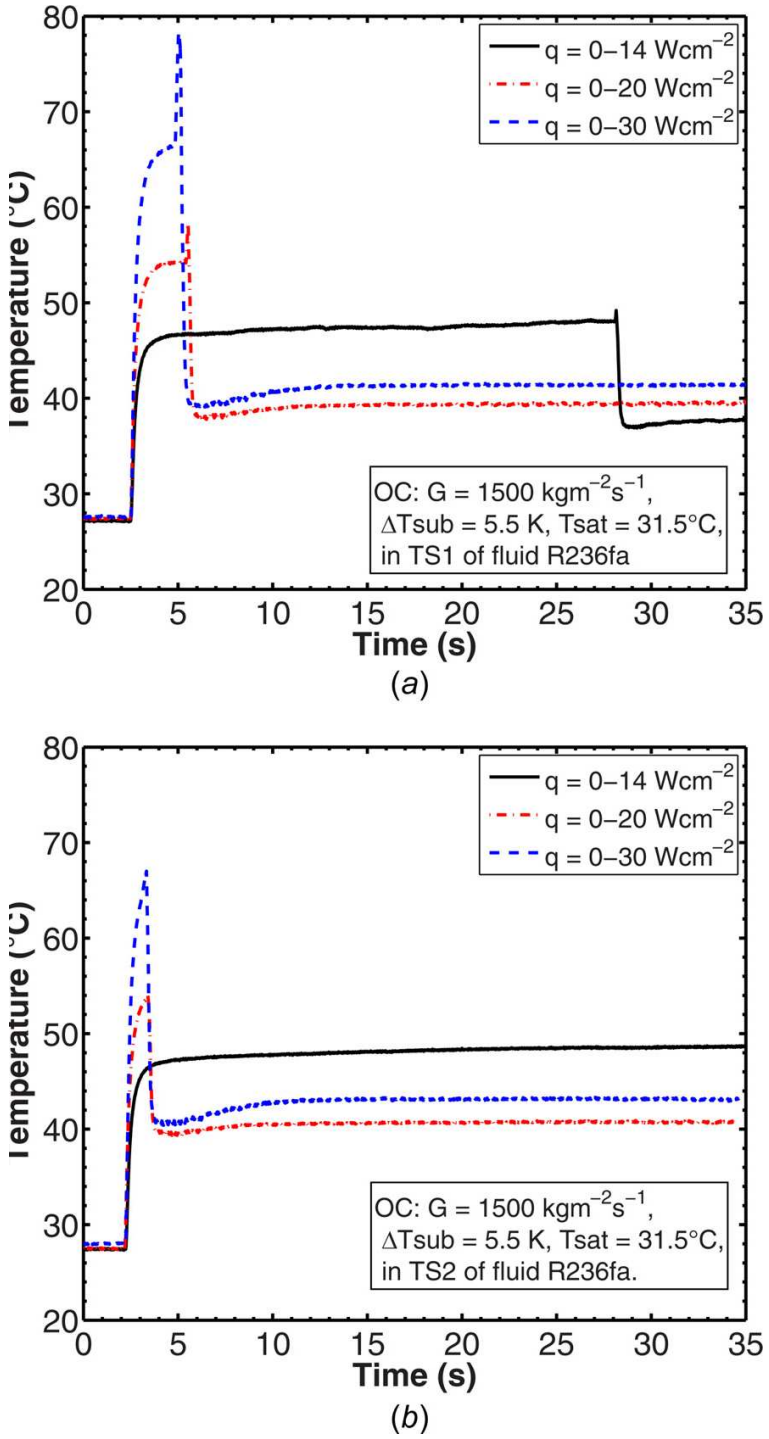

Fig. 35 The Effect of heat flux magnitudes on the thermal response of micro-evaporators: (a) test section 1 and (b) test section 2 by Huang et al. [116].